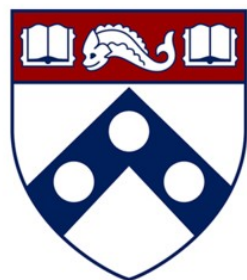


First Direct Measurement of Nuclear Dependence of Coherent Pion Production

Alejandro Ramírez Delgado

INTERSECTIONS @ Lake Buena Vista, FL

September 3rd 2022



Penn
UNIVERSITY of PENNSYLVANIA



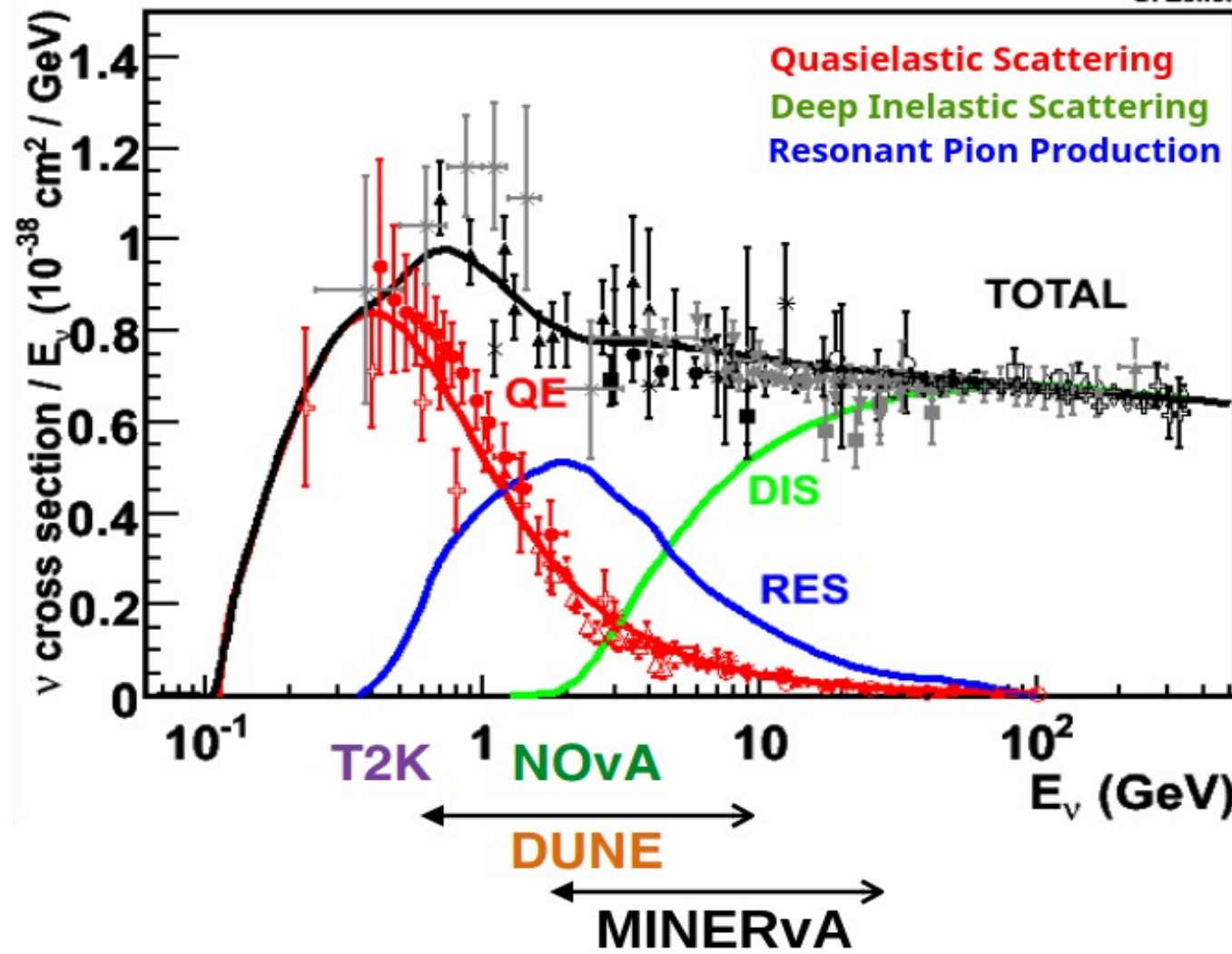
MINERvA

- 1 Neutrino Interactions (Briefly)**
- 2 What is Coherent Pion Production?**
- 3 Previous Measurements – High E_ν & Low E_ν**
- 4 A-Dependence of Coherent Pion Production**
- 5 Results**
- 6 Summary**

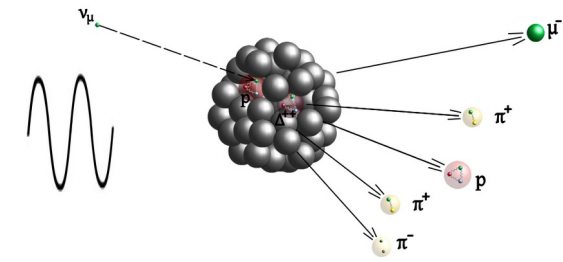
1 – Neutrino Interactions (Briefly)

Types of Neutrino Interactions ($E_\nu \sim 0.1\text{-}20\text{ GeV}$)

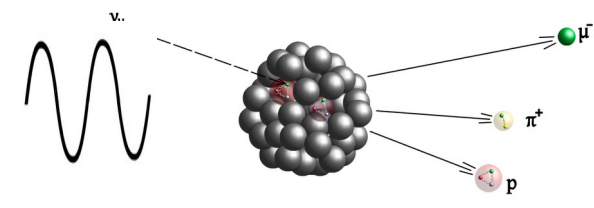
G. Zeller



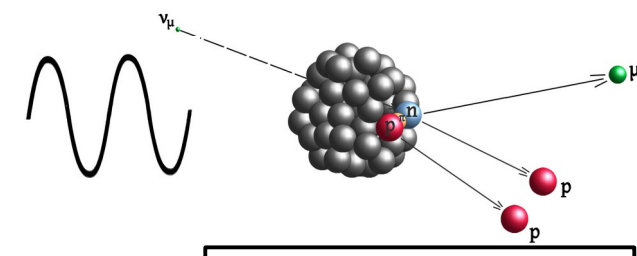
J.A. Formaggio, G. Zeller, Reviews of Modern Physics, 84 (2012)



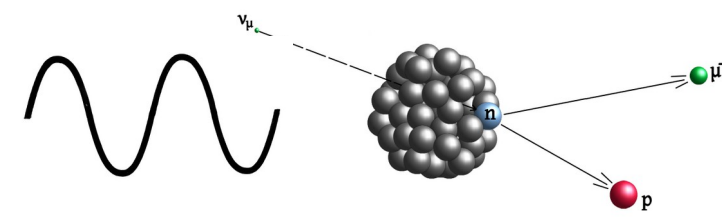
Deep Inelastic Scattering



Resonant Pion Production



2p2h Scattering

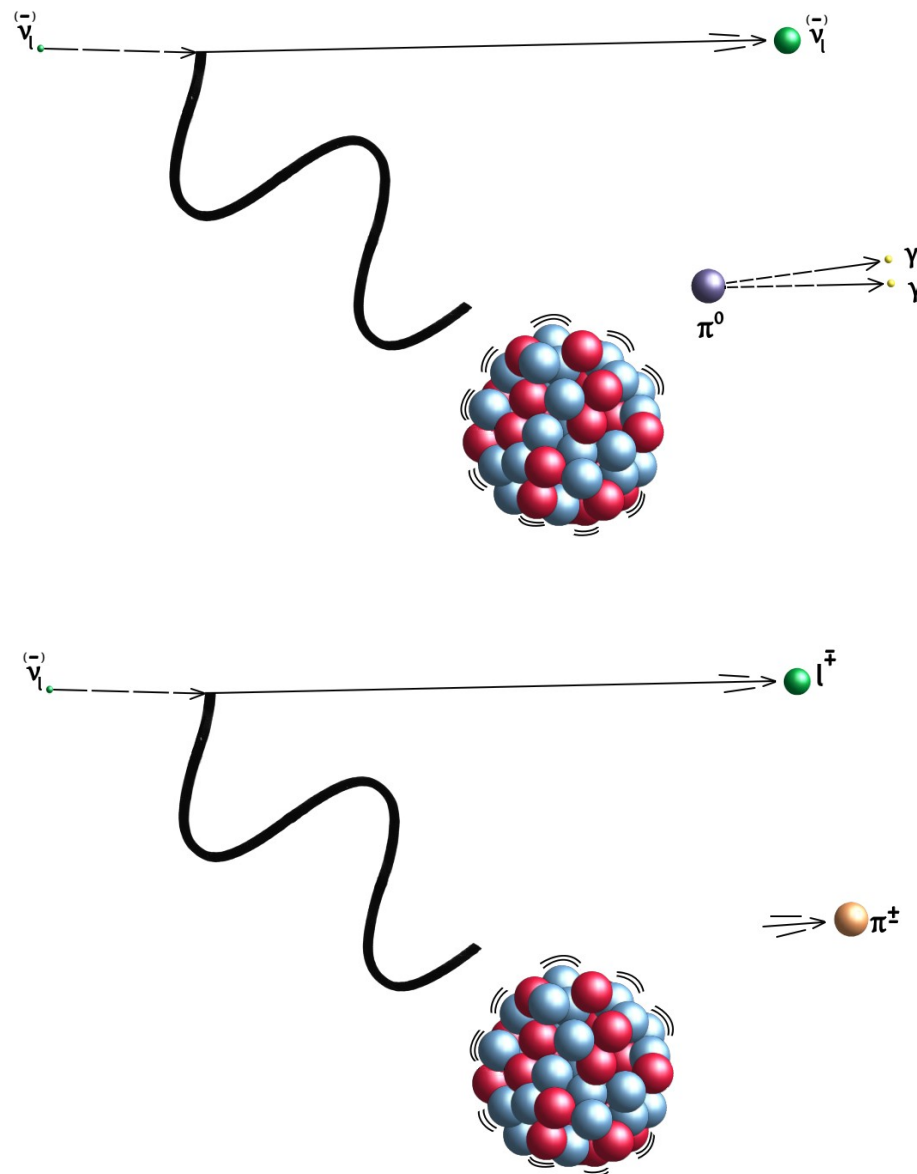


Quasielastic Scattering

2 – What Is Coherent Pion Production?

Features

- Neutrino-nucleus interaction.
- All nucleons react in phase (coherently).
- Nucleus left in its initial state (no breakup).
- Nucleus recoils undetected, $O(\sim \text{keV})$.
- Forward lepton and forward pion created.
- Pion scatters coherently off the nucleus.
- Occurs in both **charged (CC)** and **neutral (NC)** channels.
- It can be induced by a neutrino or anti neutrino of any flavor.



Features

- Coherence depends on the magnitude of the four-momentum transfer to the nucleus, $|\mathbf{t}|$

$$|t| = \left| (p_\nu - p_l - p_\pi)^2 \right|$$

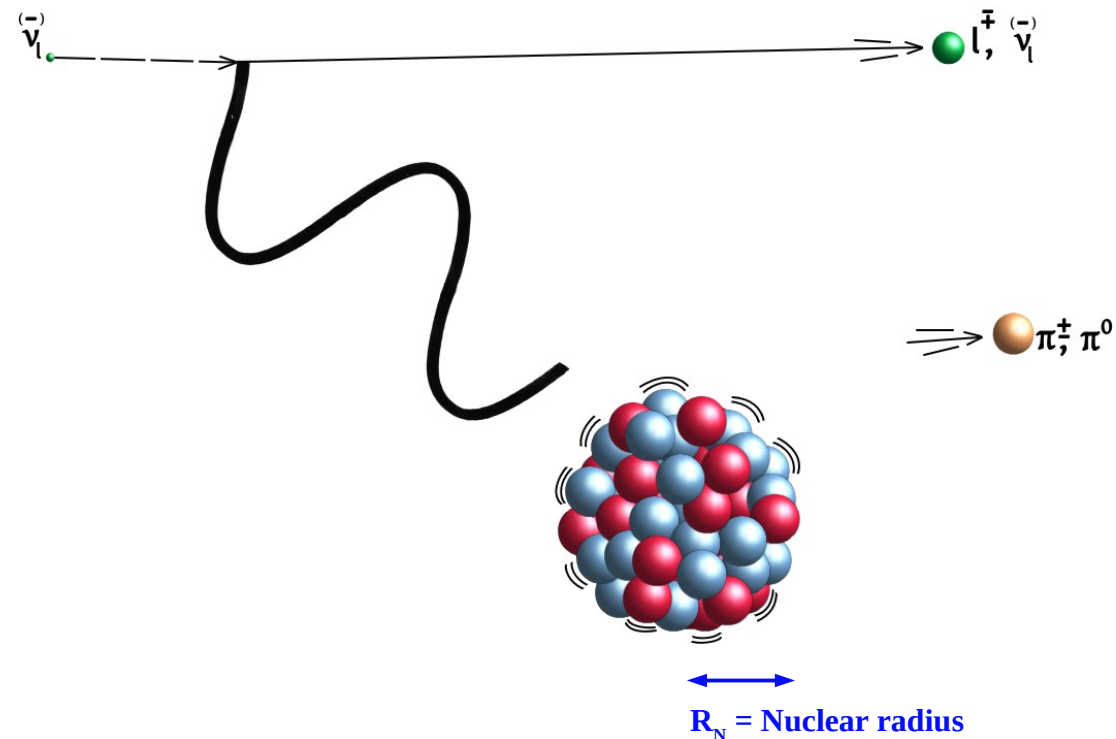
- There is a threshold $|\mathbf{t}_{\min}|$

$$|t_{\min}| \simeq \left(\frac{Q^2 + m_\pi^2}{2E_\pi} \right)^2$$

- and a maximum $|\mathbf{t}_{\max}|$

$$|t_{\max}| \simeq 1/R_N^2$$

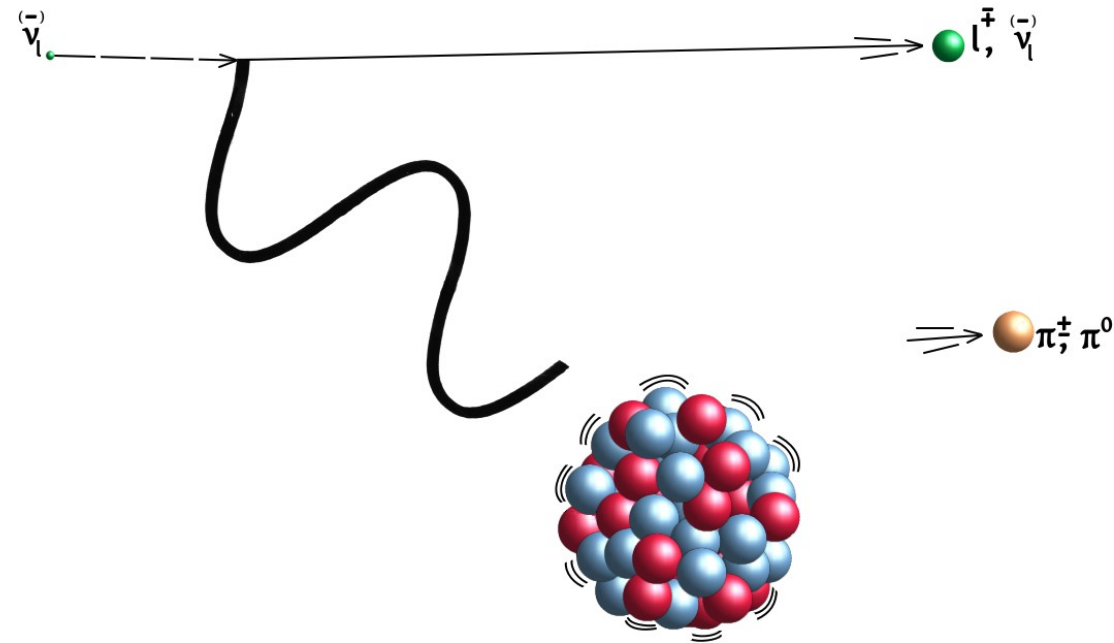
within which the interaction takes place.



Phenomenology

Underlying details of the interaction
not truly understood.

- **Partially Conserved Axial Current (PCAC) hypothesis:**
A neutrino exchanges a W or Z boson in the presence of a nucleus. The boson then fluctuates to a π meson.
- **Microscopic Interpretation:**
Coherent addition of all neutrino-nucleon interactions in the nucleus.
 Δ resonance production is the main process contributing to the final state.



The Rein-Sehgal Model

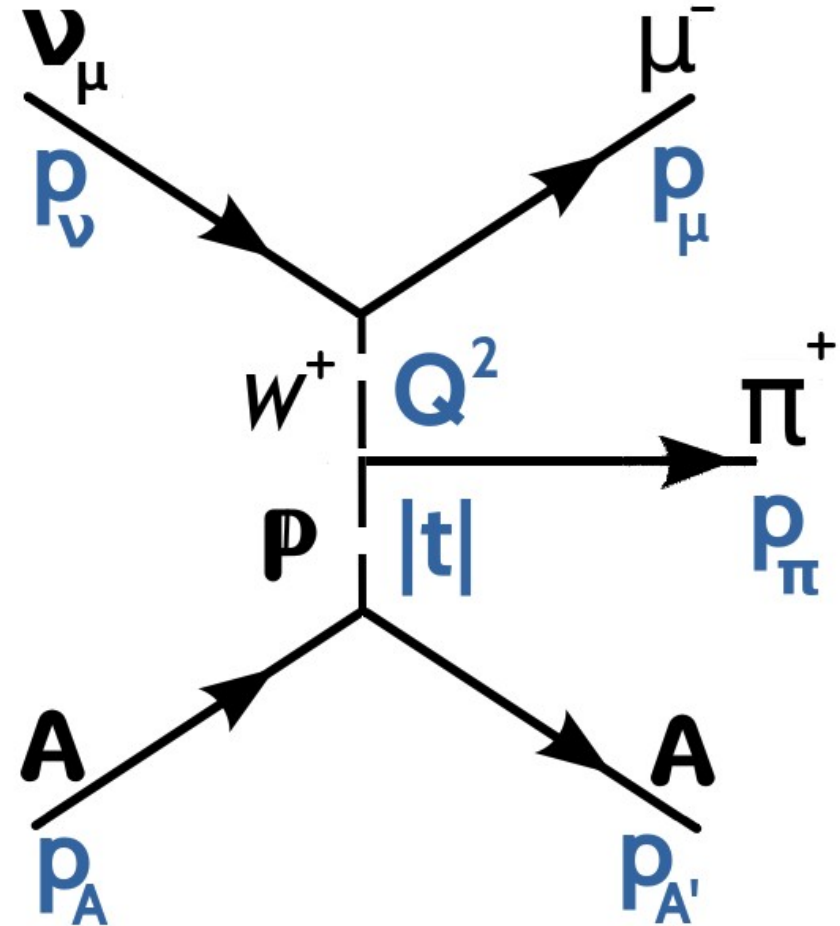
- Uses **Adler's theorem** to relate the inelastic process

$$\nu + A \rightarrow l + \pi + A$$

to the elastic process

$$\pi + A \rightarrow \pi + A$$

- It assumes the incoming neutrino and the outgoing lepton are parallel (**when $Q^2 = 0$**), and neglects the lepton mass.

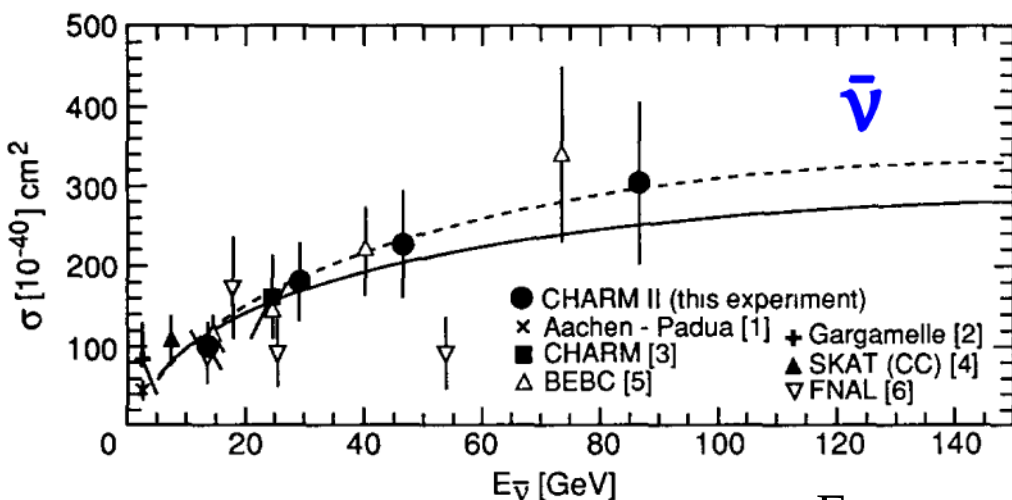
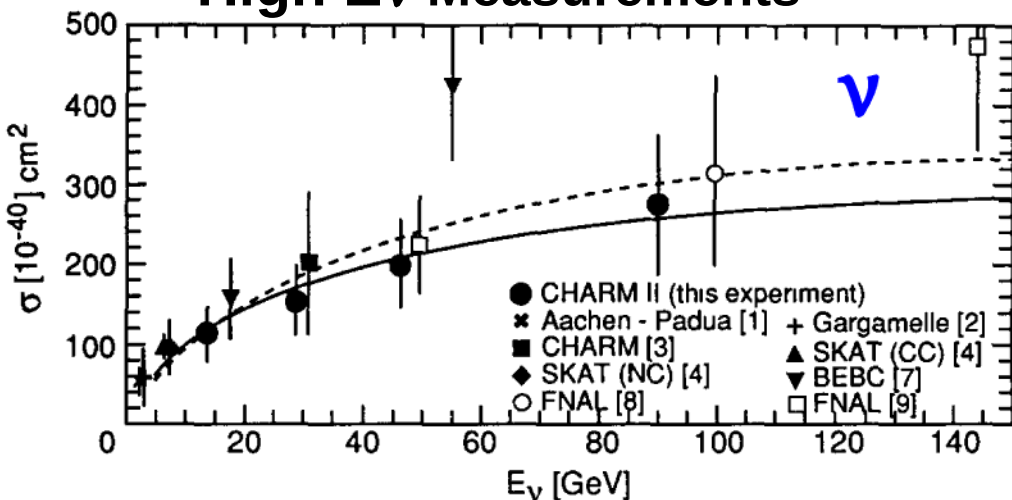


3 – Previous Measurements

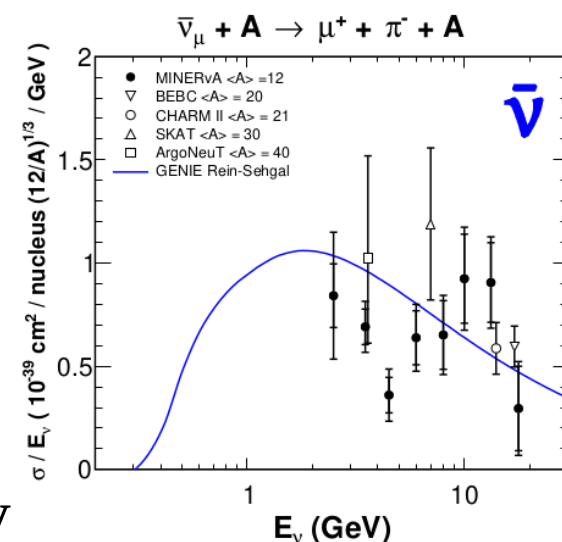
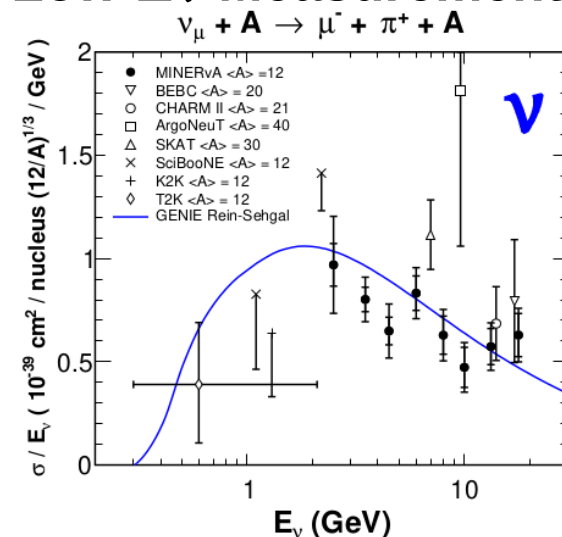
[Phys.Lett.B 313 (1993) 267-275]

[Phys.Rev.D 97 (2018) 3, 032014]

High E_ν Measurements



Low E_ν Measurements



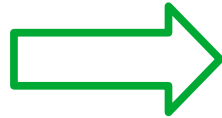
- E_ν range: ~ 2 to ~ 300 GeV
- A (nuclear mass) range: ^{12}C to ^{80}Br
- Neutrino and anti-neutrino modes
- Cross sections scaled as $A^{1/3}$

What Else? A-Scaling Measurements!

- So far, **NO** measurements for **nuclei beyond $A = 80$** . **A**-scaling of the cross section requires measurements in nuclei of very different mass.
- Different models predict different scaling of the coherent cross section with regards to the mass number **A**:
 - A set of models, like the **Rein-Sehgal** model, predict an **A**-scaling as $A^{1/3}$.
 - Other models, like the **Berger-Sehgal** model, predict a **A**-scaling as $A^{2/3}$.
 - The **Belkov-Kopeliovich** model predicts an “energy-dependent” **A**-scaling. Scaling as $A^{1/3}$ at **low E_ν** , and as $A^{2/3}$ at **high E_ν** .

4 – A-Dependence of Coherent Pion Production

What Else?



A-Scaling Measurements!

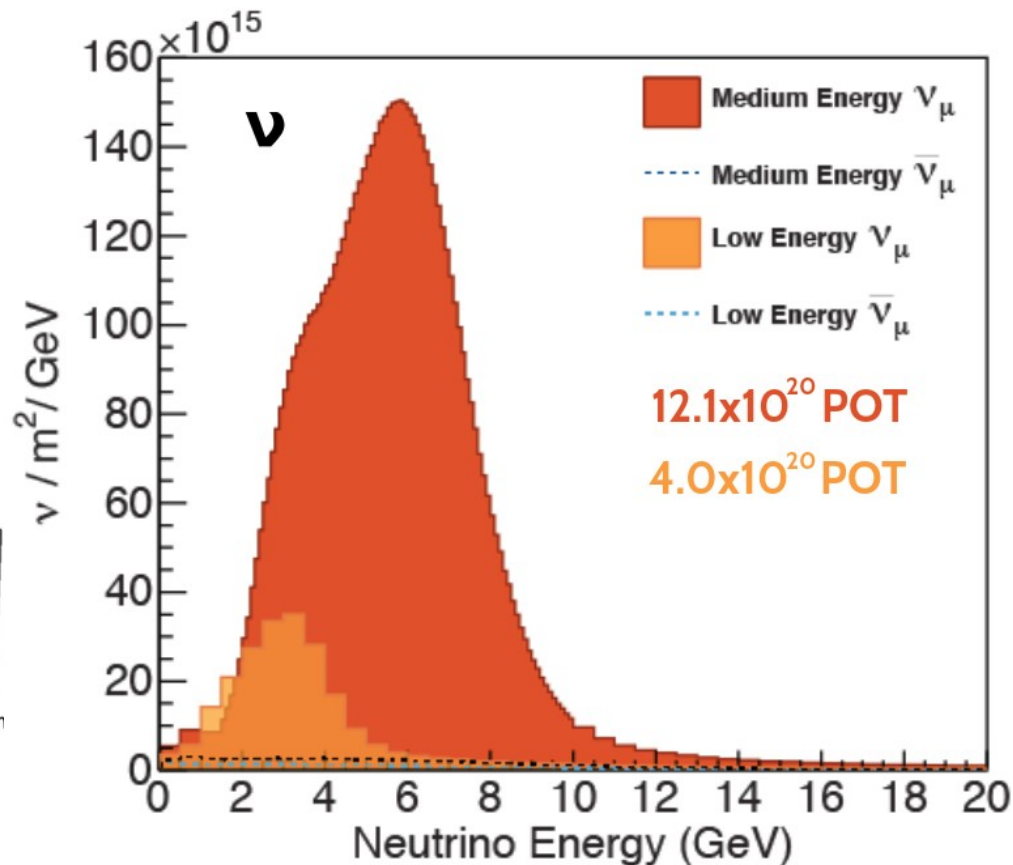
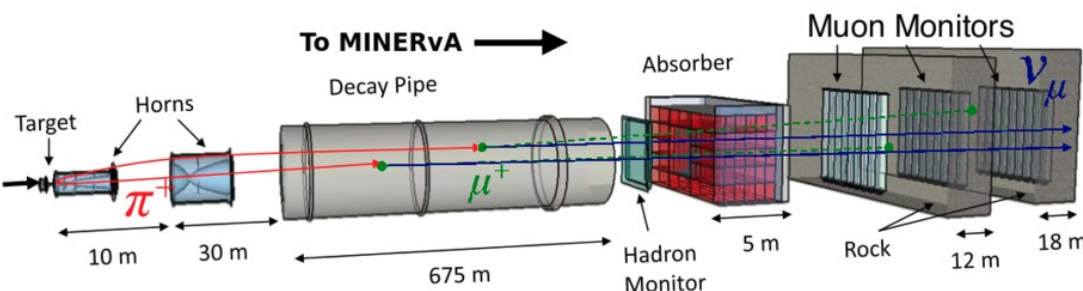
$$A = 12, 56, 207$$

| | | | | | | | | | | | | | | | | | |
|-------------------------------------|-----------------------------------|-----------------------------------|-------------------------------------|-----------------------------------|----------------------------------|------------------------------------|---------------------------------|----------------------------------|------------------------------------|-----------------------------------|-----------------------------------|------------------------------------|---------------------------------|---------------------------------------|-----------------------------------|------------------------------------|---------------------------------|
| 1 H Hydrogen 1.008 | | | | | | | | | | | | | | | | | 2 He Helium 4.002602 |
| 3 Li Lithium 6.94 | 4 Be Beryllium 9.0121831 | | | | | | | | | | | 5 B Boron 10.81 | 6 C Carbon 12.011 | 7 N Nitrogen 14.007 | 8 O Oxygen 15.999 | 9 F Fluorine 18.998403163 | 10 Ne Neon 20.1797 |
| 11 Na Sodium 22.98976928 | 12 Mg Magnesium 24.305 | | | | | | | | | | | 13 Al Aluminum 26.9815385 | 14 Si Silicon 28.085 | 15 P Phosphorus 30.973761998 | 16 S Sulfur 32.06 | 17 Cl Chlorine 35.45 | 18 Ar Argon 39.948 |
| 19 K Potassium 39.0983 | 20 Ca Calcium 40.078 | 21 Sc Scandium 44.955908 | 22 Ti Titanium 47.867 | 23 V Vanadium 50.9415 | 24 Cr Chromium 51.9961 | 25 Mn Manganese 54.938044 | 26 Fe Iron 55.845 | 27 Co Cobalt 58.933194 | 28 Ni Nickel 58.6934 | 29 Cu Copper 63.546 | 30 Zn Zinc 65.38 | 31 Ga Gallium 69.723 | 32 Ge Germanium 72.630 | 33 As Arsenic 74.921595 | 34 Se Selenium 78.971 | 35 Br Bromine 79.904 | 36 Kr Krypton 83.798 |
| 37 Rb Rubidium 85.4678 | 38 Sr Strontium 87.62 | 39 Y Yttrium 88.90584 | 40 Zr Zirconium 91.224 | 41 Nb Niobium 92.90637 | 42 Mo Molybdenum 95.95 | 43 Tc Technetium (98) | 44 Ru Ruthenium 101.07 | 45 Rh Rhodium 102.90550 | 46 Pd Palladium 106.42 | 47 Ag Silver 107.8682 | 48 Cd Cadmium 112.414 | 49 In Indium 114.818 | 50 Sn Tin 118.710 | 51 Sb Antimony 121.760 | 52 Te Tellurium 127.60 | 53 I Iodine 126.90447 | 54 Xe Xenon 131.293 |
| 55 Cs Caesium 132.90545196 | 56 Ba Barium 137.327 | 57 - 71 Lanthanoids | 72 Hf Hafnium 178.49 | 73 Ta Tantalum 180.94788 | 74 W Tungsten 183.84 | 75 Re Rhenium 186.207 | 76 Os Osmium 190.23 | 77 Ir Iridium 192.217 | 78 Pt Platinum 195.084 | 79 Au Gold 196.966569 | 80 Hg Mercury 200.592 | 81 Tl Thallium 204.38 | 82 Pb Lead 207.2 | 83 Bi Bismuth 208.98040 | 84 Po Polonium (209) | 85 At Astatine (210) | 86 Rn Radon (222) |
| 87 Fr Francium (223) | 88 Ra Radium (226) | 89 - 103 Actinoids | 104 Rf Rutherfordium (267) | 105 Db Dubnium (268) | 106 Sg Seaborgium (269) | 107 Bh Bohrium (270) | 108 Hs Hassium (269) | 109 Mt Meitnerium (278) | 110 Ds Darmstadtium (281) | 111 Rg Roentgenium (282) | 112 Cn Copernicium (285) | 113 Nh Nihonium (286) | 114 Fl Flerovium (289) | 115 Mc Moscovium (289) | 116 Lv Livermorium (293) | 117 Ts Tennessine (294) | 118 Og Oganesson (294) |

| | | | | | | | | | | | | | | |
|------------------------------------|---------------------------------|---------------------------------------|----------------------------------|---------------------------------|--------------------------------|---------------------------------|----------------------------------|----------------------------------|-----------------------------------|----------------------------------|-------------------------------|-----------------------------------|----------------------------------|----------------------------------|
| 57 La Lanthanum 138.90547 | 58 Ce Cerium 140.116 | 59 Pr Praseodymium 140.90766 | 60 Nd Neodymium 144.242 | 61 Pm Promethium (145) | 62 Sm Samarium 150.36 | 63 Eu Europium 151.964 | 64 Gd Gadolinium 157.25 | 65 Tb Terbium 158.92535 | 66 Dy Dysprosium 162.500 | 67 Ho Holmium 164.93033 | 68 Er Erbium 167.259 | 69 Tm Thulium 168.93422 | 70 Yb Ytterbium 173.045 | 71 Lu Lutetium 174.9668 |
| 89 Ac Actinium (227) | 90 Th Thorium 232.0377 | 91 Pa Protactinium 231.03588 | 92 U Uranium 238.02891 | 93 Np Neptunium (237) | 94 Pu Plutonium (244) | 95 Am Americium (243) | 96 Cm Curium (247) | 97 Bk Berkelium (247) | 98 Cf Californium (251) | 99 Es Einsteinium (252) | 100 Fm Fermium (257) | 101 Md Mendelevium (258) | 102 No Nobelium (259) | 103 Lr Lawrencium (260) |

Beamline and Fluxes

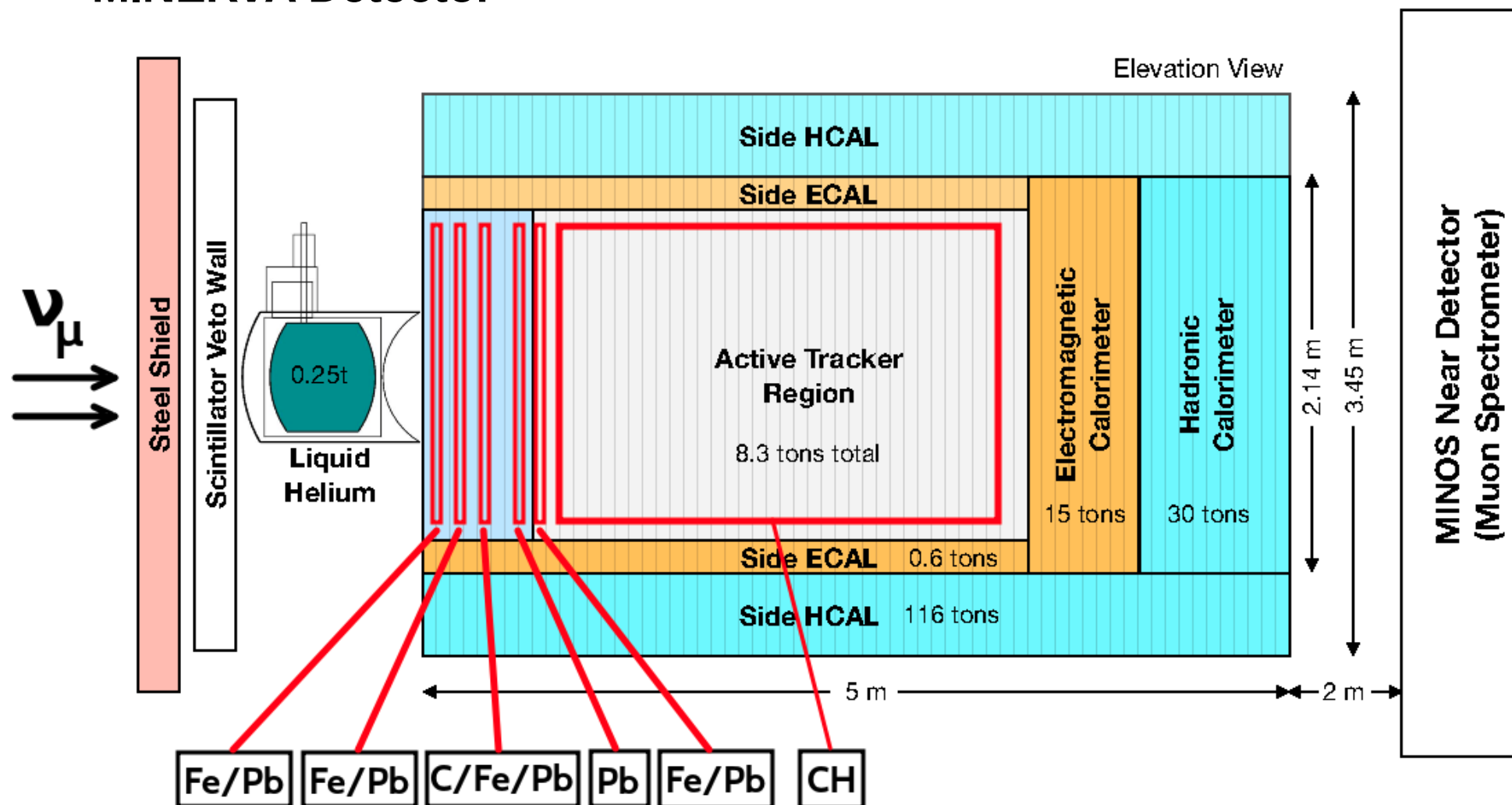
Beamline



Flux used in previous
MINERvA
measurement
 $\langle E_\nu \rangle \sim 3.5 \text{ GeV}$

Flux used in this
measurement
 $\langle E_\nu \rangle \sim 6 \text{ GeV}$

MINERvA Detector



Event Selection

CUTS APPLIED

Vertex in Iron

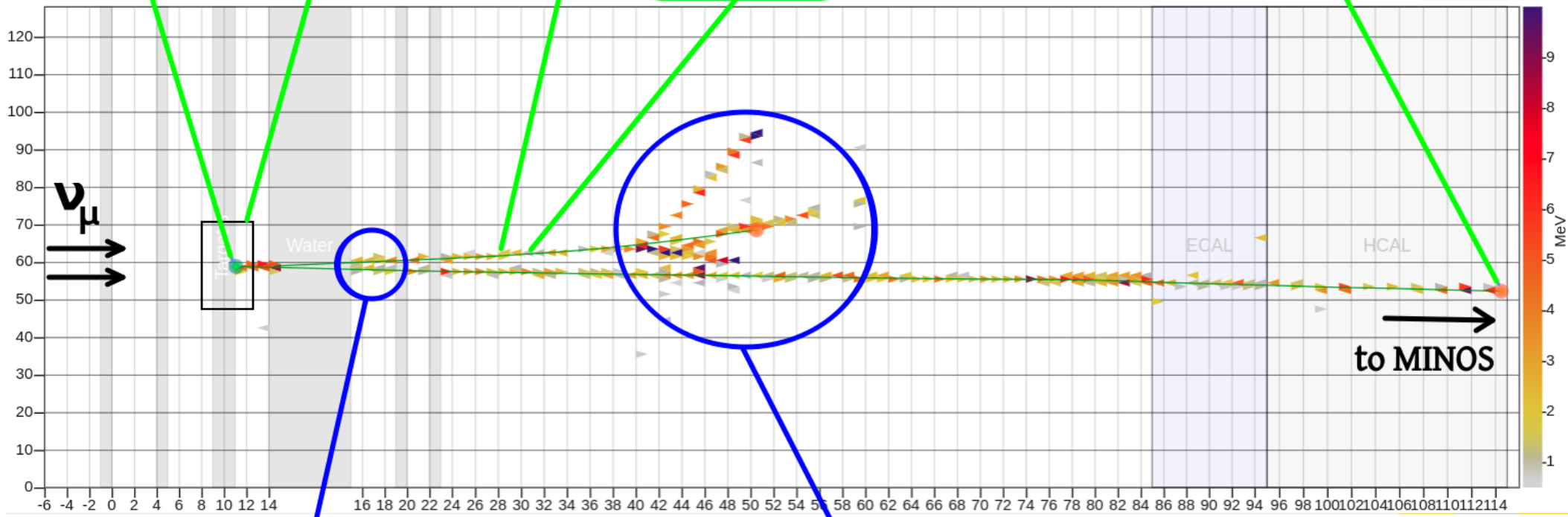
Low Energy Around the Vertex

π^+ Candidate Fully Contained

π^+ -Like dE/dx Profile

$|t| < 1/R^2$,
R = Nuclear Radius

μ^- Candidate to MINOS Detector



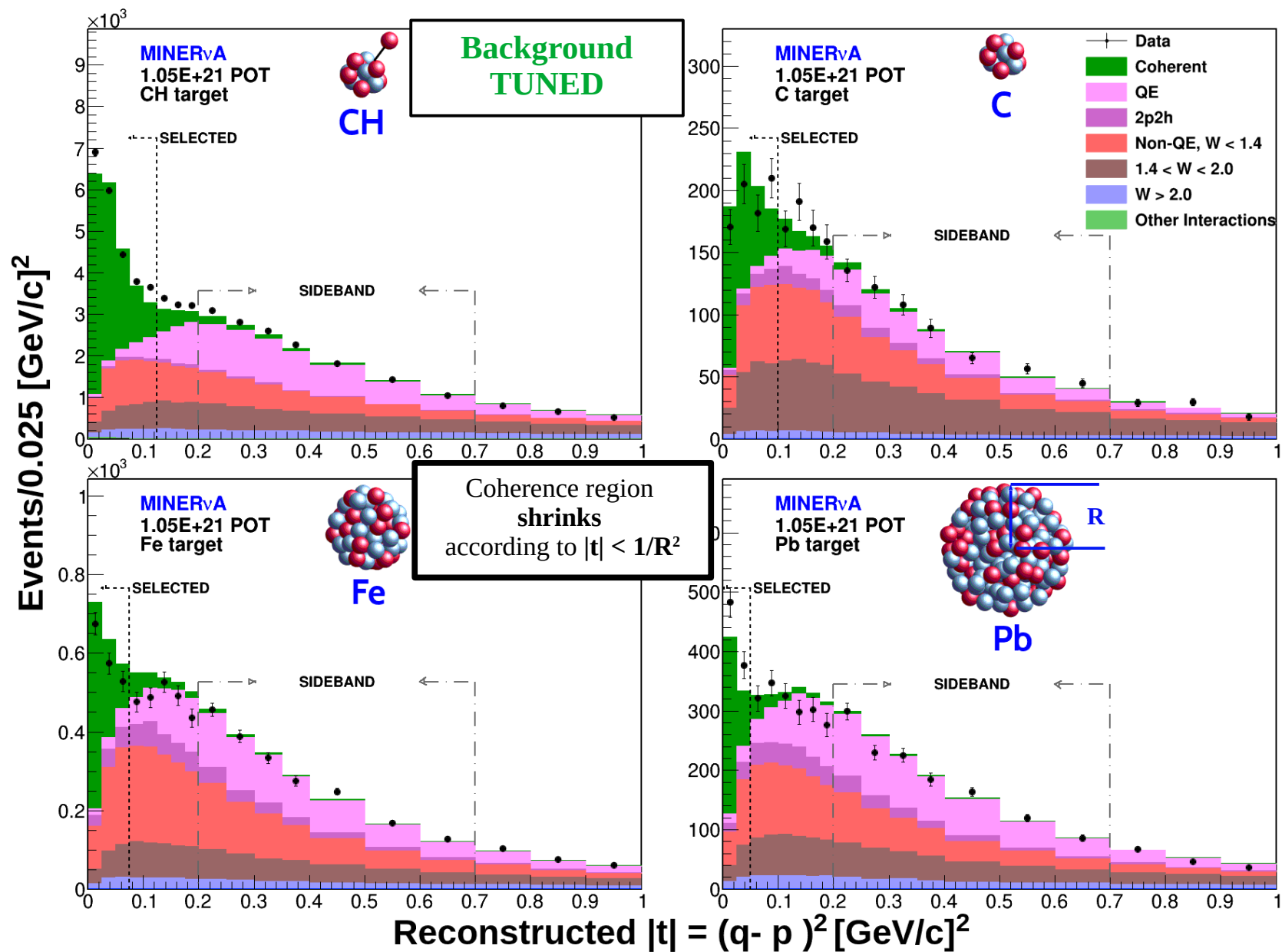
Small Opening Angle

Small π^+ and μ^- Angles WRT ν_μ

Interaction of π^+ Candidate

OBSERVABLES

Tuned $|t|$ Distributions



Cross Section Extraction

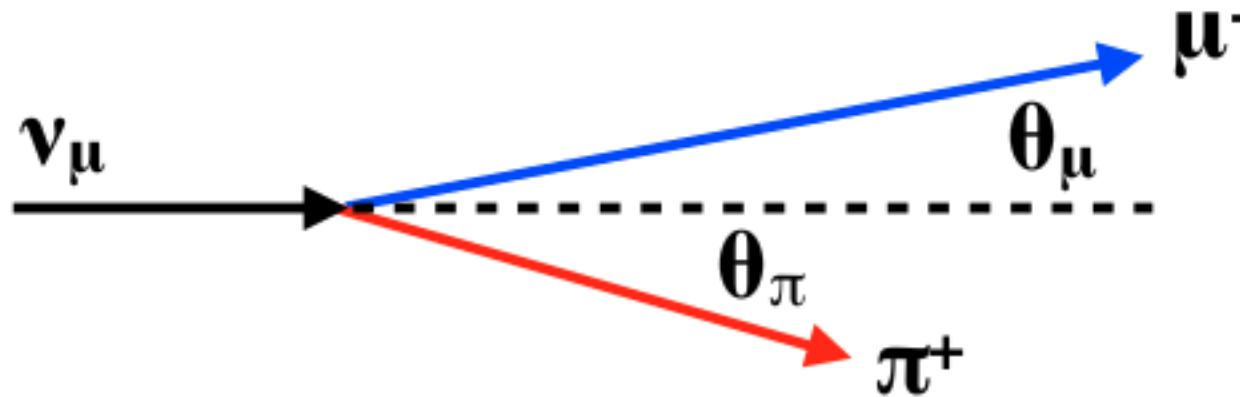
$$\sigma_i = \frac{\sum_j U_{ij} (N_j^{DATA} - N_j^{BKGD})}{\epsilon_i \phi_i T}$$

The equation is annotated with blue arrows and text:

- Total Cross Section** points to σ_i .
- True Bin** points to the subscript i of σ_i .
- Unfolding Matrix** points to U_{ij} .
- Reco Bin** points to the subscript j of \sum_j .
- Number of Selected Data Events** points to N_j^{DATA} .
- Number of Predicted Background Events** points to N_j^{BKGD} .
- Efficiency** points to ϵ_i .
- Flux Per Bin** points to ϕ_i .
- Number of Nuclei** points to T .

Cross Sections

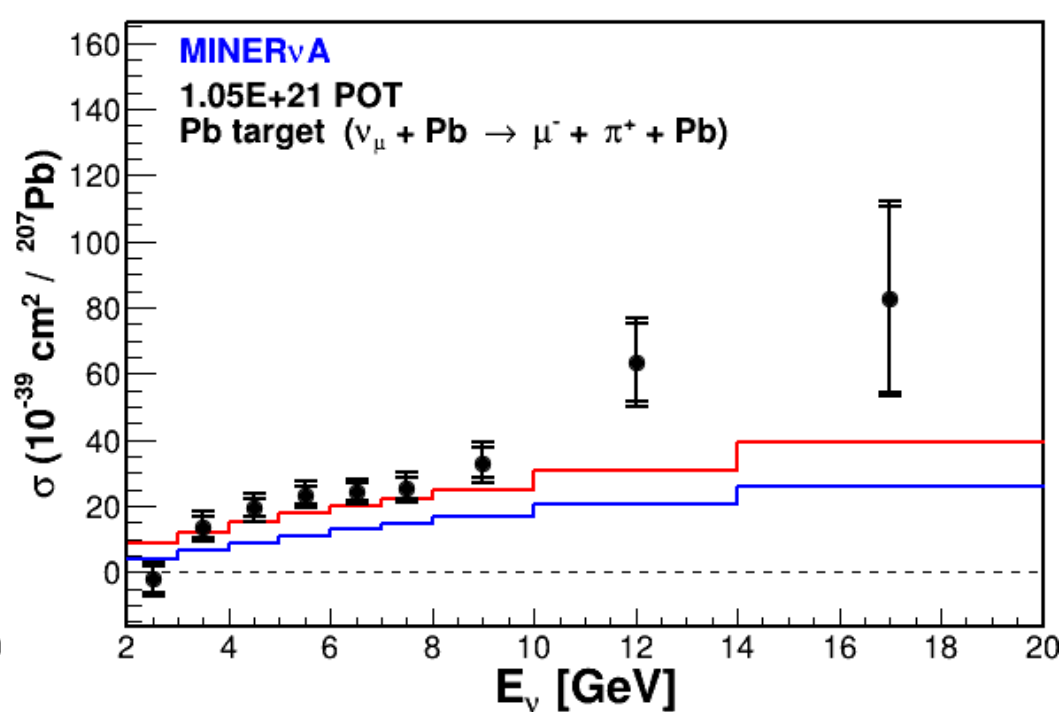
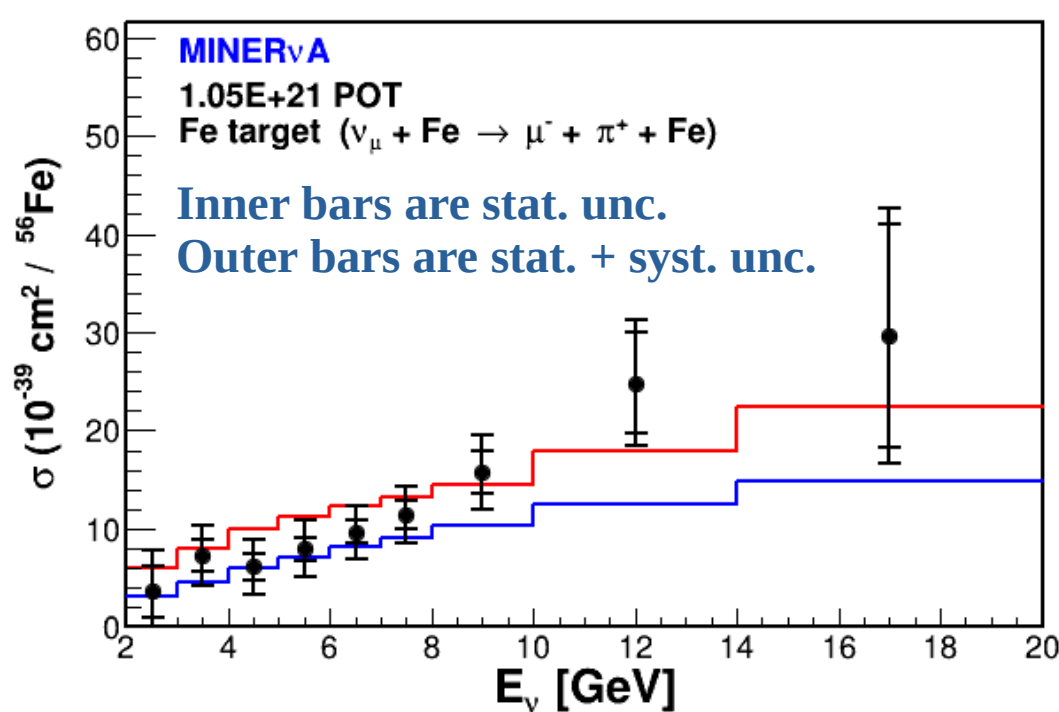
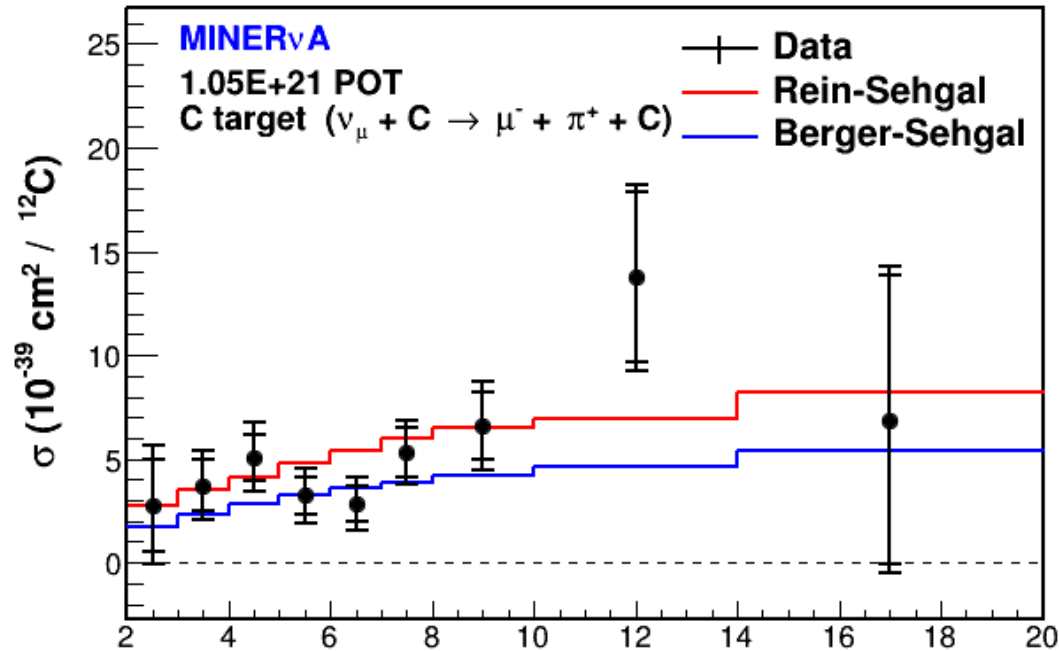
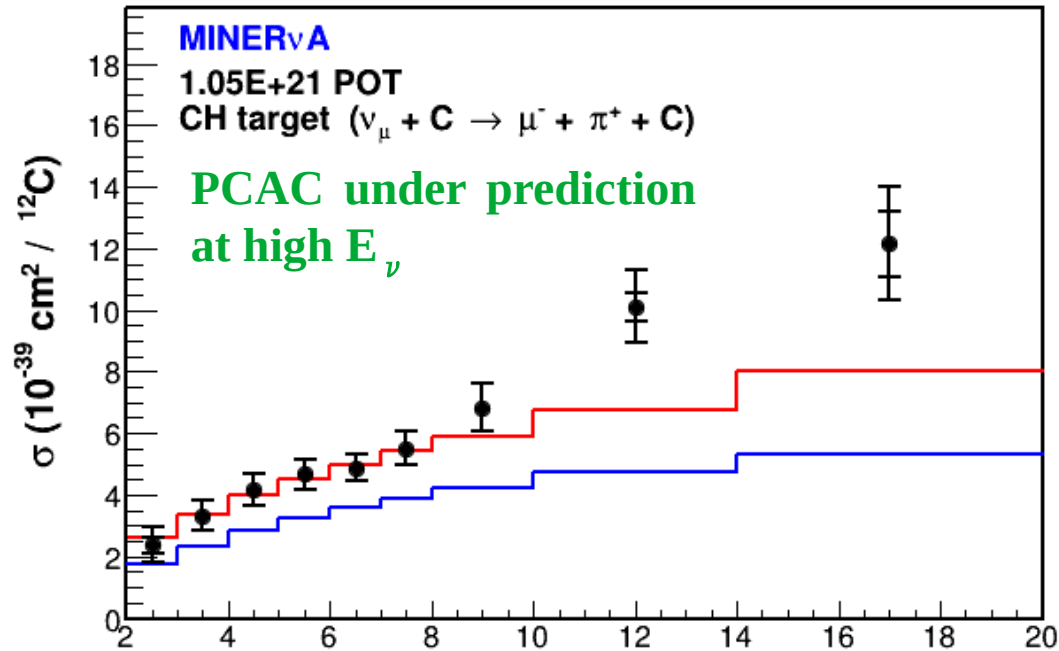
In 6 variables: E_ν , E_π , Q^2 , θ_π , θ_μ , E_μ



- $E_\nu \approx E_\mu + E_\pi$
- E_π from calorimetry in MINERvA
- E_μ from range in MINERvA + range/curvature in MINOS
- $Q^2 = -(p_\nu - p_\mu)^2 \approx 2E_\nu (E_\mu - P_\mu \cos \theta_\mu) - m_\mu^2$
- θ_π and θ_μ from reconstructed tracks in MINERvA

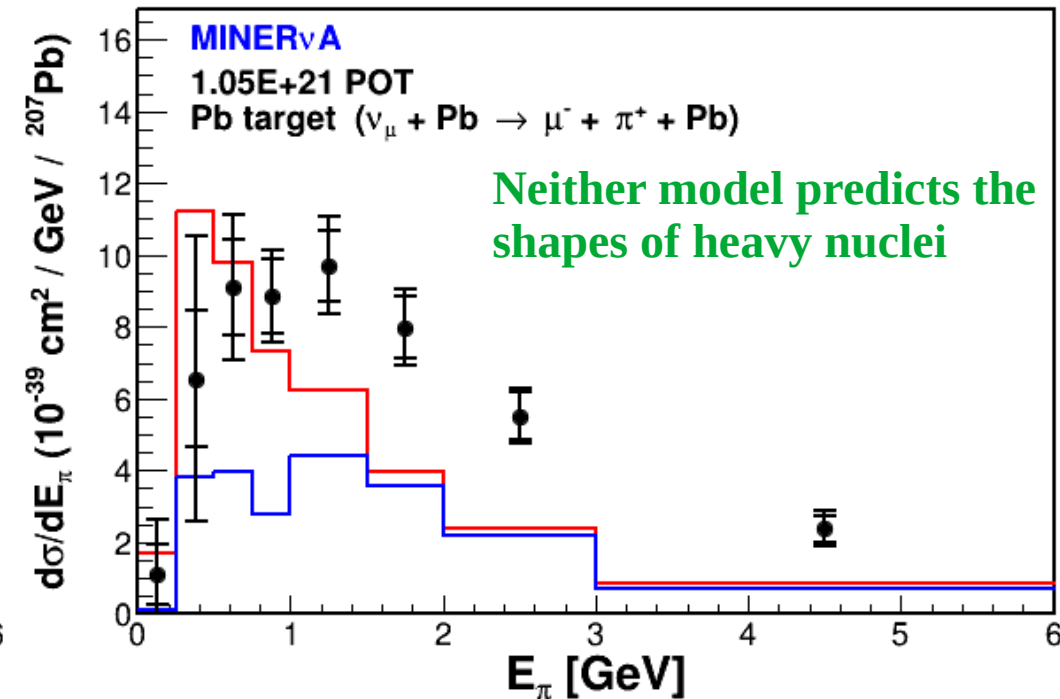
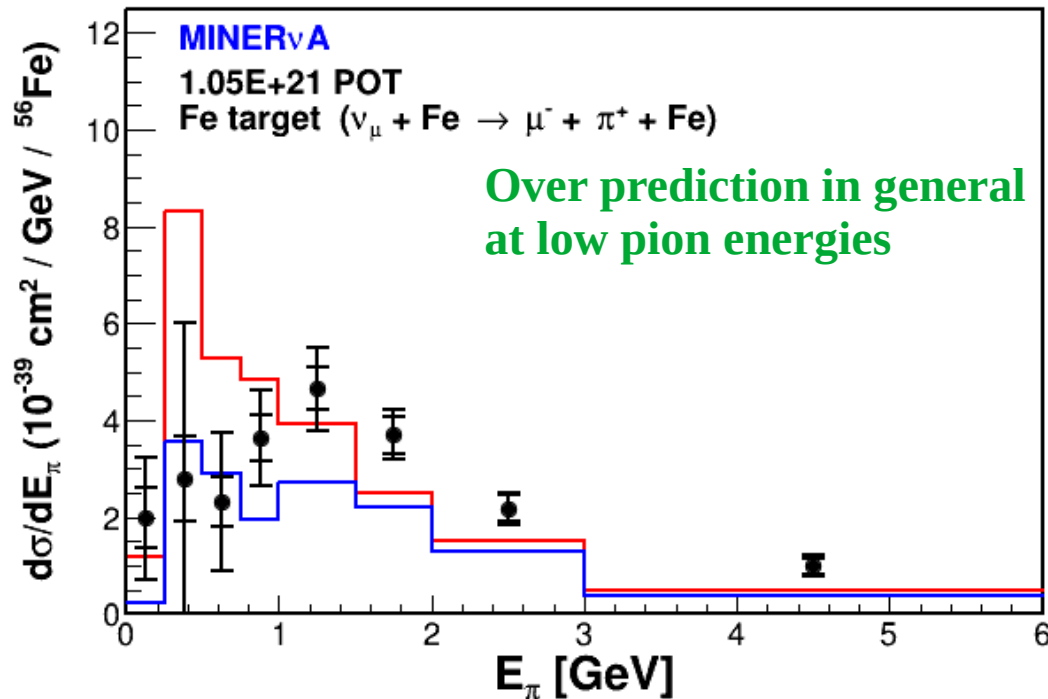
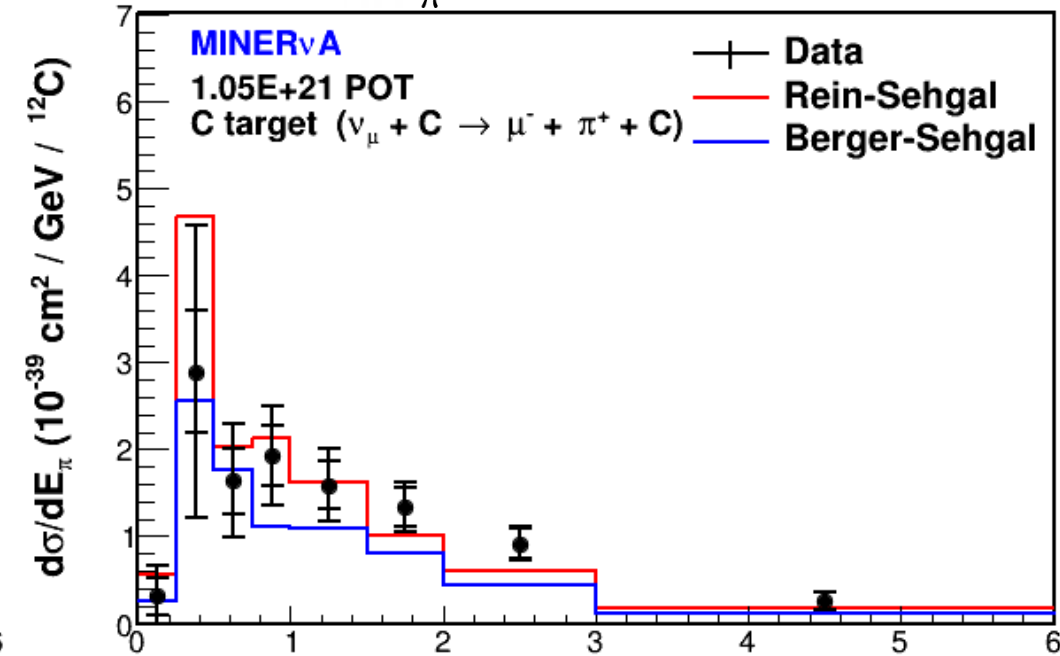
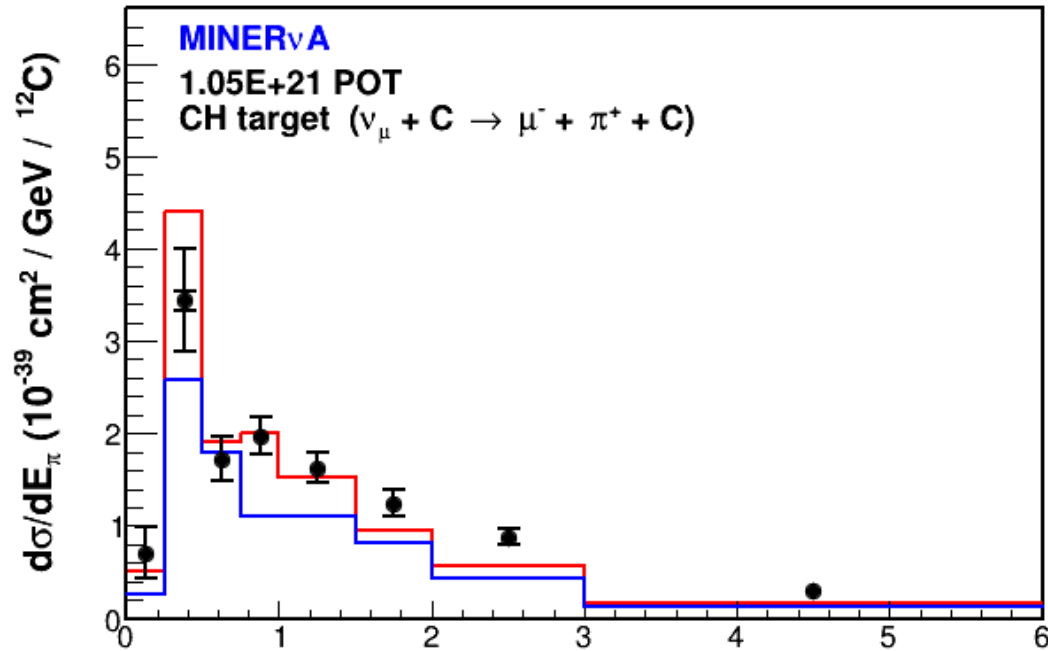
5 - Results: Cross Sections

$$\sigma E_\nu$$



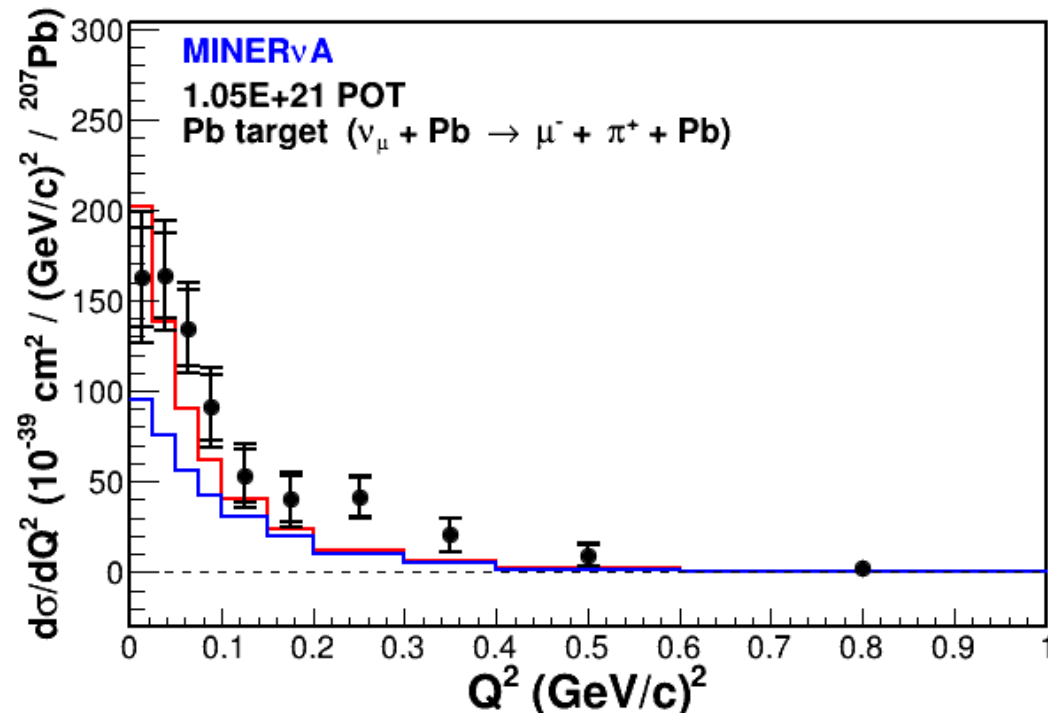
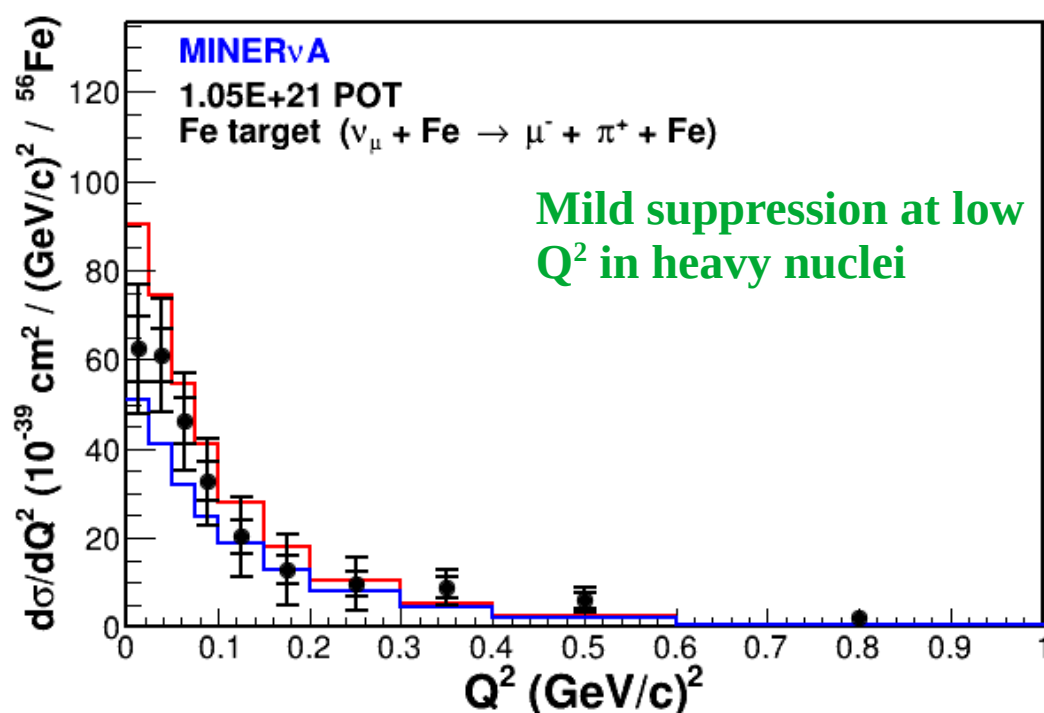
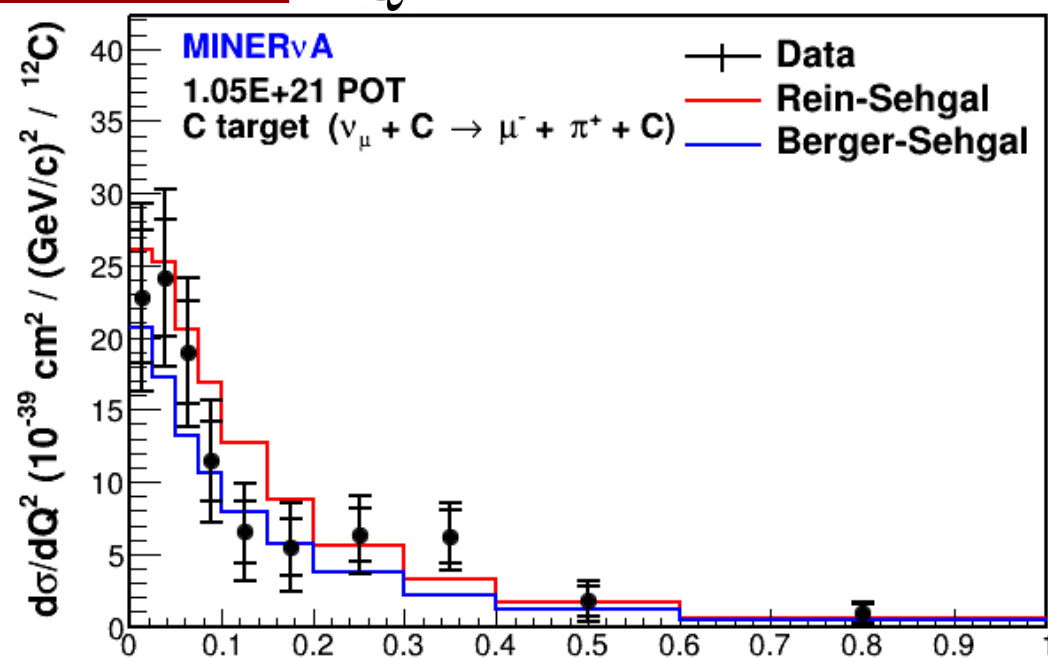
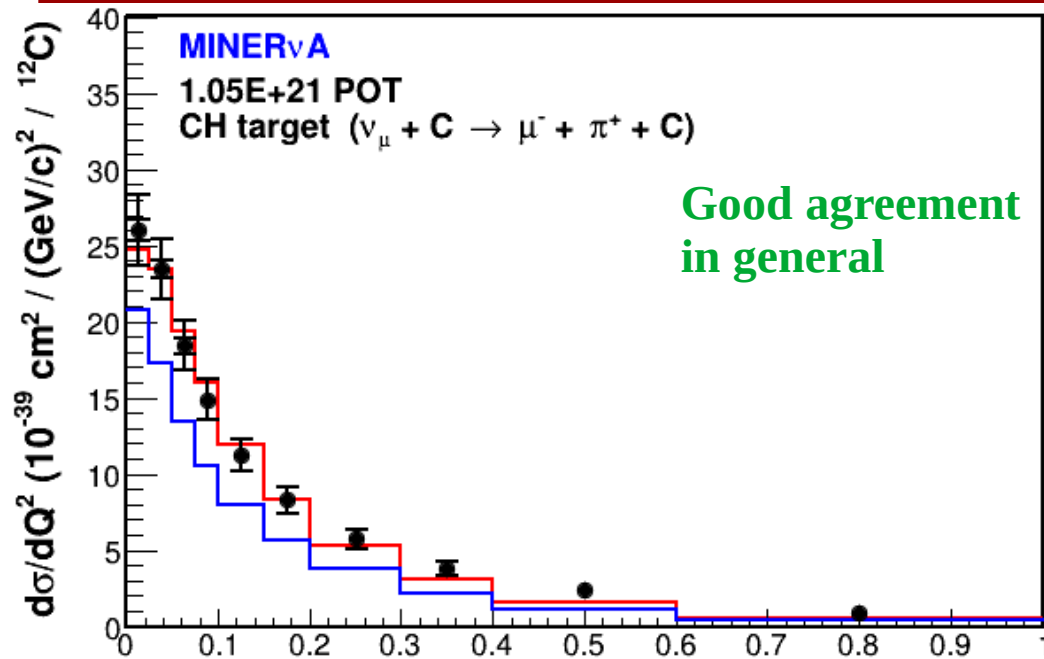
Results: Cross Sections

$$\frac{d\sigma}{dE_\pi}$$



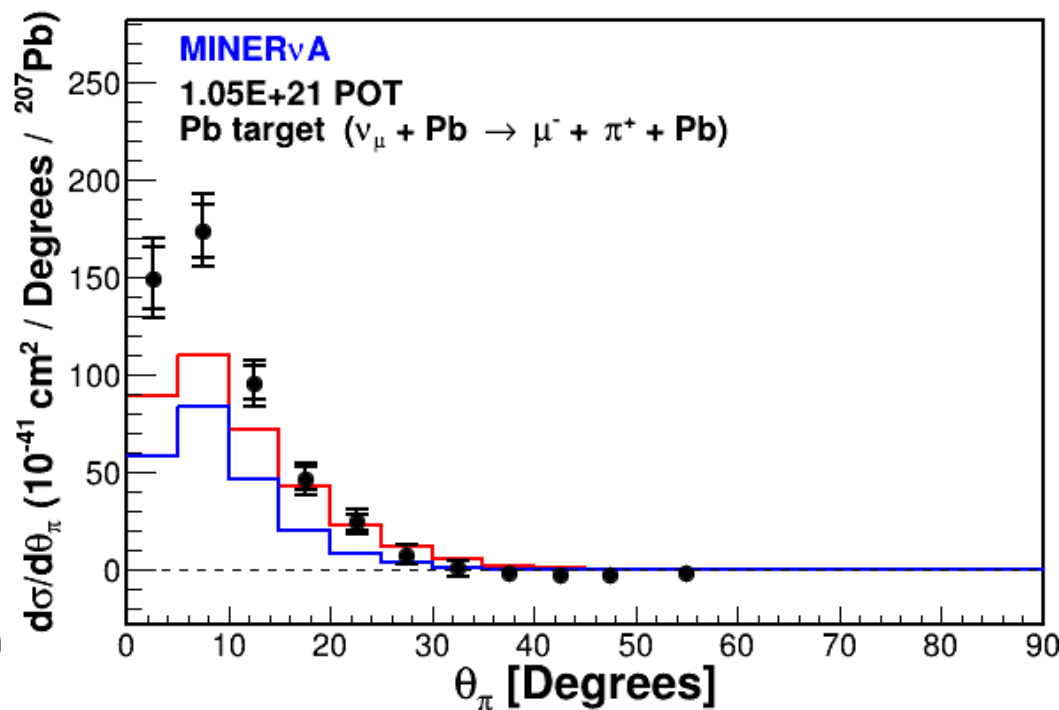
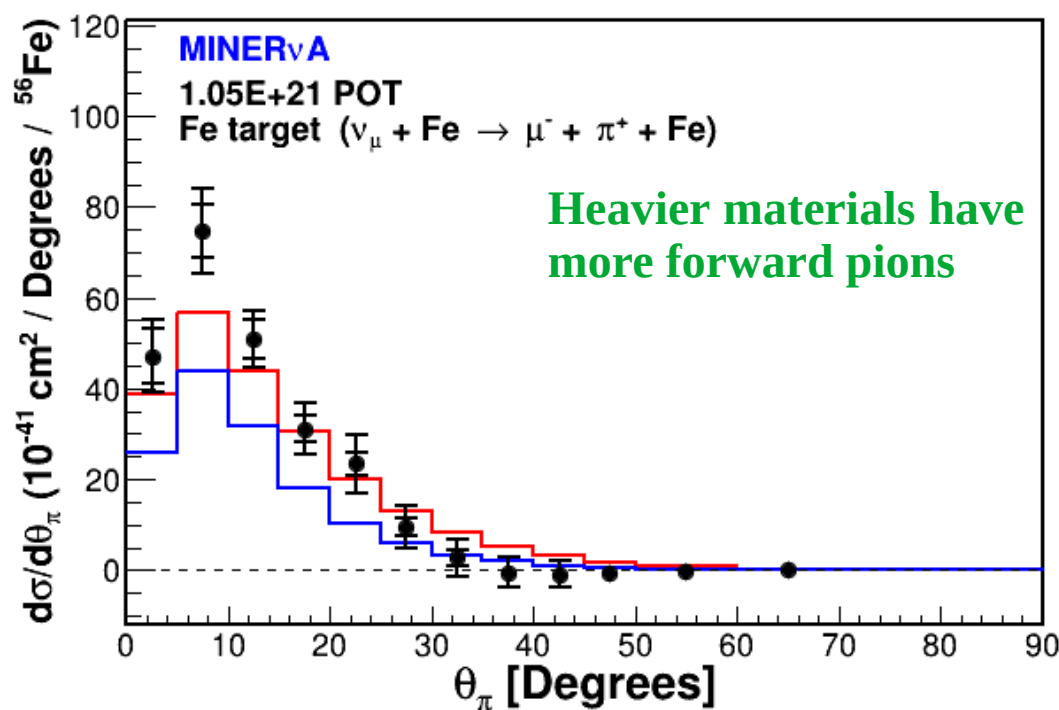
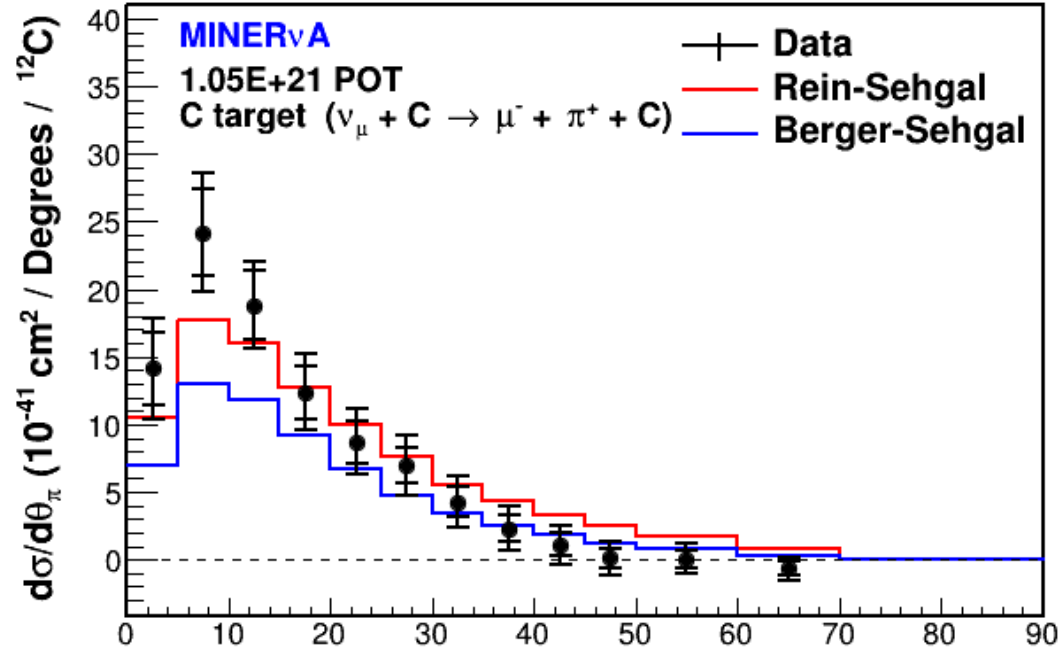
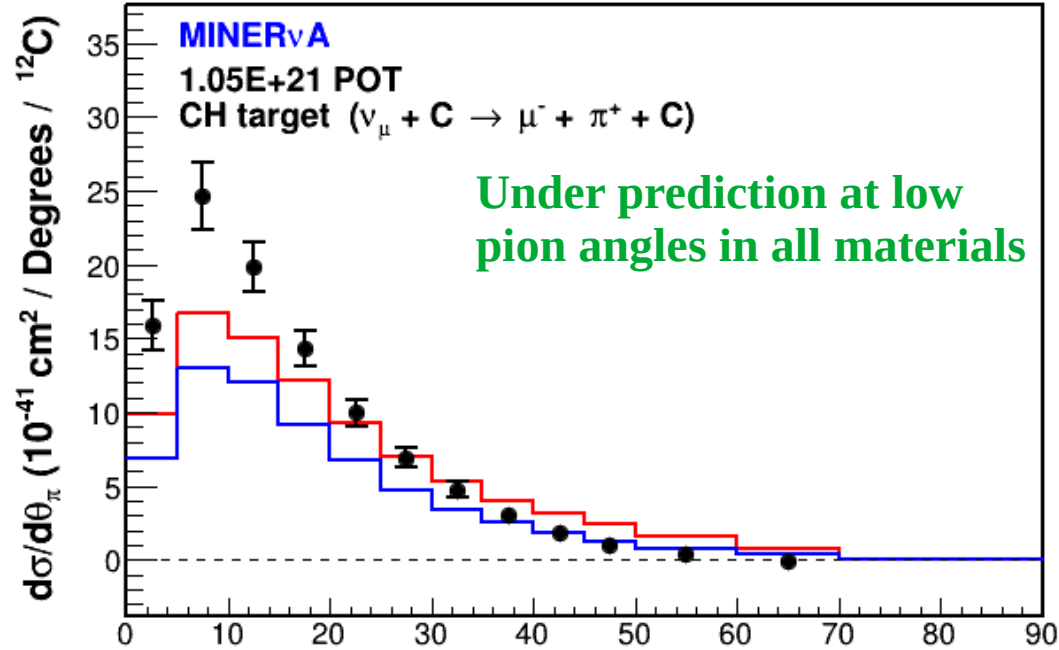
Results: Cross Sections

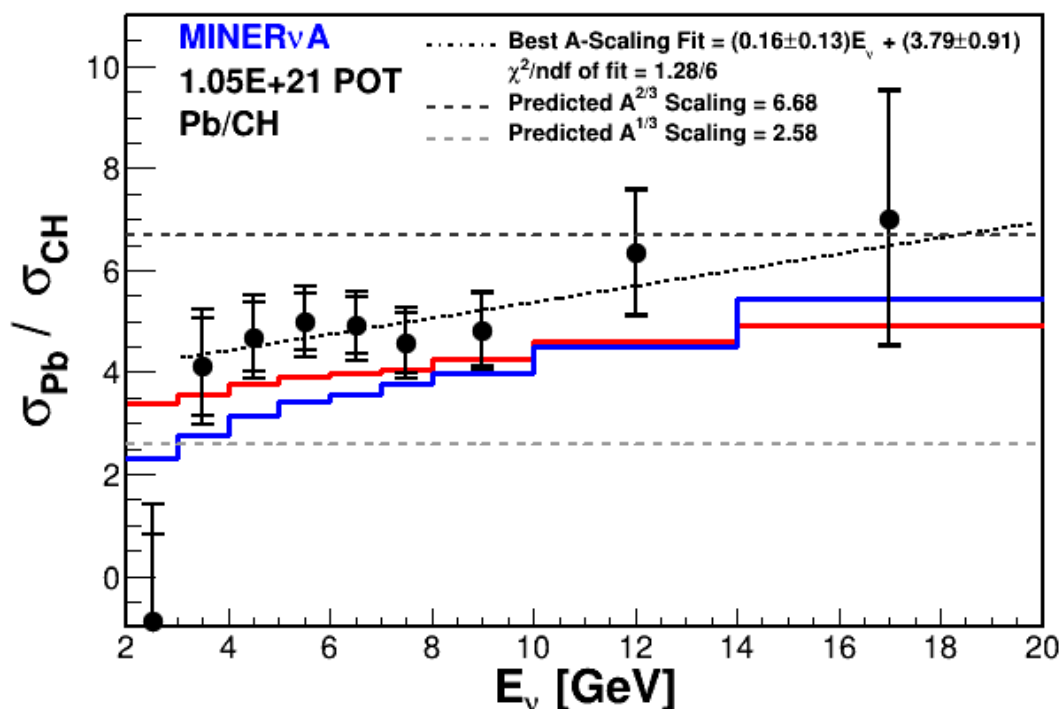
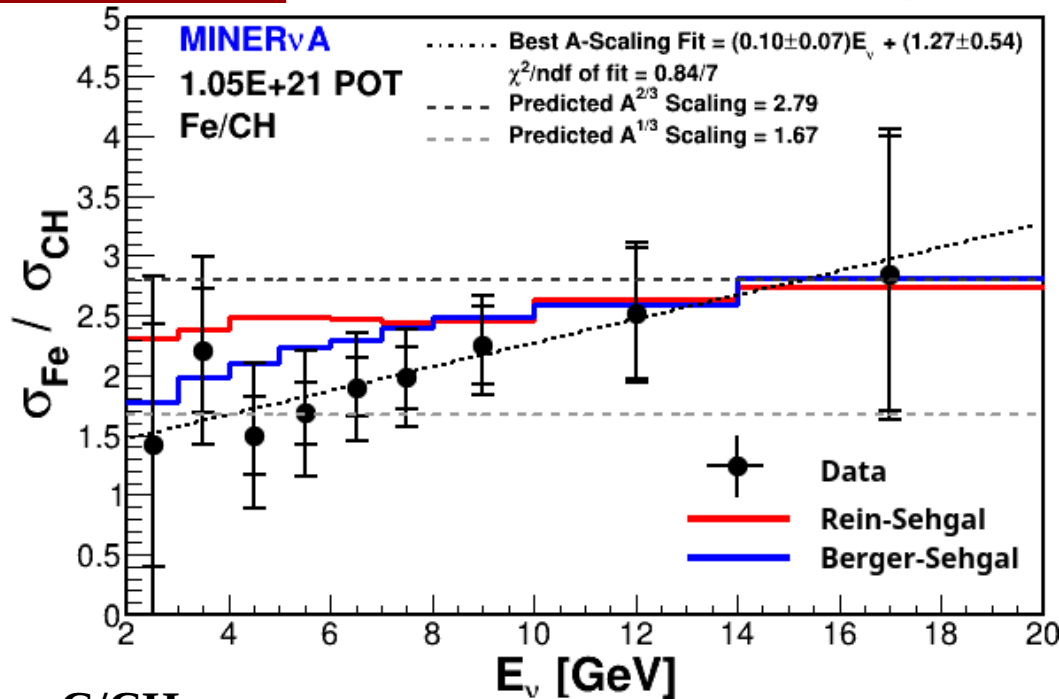
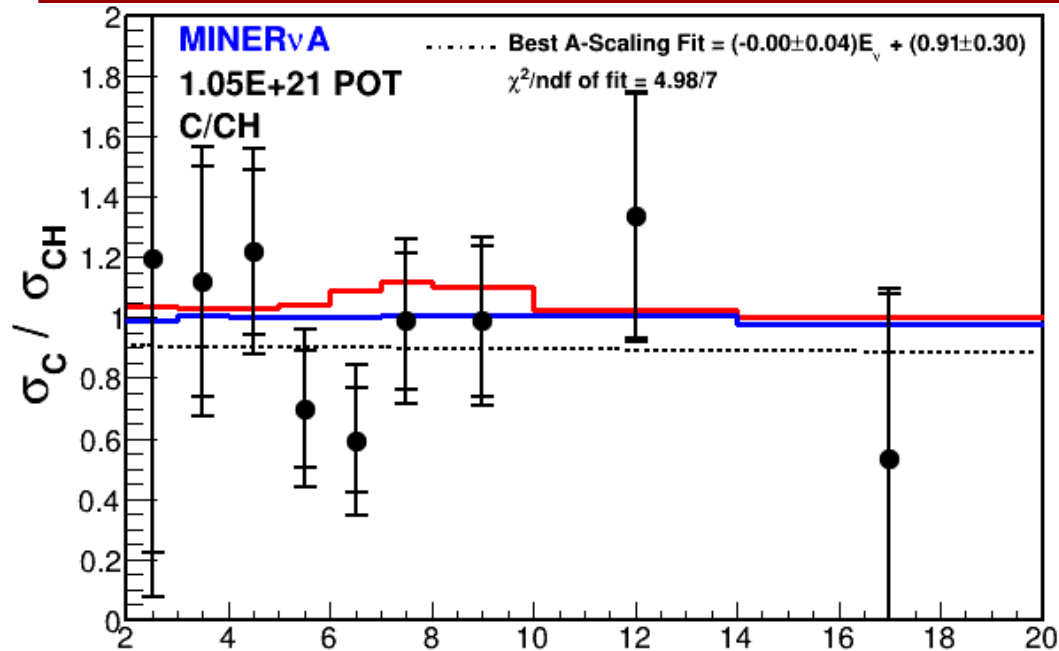
$$\frac{d\sigma}{dQ^2}$$



Results: Cross Sections

$$\frac{d\sigma}{d\theta_\pi}$$





C/CH

- consistent with unity.

A-Scaling linear fit

Fe/CH

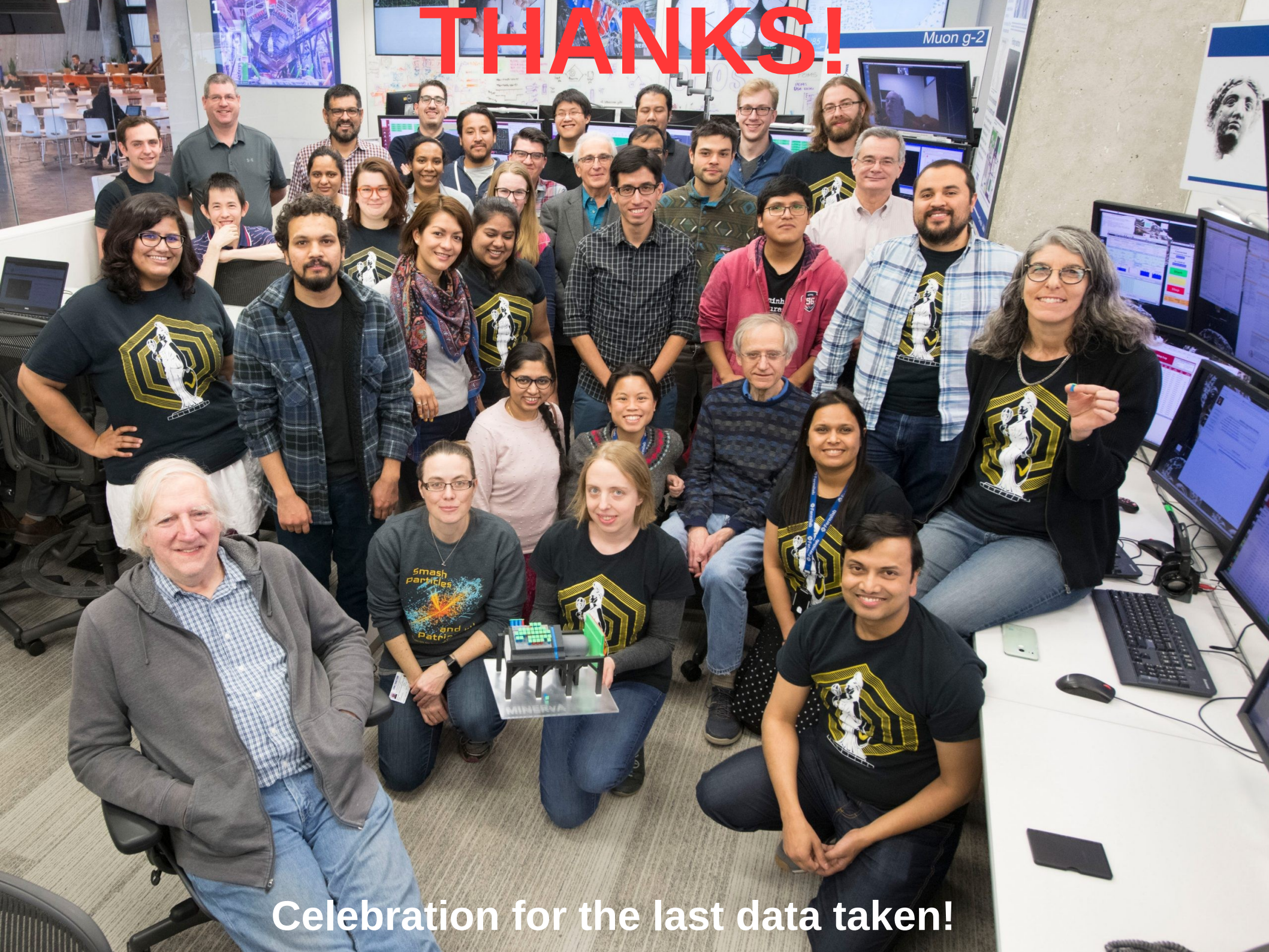
- Neither model does a good description.
- Closer to $A^{1/3}$ scaling for $E_\nu < 8$ GeV.
- Closer to $A^{2/3}$ scaling for $E_\nu > 10$ GeV.

Pb/CH

- Neither model does a good description.
- Closer to $A^{2/3}$ scaling for $E_\nu > 10$ GeV.
- Low E_ν A-scaling in between predictions.

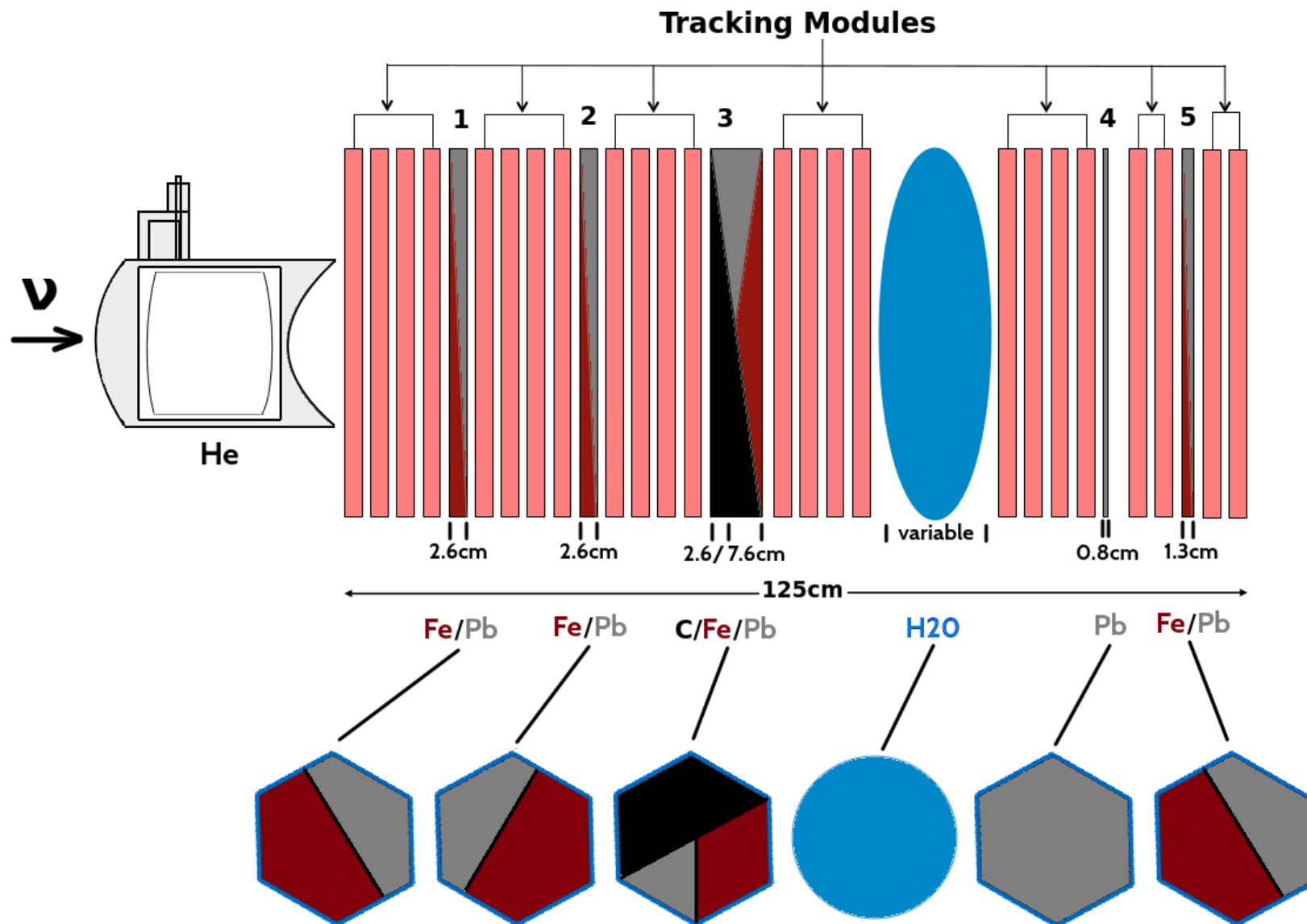
- 1) **MINERvA** has performed the **first simultaneous measurement** in (four) different materials, of the **neutrino-induced coherent production of π^+** .
- 2) **First evidence** of the interaction in iron and lead nuclei (**^{56}Fe** and **^{207}Pb**).
Lead being the **largest nucleus probed** so far.
- 3) **First measurement** in a **pure carbon** target.
- 4) **World's largest ^{12}C , ^{56}Fe and ^{82}Pb samples: ~ 15 k, ~ 0.7 k and ~ 0.5 k events and most precise measurement** (using the CH target).
- 5) **First cross section ratios** of the interaction: $\sigma_{\text{C}}/\sigma_{\text{CH}}$, $\sigma_{\text{Fe}}/\sigma_{\text{CH}}$ and $\sigma_{\text{Pb}}/\sigma_{\text{CH}}$.
- 6) **Apparent energy-dependence** of the **A-Scaling** of the $\sigma(E_\nu)$ cross section with an apparent **E_π -dependence** origin.

THANKS!

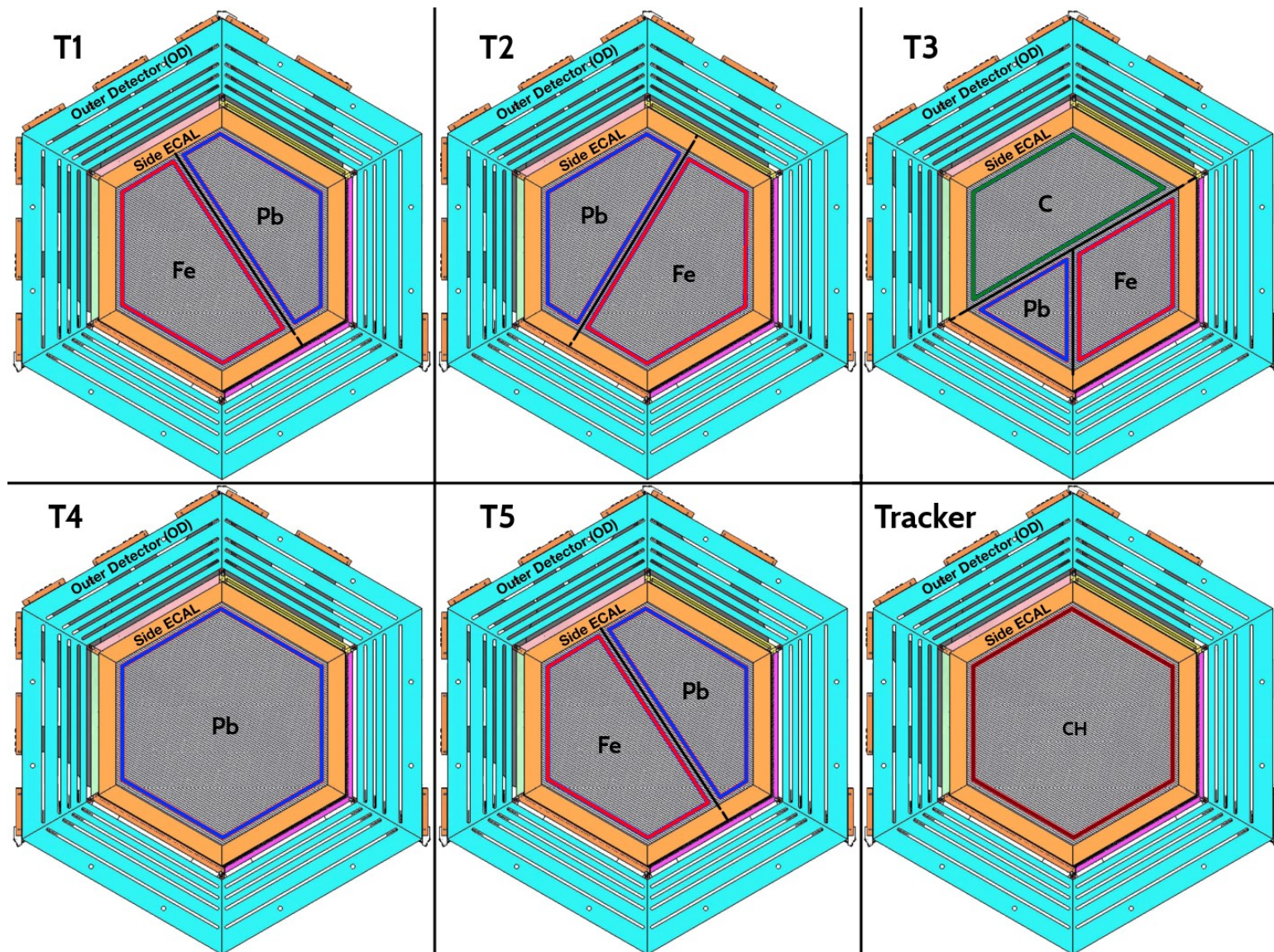


Celebration for the last data taken!

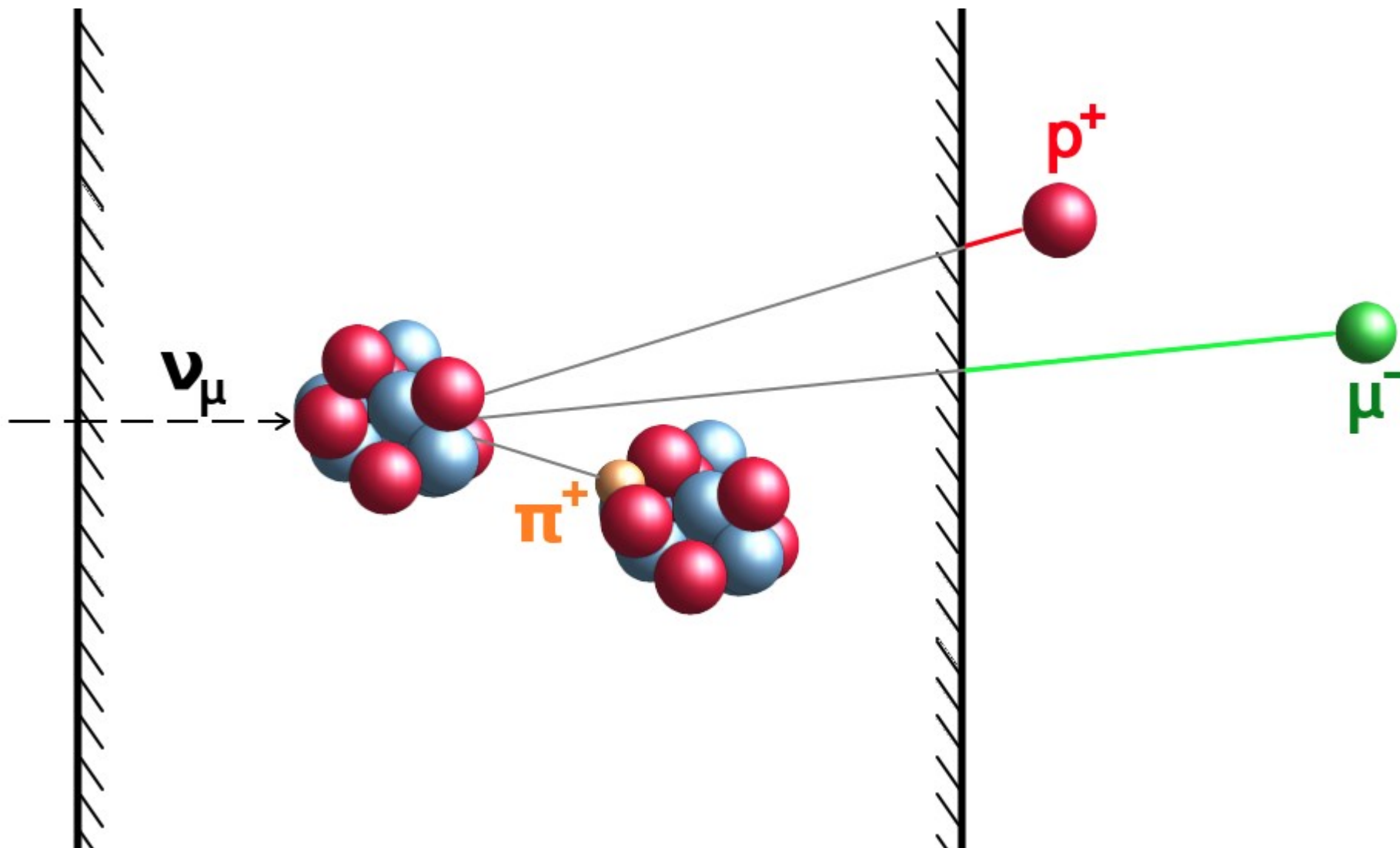
Side View of the Passive Target Region



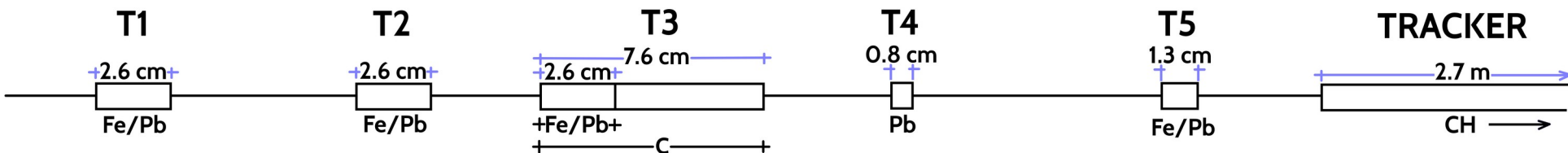
Target Segments (Beam goes out of the page)



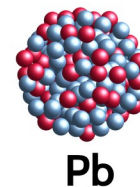
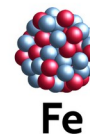
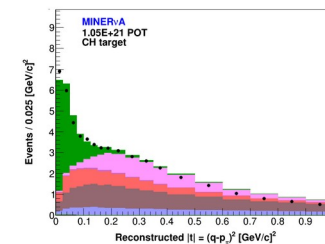
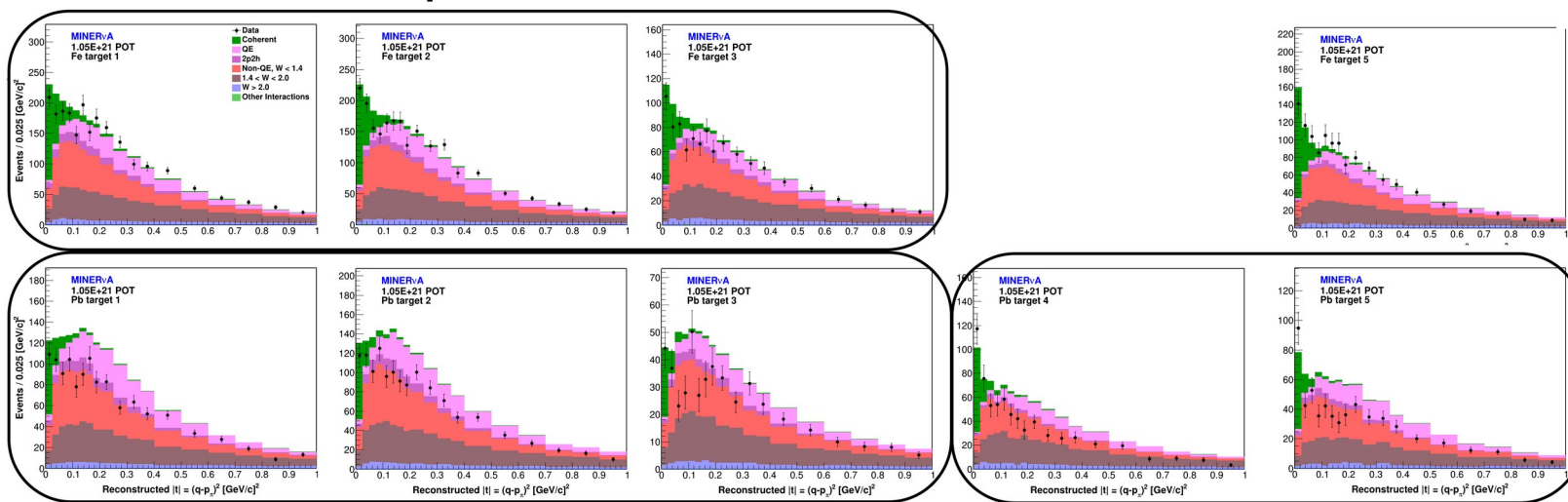
Effect of Target Thickness – C and CH |t| Shapes Are Different



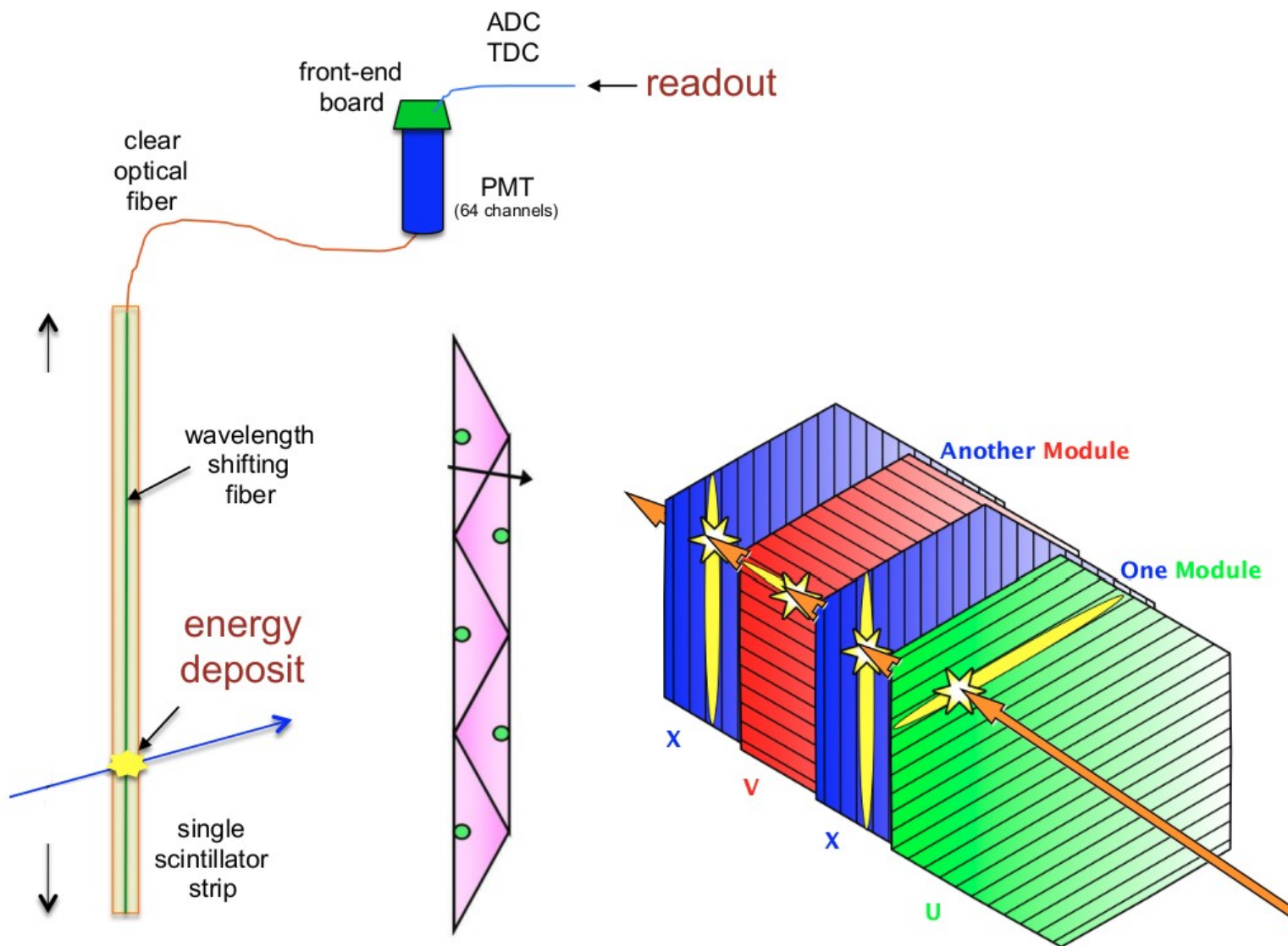
Effect of Target Thickness - $|t|$ Shapes Depend on Thickness



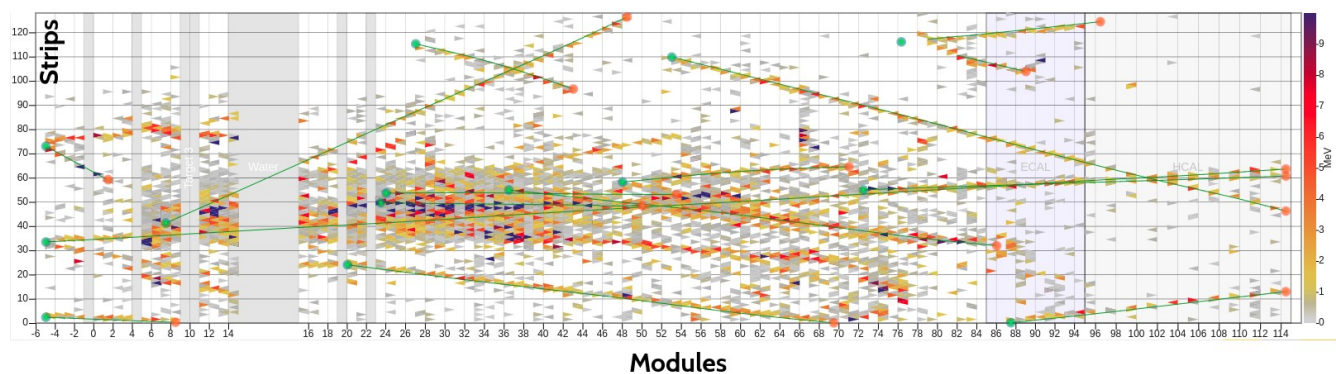
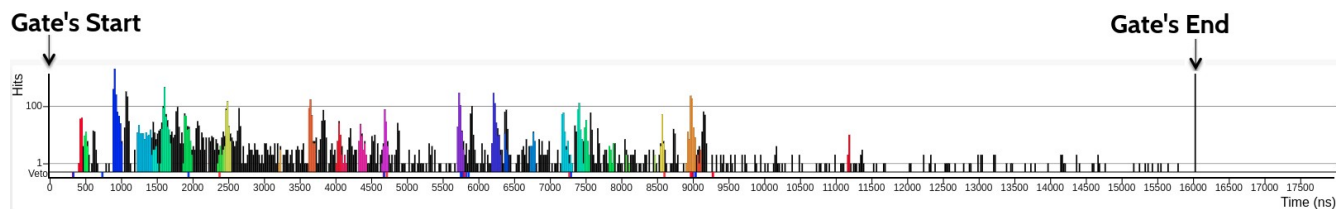
Boxes of Similar Shapes



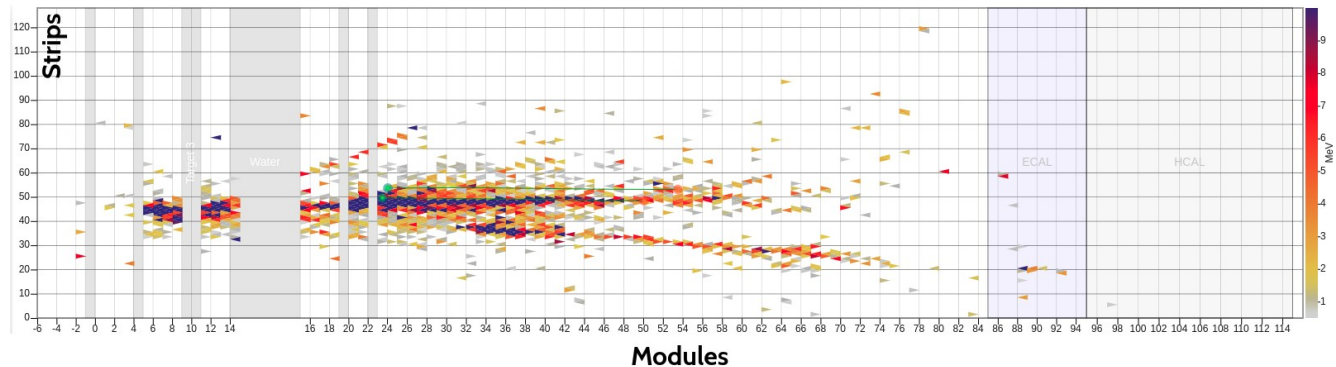
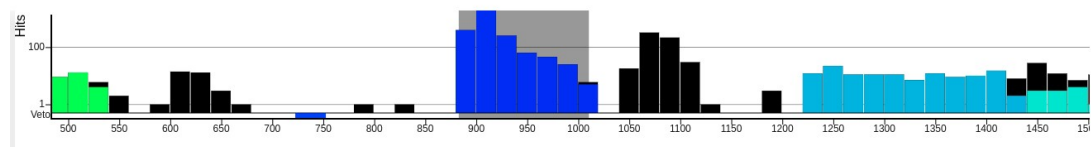
Data Acquisition



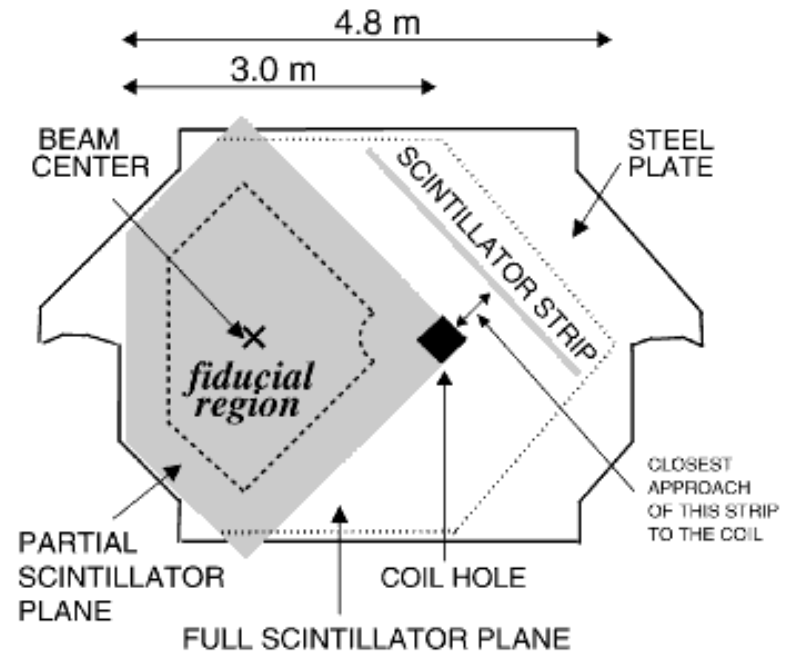
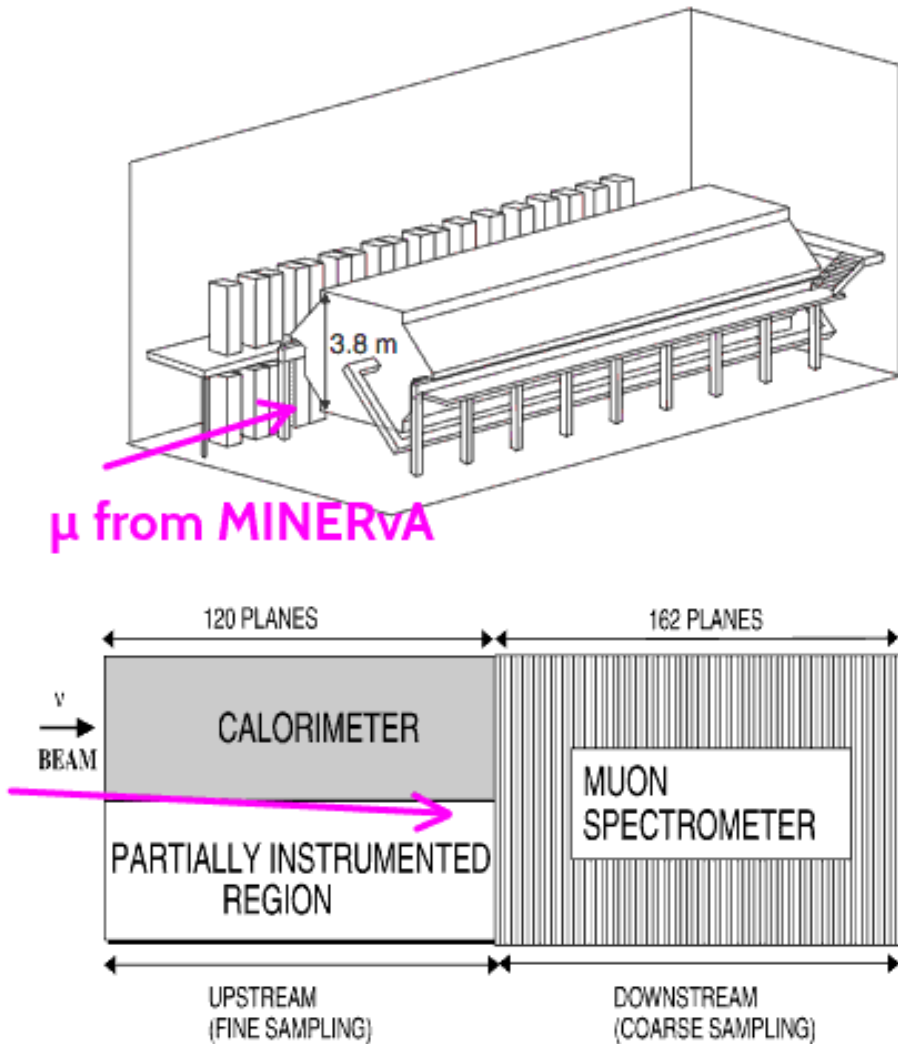
Data Acquisition



Zoom 500-1500 ns

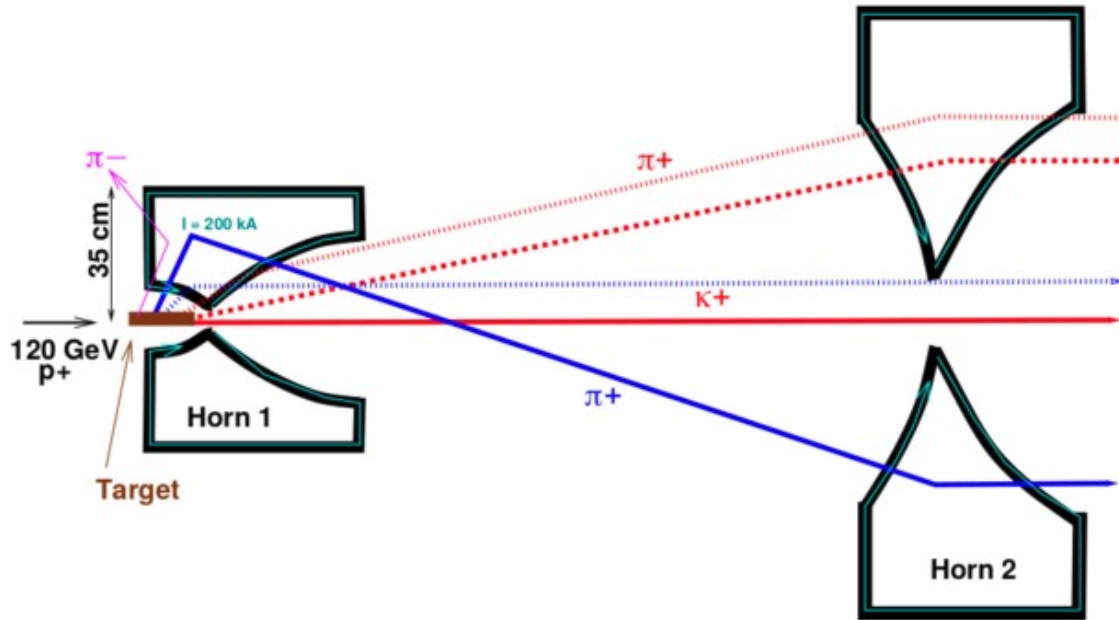


The MINOS Detector

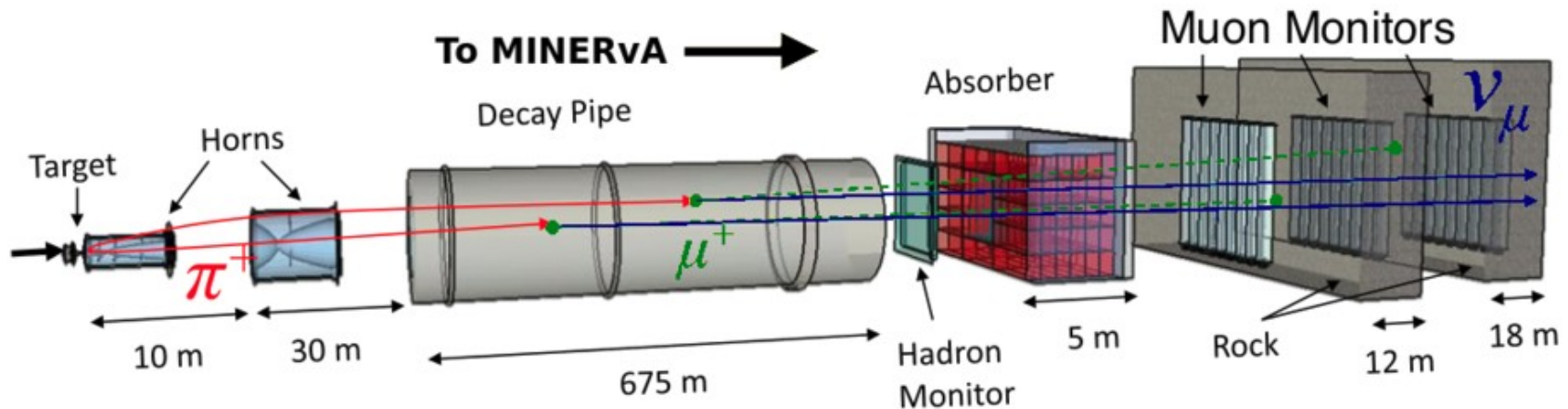


The NuMI Beam at FNAL

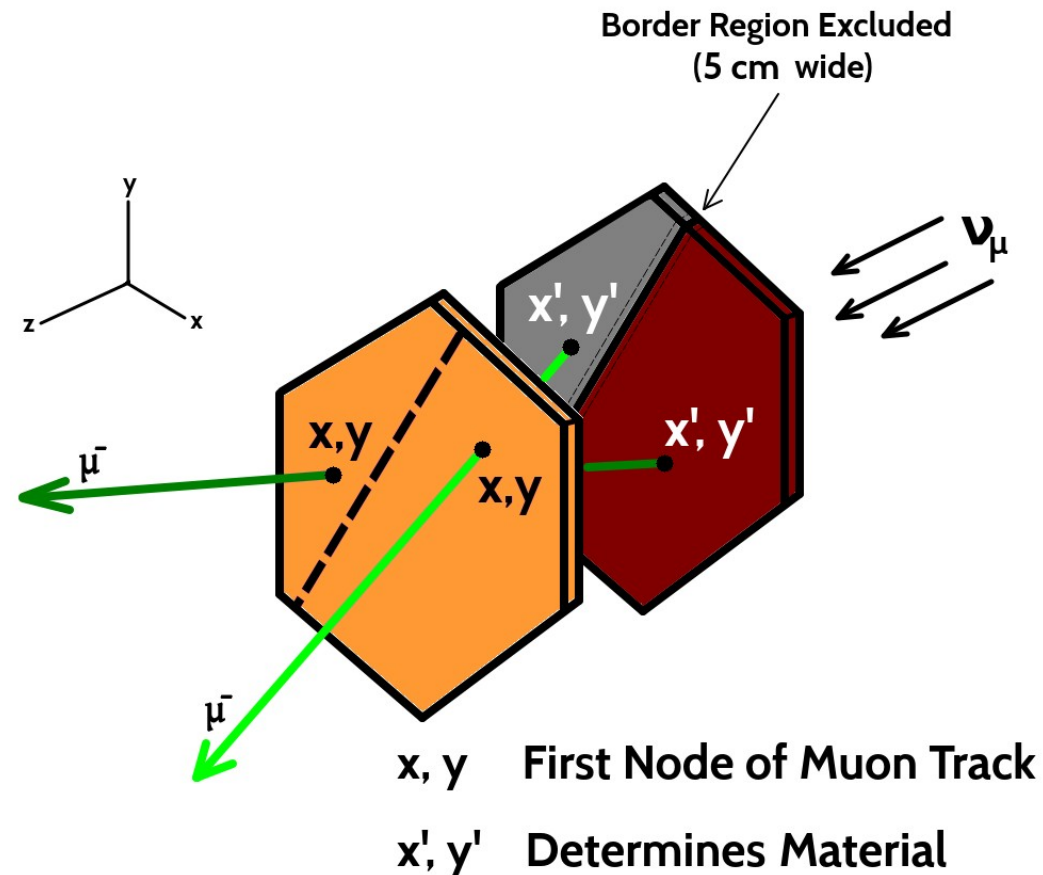
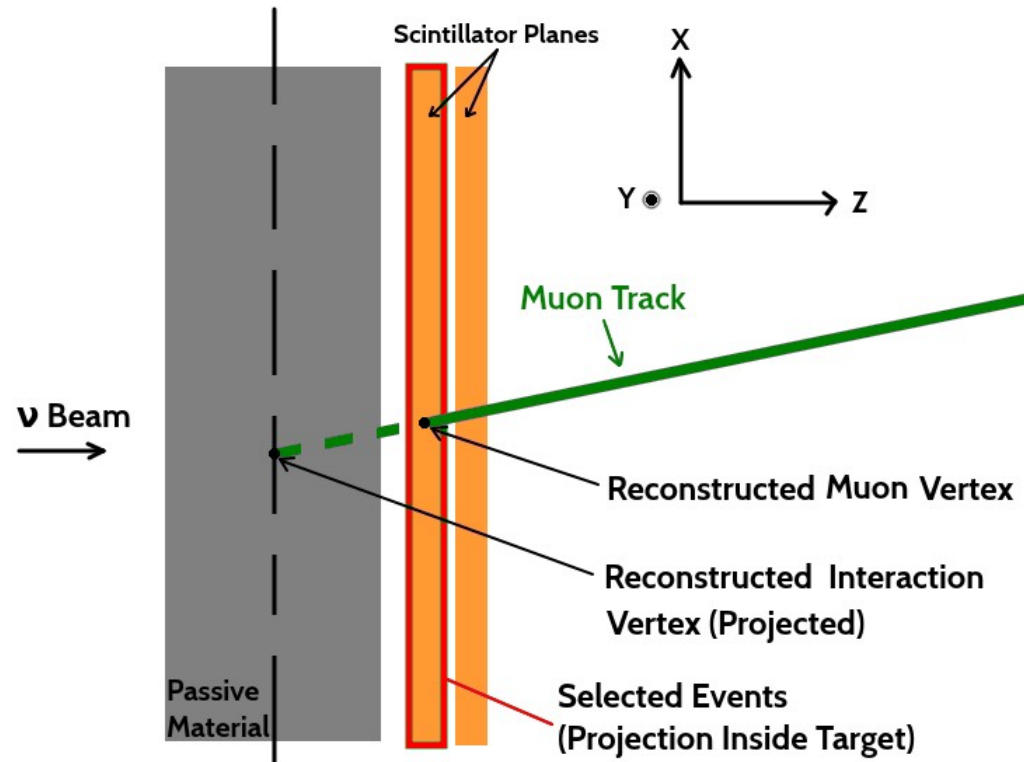
Horns



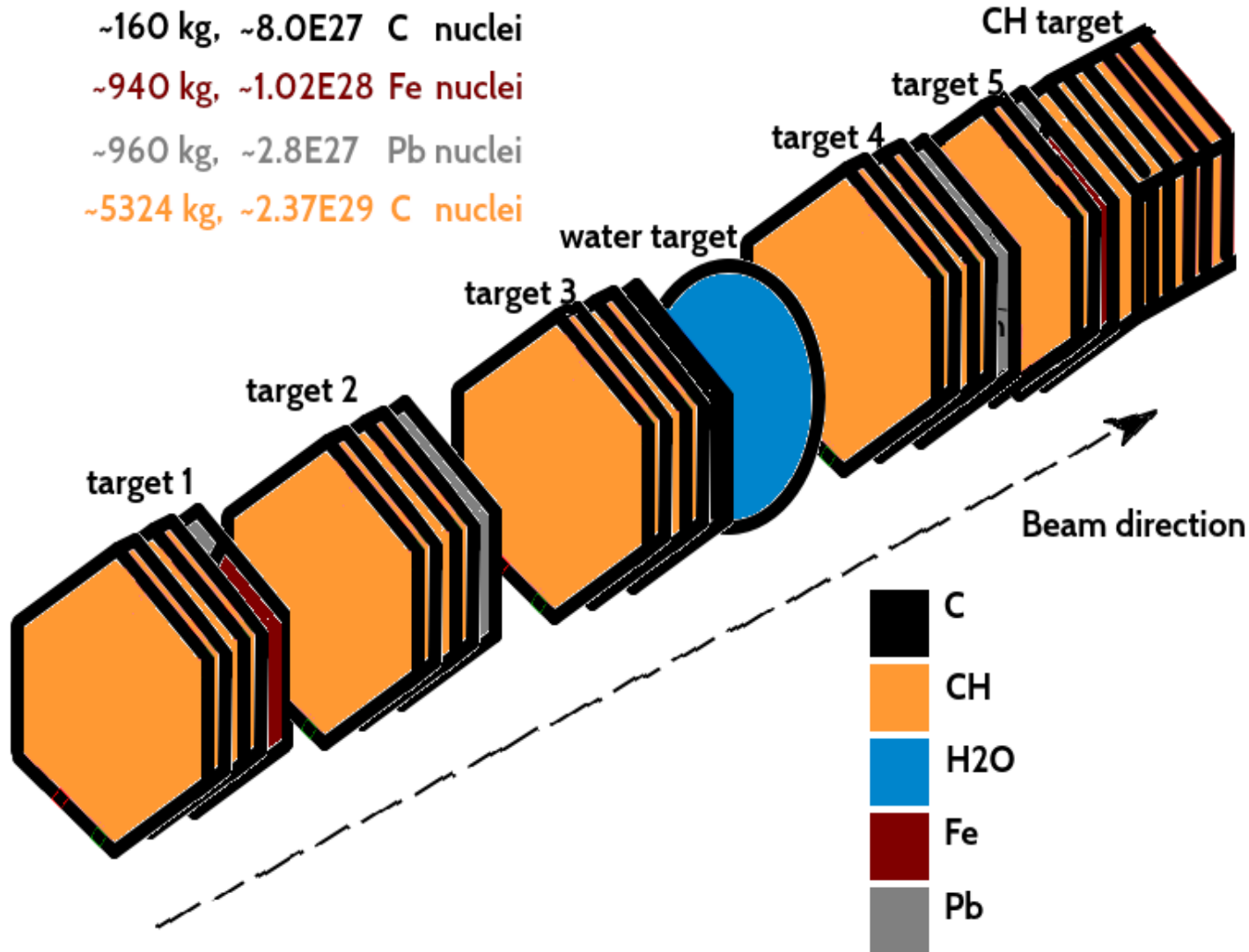
Beamline



Event Selection – Determining the Material

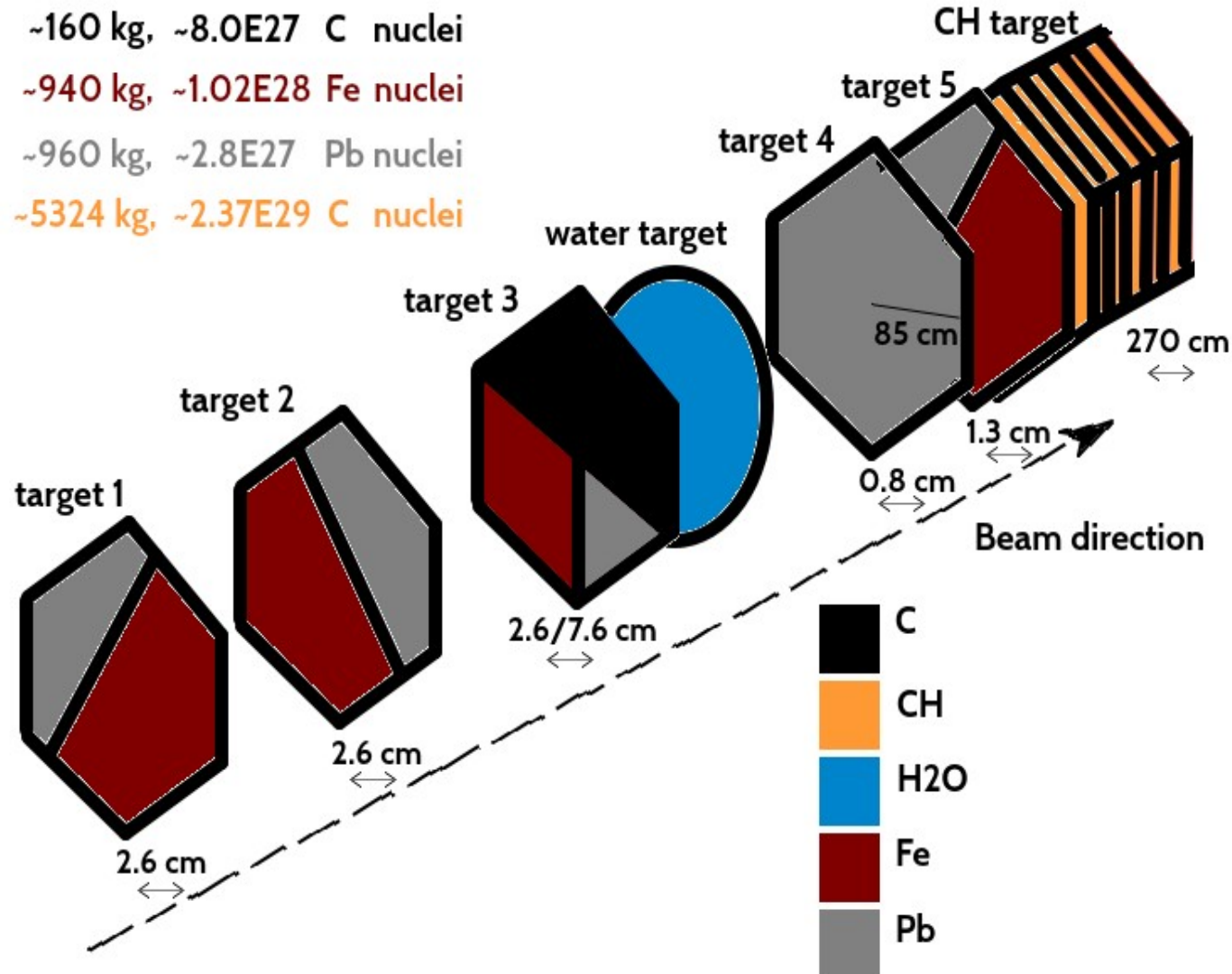


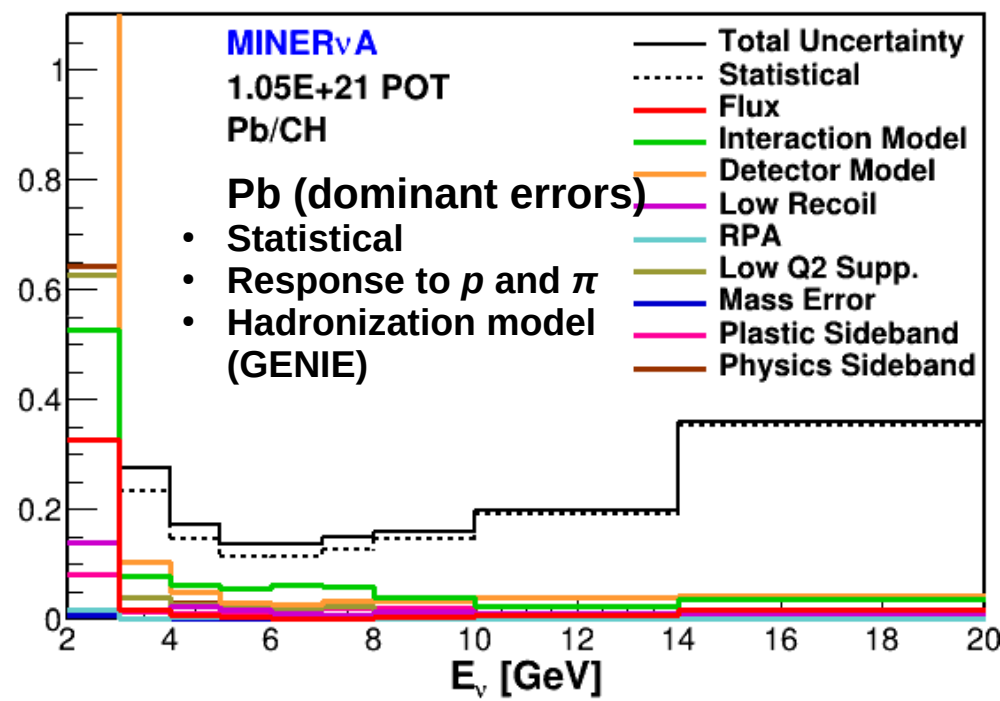
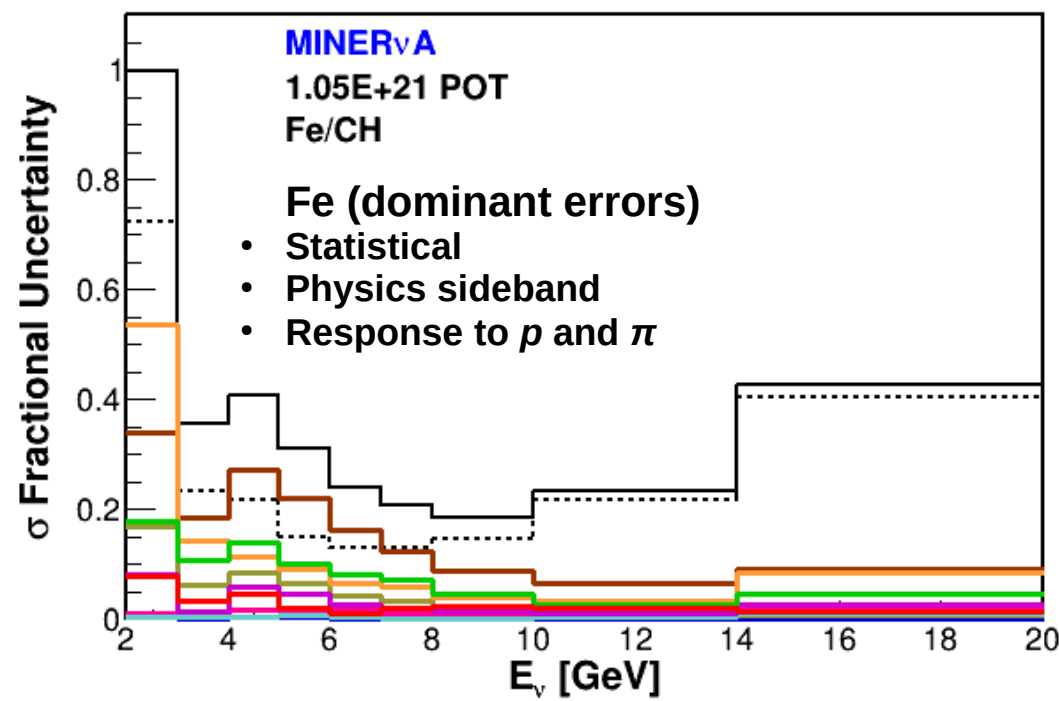
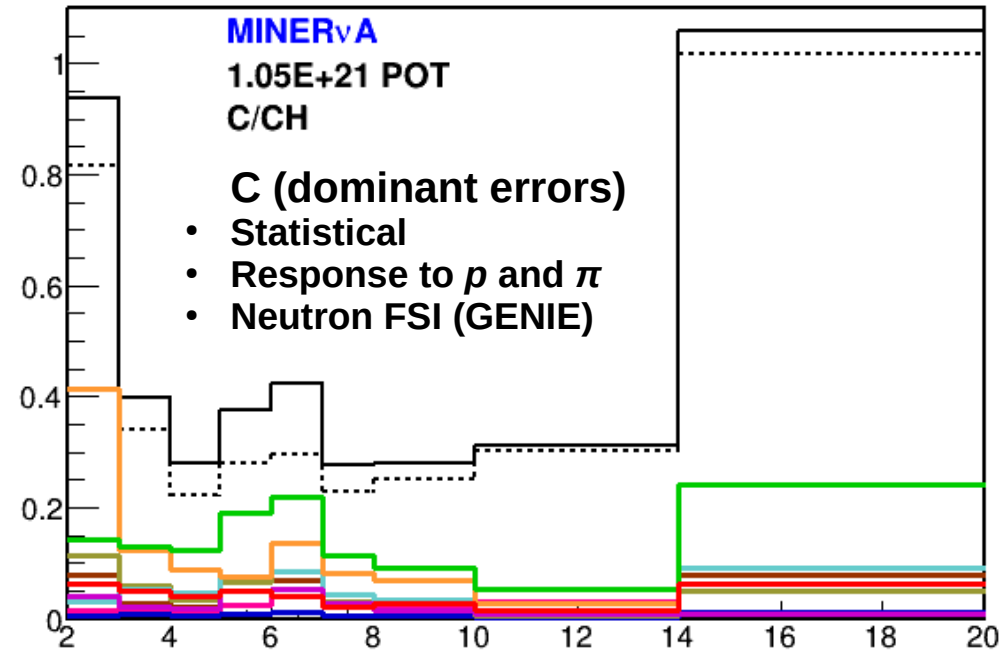
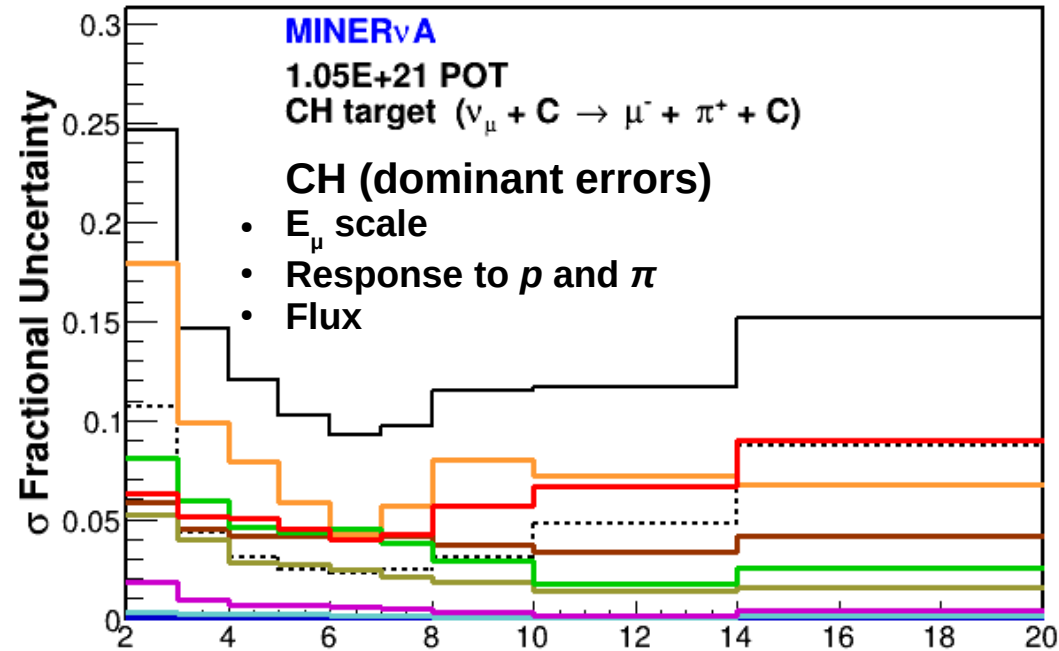
Passive Target Region



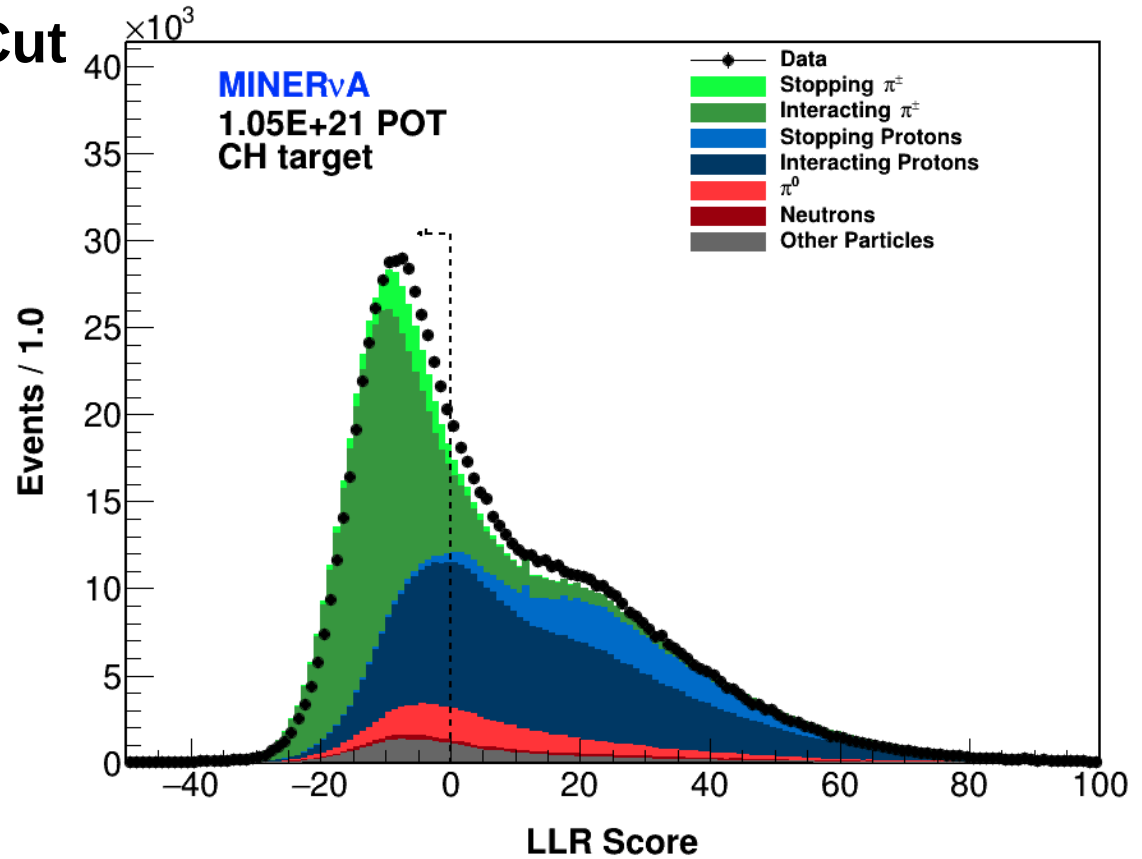
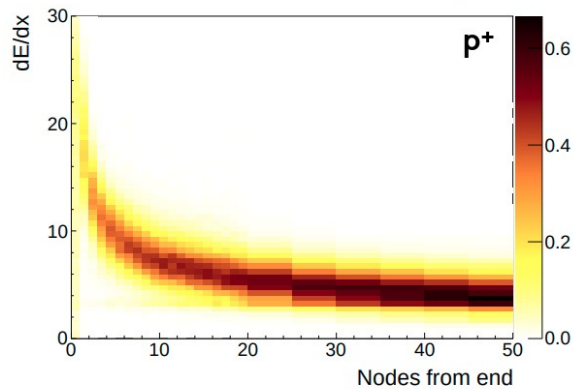
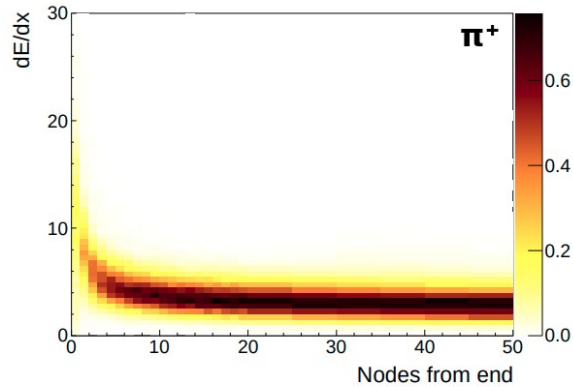
Passive Target Region – Enabled Due to High Statistics!

- ~160 kg, ~8.0E27 C nuclei
- ~940 kg, ~1.02E28 Fe nuclei
- ~960 kg, ~2.8E27 Pb nuclei
- ~5324 kg, ~2.37E29 C nuclei

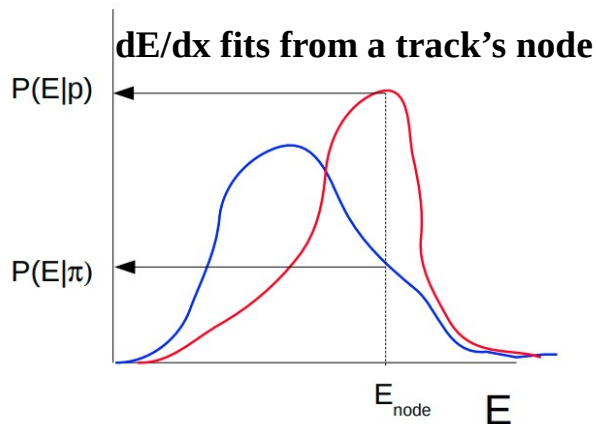




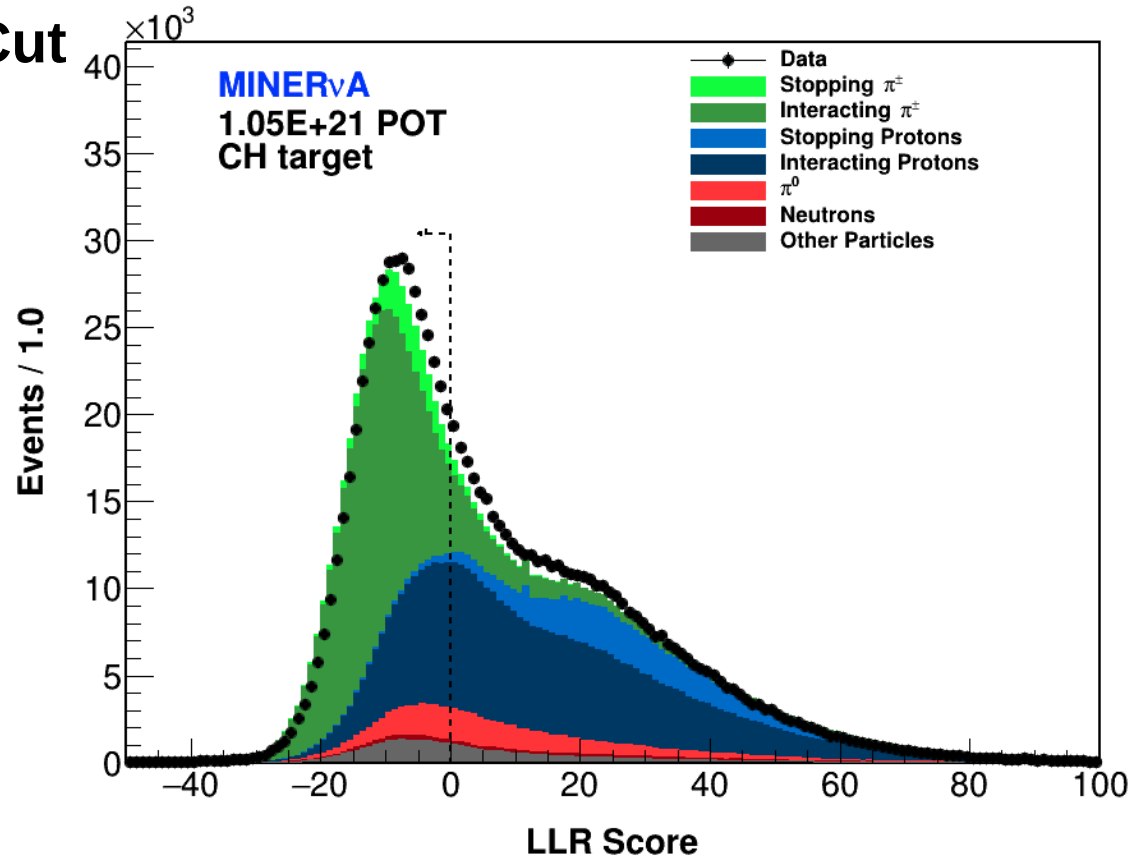
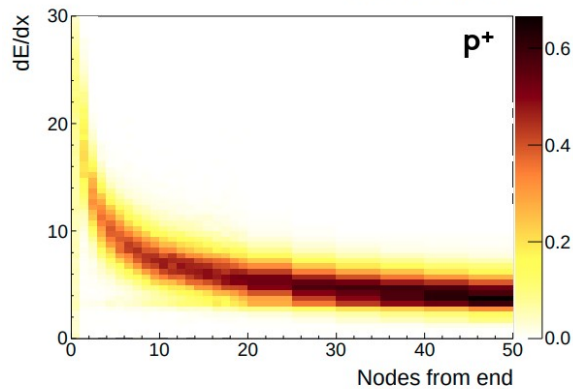
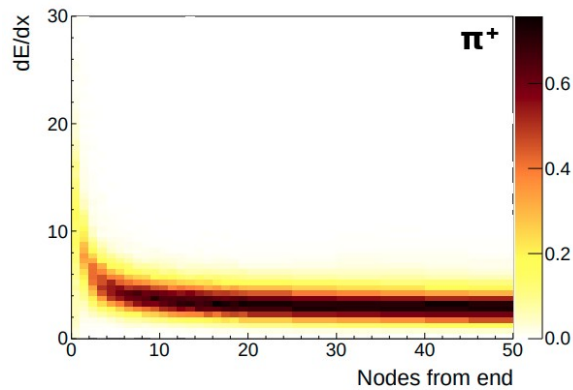
Event Selection – dE/dx Cut



- Log Likelihood Ratio between proton and pion hypotheses.
- Contained track consistent with charged pion.
- Cut keeps ~70% of pions.
- And removes ~87% protons.



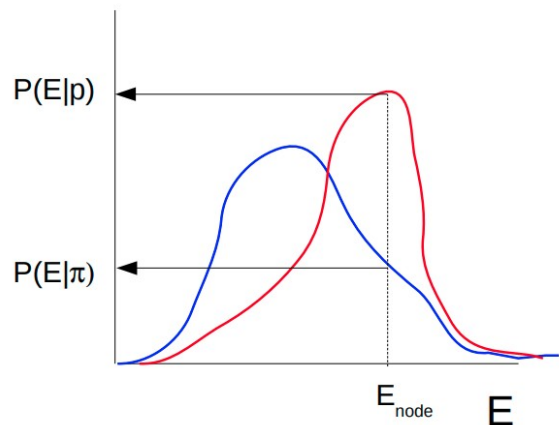
Event Selection – dE/dx Cut



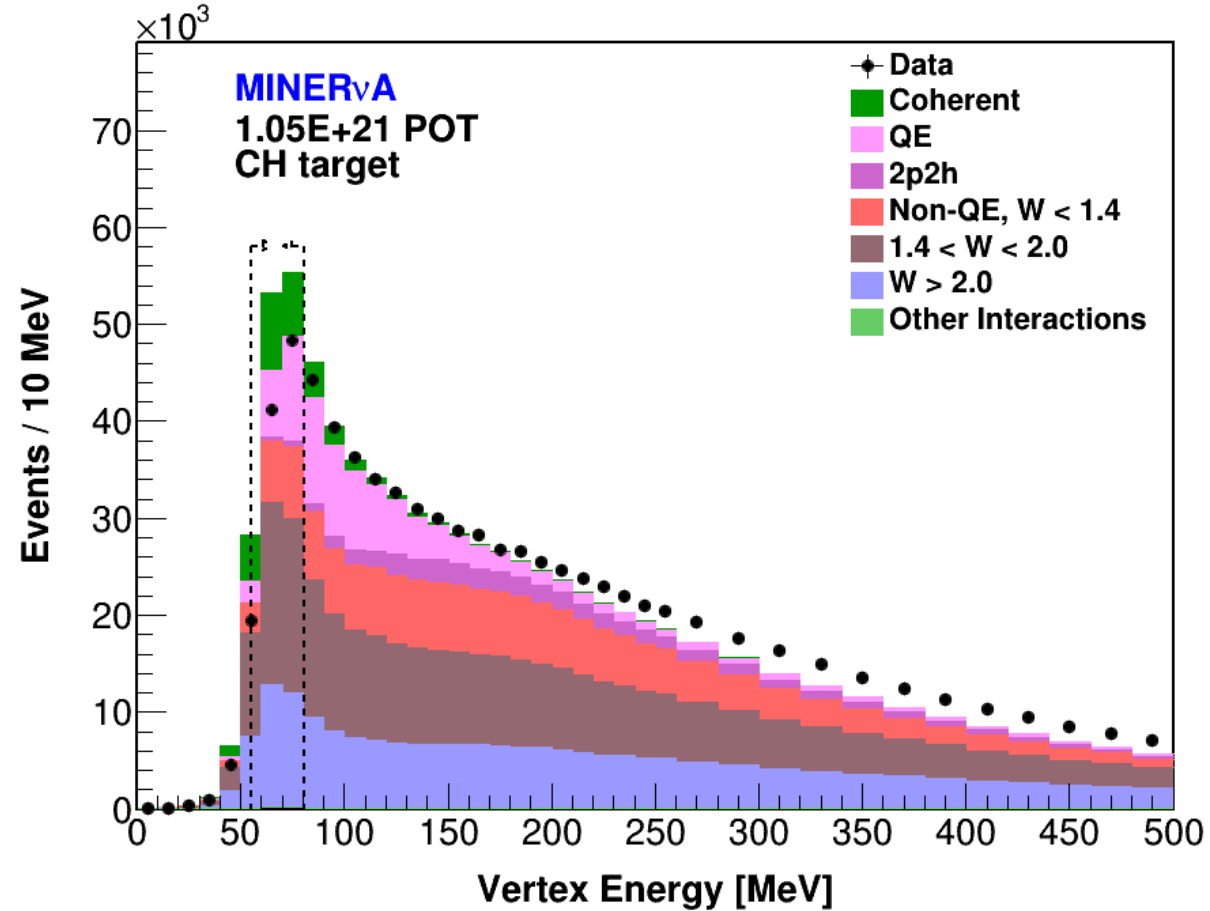
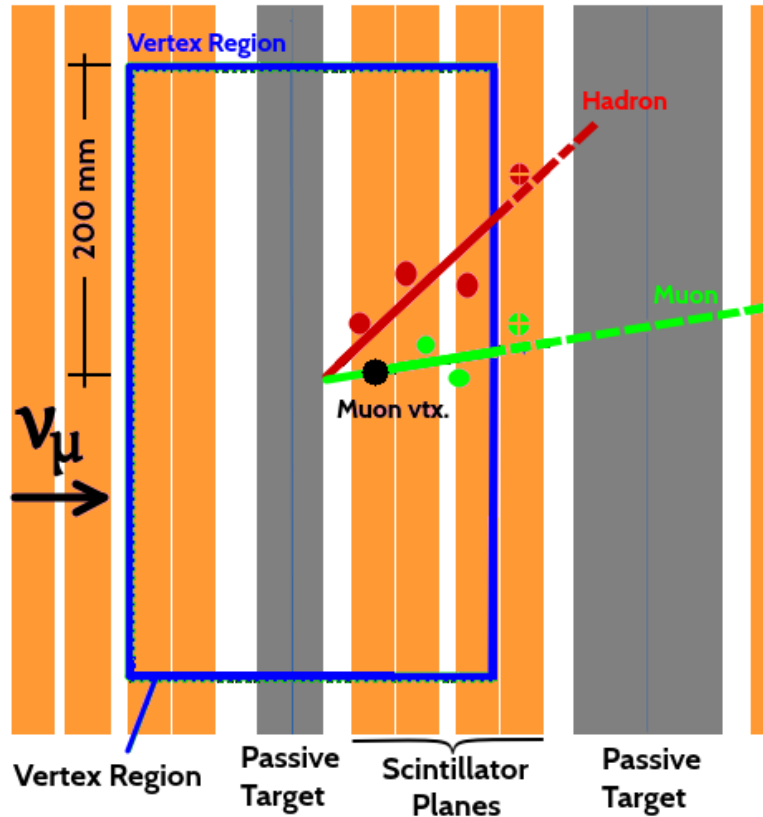
$$\mathcal{L}_{\pi^+, p} = \prod_{nodes} P(E_{node} | \pi^+, p) \quad \leftarrow \text{pion/proton hypotheses}$$

$$LR = \mathcal{L}_p / \mathcal{L}_{\pi^+} \quad \leftarrow \text{Likelihood ratio}$$

$$LLR = \sum_{nodes} [\log P(E_{node} | p) - \log P(E_{node} | \pi^+)]$$



Event Selection – Energy of Vertex Region



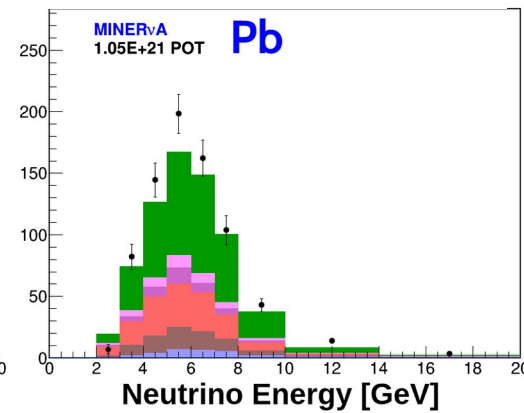
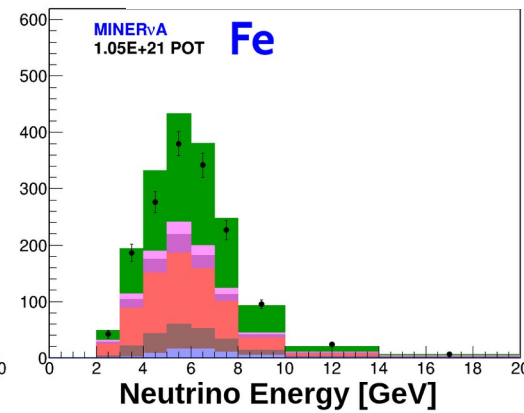
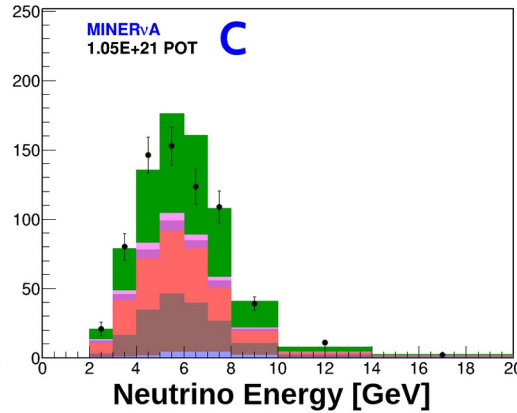
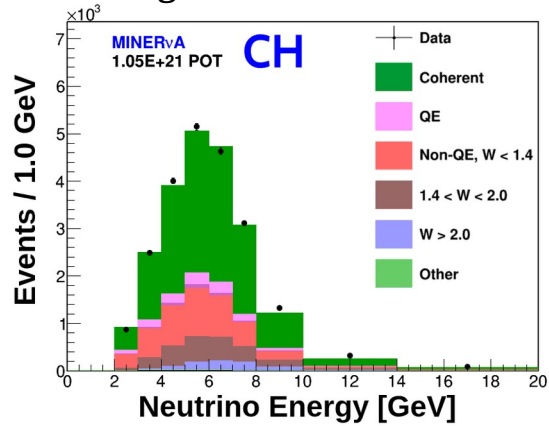
- Vertex energy consistent with 2 MIP ($\mu^- + \pi^+$).
- Cut keeps $\sim 60\%$ of signal.
- And removes $\sim 86\%$ background.

Cross Section Extraction Selected Sample

$$\sigma_i = \frac{\sum_j U_{ij} (N_j^{DATA} - N_j^{BKGD})}{\epsilon_i \phi_i T}$$

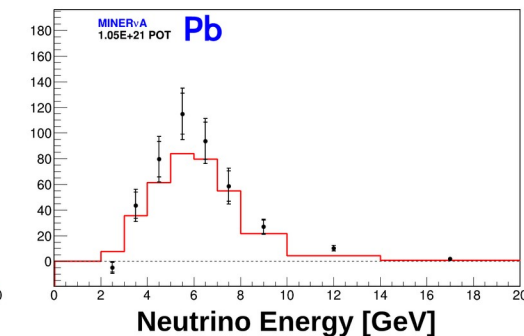
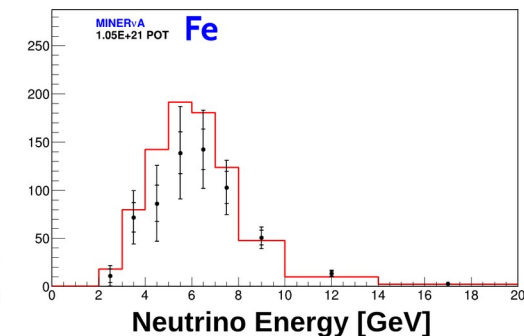
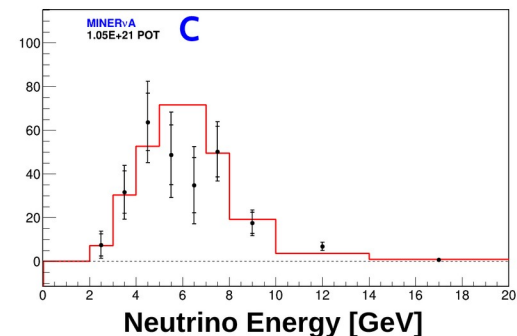
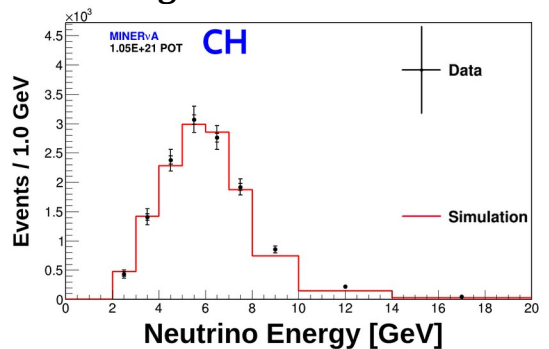
Total Cross Section $\rightarrow \sigma_i$
 Unfolding Matrix $\rightarrow U_{ij}$
 Number of Selected Data Events $\rightarrow N_j^{DATA}$
 Number of Predicted Background Events $\rightarrow N_j^{BKGD}$
 Reco Bin $\rightarrow j$
 True Bin $\rightarrow i$
 Efficiency $\rightarrow \epsilon_i$
 Flux Per Bin $\rightarrow \phi_i$
 Number of Nuclei $\rightarrow T$

Background Tuned



| Material | <i>CH</i> | <i>C</i> | <i>Fe</i> | <i>Pb</i> |
|------------------|-----------|----------|-----------|-----------|
| Candidate Events | 14855 | 303 | 726 | 492 |

Background Subtracted



Cross Section Extraction

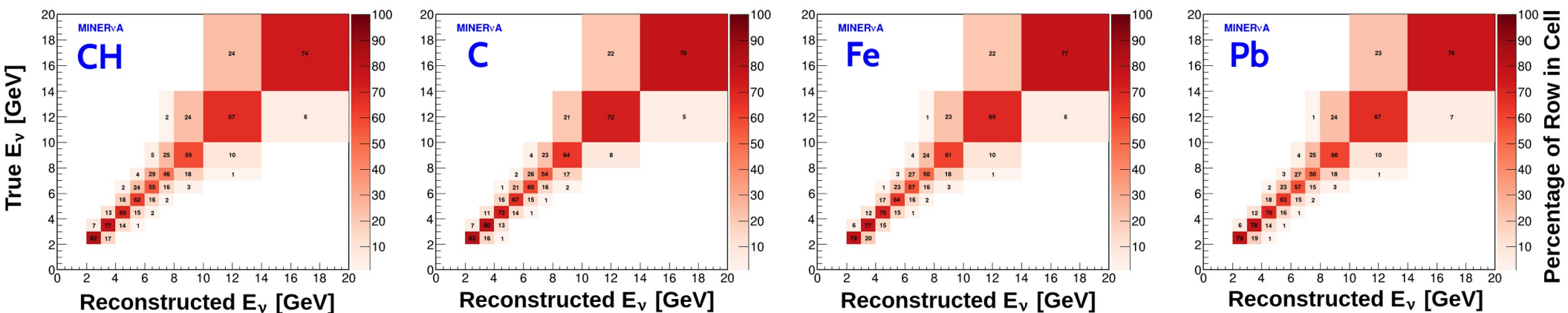
Unfolding

- Iterative Approach
- D'Agostini Method

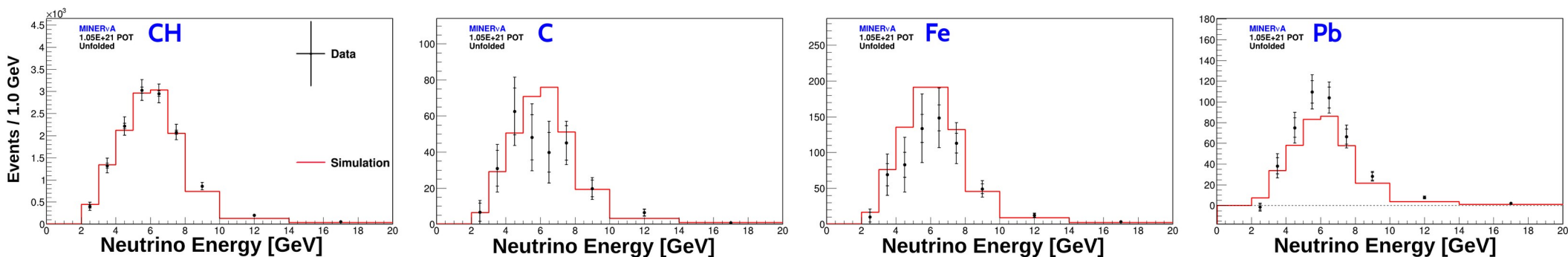
$$\sigma_i = \frac{\sum_j U_{ij} (N_j^{DATA} - N_j^{BKGD})}{\epsilon_i \phi_i T}$$

Total Cross Section $\rightarrow \sigma_i$
 True Bin $\rightarrow i$
 Reco Bin $\rightarrow j$
 Unfolding Matrix $\rightarrow U_{ij}$
 Number of Selected Data Events $\rightarrow N_j^{DATA}$
 Number of Predicted Background Events $\rightarrow N_j^{BKGD}$
 Efficiency $\rightarrow \epsilon_i$
 Flux Per Bin $\rightarrow \phi_i$
 Number of Nuclei $\rightarrow T$

Migration Matrices



Unfolded Distributions

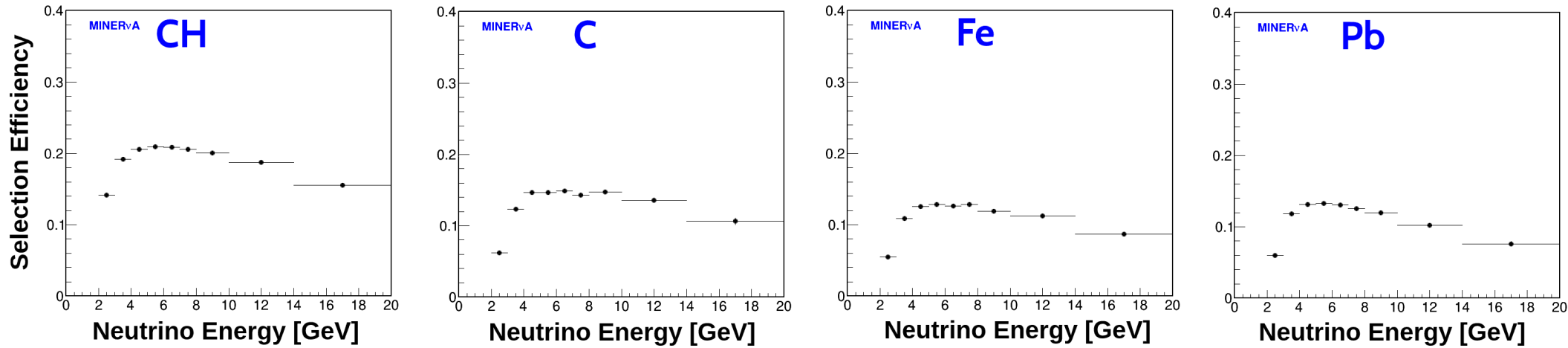


Cross Section Extraction Efficiency Correction

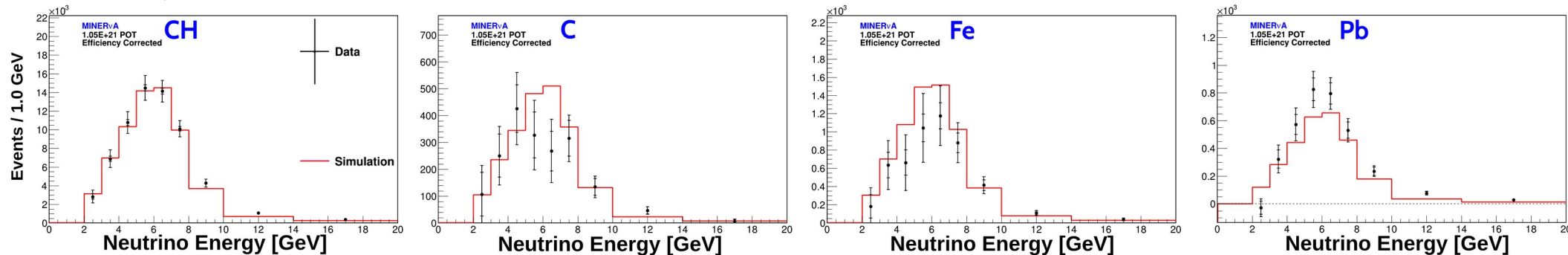
$$\sigma_i = \frac{\sum_j U_{ij} (N_j^{DATA} - N_j^{BKGD})}{\epsilon_i \phi_i T}$$

Total Cross Section (points to σ_i)
 Unfolding Matrix (points to U_{ij})
 Number of Selected Data Events (points to N_j^{DATA})
 Number of Predicted Background Events (points to N_j^{BKGD})
 Reco Bin (points to j)
 True Bin (points to i)
 Efficiency (points to ϵ_i)
 Flux Per Bin (points to ϕ_i)
 Number of Nuclei (points to T)

Selection Efficiency



Efficiency Corrected

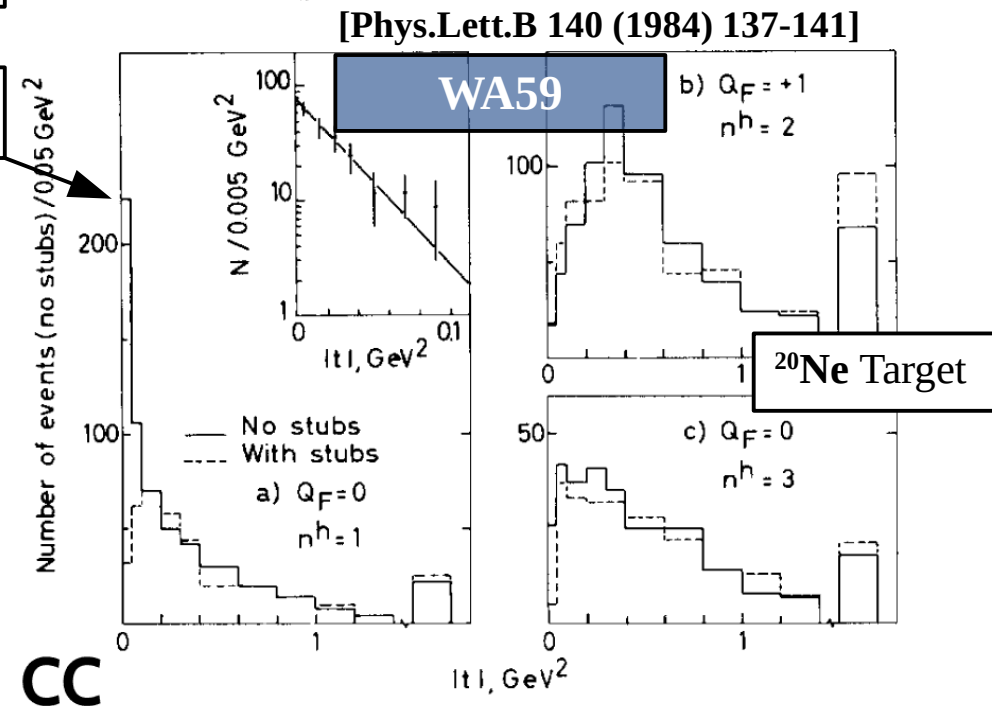
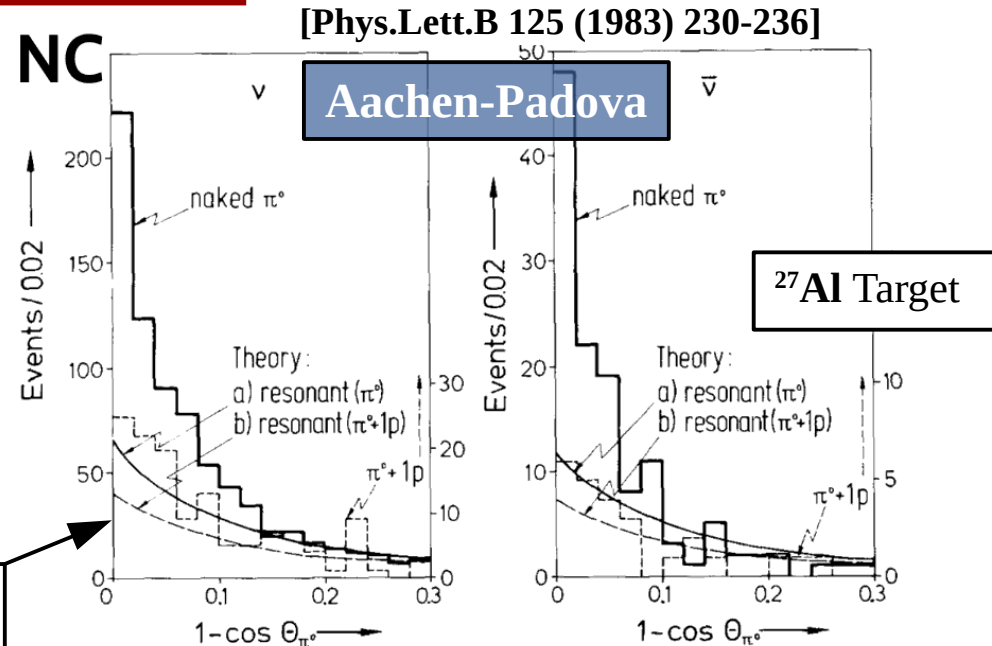


Purpose

- Meant to test **PCAC** hypothesis. Focused on understanding the nature of the weak currents.
- Mostly compared against the Rein-Sehgal and Belkov-Kopeliovich models

First NC Measurement

First CC Measurement

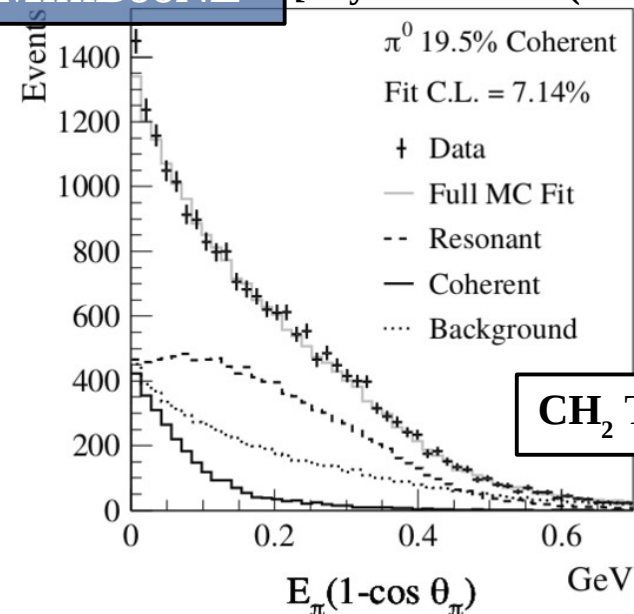


Purpose

- Characterize it as **background for ν -oscillations**.
- **NC channel** can **mimic** the signal of ν_e **appearance** if one the photons goes undetected.
- **CC channel** can **mimic** the signal of ν_μ **disappearance** if the π^+ is misidentified as a proton, or if the π^- is not detected.
- Proof of existence at $E_\nu < 2$ GeV (NC).
- Proof of existence at $E_\nu < 5$ GeV (CC).
- Most used model was also the one by Rein-Sehgal.

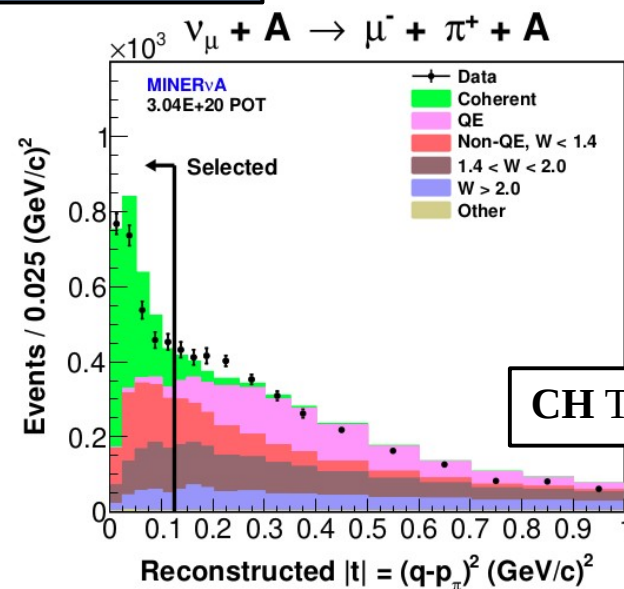
MiniBooNE

[Phys.Lett.B 664 (2008) 41-46]



MINERvA

[Phys.Rev.Lett. 113 (2014) 26]



$|t|$ in Terms of the Muon and Pion Kinematics

- Considering the nucleus at rest and the energy transferred to it negligible, the neutrino energy can be expressed like:

$$E_\nu \approx E_\mu + E_\pi$$

- With that assumption, it follows

$$|t| = \left| (p_\nu - p_l - p_\pi)^2 \right| \approx \left(\sum_{i=l,\pi} p_i^T \right)^2 + \left(\sum_{i=l,\pi} E_i - p_i^L \right)^2$$

- After deploying the algebra, is written like

$$\begin{aligned} |t| &\simeq \left| 2(E_\mu + E_\pi)(E_\mu - p_\mu \cos \theta_{\nu\mu}) - m_\mu^2 \right. \\ &\quad \left. - 2(E_\pi^2 - (E_\mu + E_\pi)p_\pi \cos \theta_{\nu\pi} + p_\mu p_\pi \cos \theta_{\mu\pi}) + m_\pi^2 \right| \end{aligned}$$

Diffractive Process

- Coherent inelastic pion production is also a diffractive process. This means that the momentum transfer to the target is “small”

$$\frac{d\sigma}{dt} \sim A(E_\pi) e^{-b|t|}$$

where b [GeV/c] $^{-2}$ \sim radius of the target:

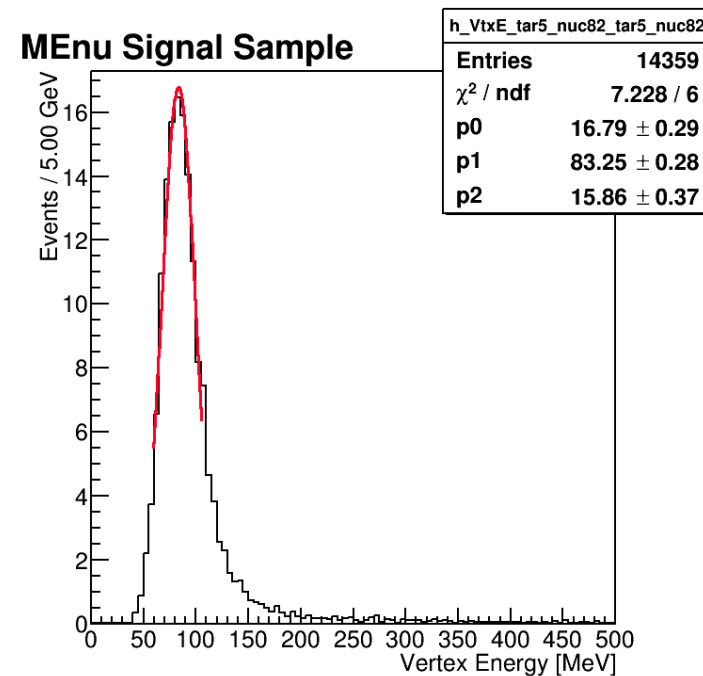
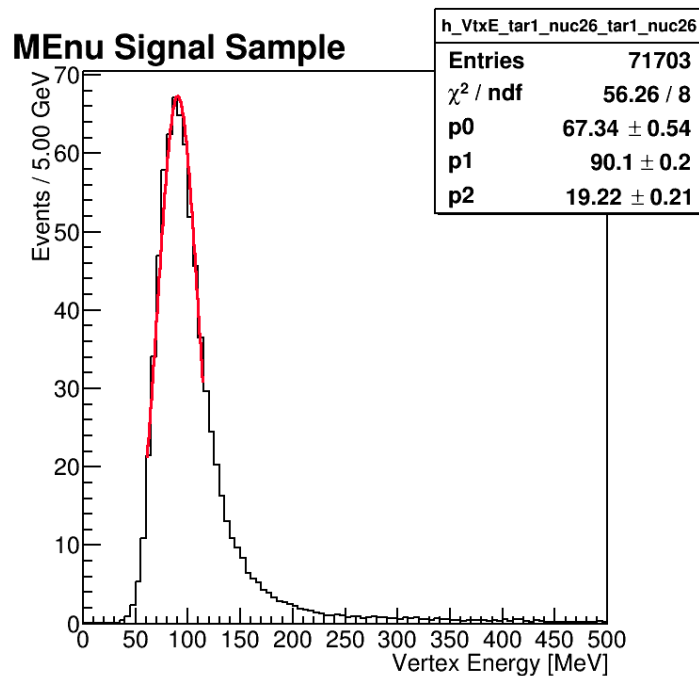
- $R_C \sim 2.77$ fm, $b \sim 40$ [GeV/c] $^{-2}$
- $R_{\text{Fe}} \sim 4.29$ fm, $b \sim 110$ [GeV/c] $^{-2}$
- $R_{\text{pb}} \sim 7.16$ fm, $b \sim 270$ [GeV/c] $^{-2}$

MINERvA's LE Analysis [Phys.Rev.D 97 (2018) 3, 032014]

- The cross section is $\nu + p \rightarrow \pi^+ + p$
- $|t|_{\text{diff}} = |(p_\nu - p_\mu - p_\pi)^2| = |(p_{p,f} - p_{p,i})^2| = 2m_p T_p$
- Because of the E_{vtx} cut, the protons kinetic energy T_p is restricted to small values and therefore small $|t|$.
- The slope b in the cross section is only $\sim 8 [\text{GeV}/c]^{-2}$ compared to that of $C \sim 40 [\text{GeV}/c]^{-2}$
$$\frac{d\sigma}{dt} \sim A(E_\pi) e^{-b|t|}$$
- The small acceptance and the slow falling $|t|$ -dependence of the cross section results in a small contribution to the coherent cross section.
- The LE MINERvA analysis showed that the measured diffractive cross section was consistent with zero!

E_{Vtx} Fit

- Example of T1 Fe and T5 Pb distributions of the vertex energy using signal events only.
- The $\mu \pm 1\sigma$ defines the E_{Vtx} cut.





Backgrounds From GENIE + Mnv Tune

In terms of invariant hadron mass $W = \sqrt{(M^2 + 2M\nu - Q^2)}$

M = nucleon mass, ν = energy transfer from the neutrino.

- **Quasielastic Scattering (QE)**
 - Random Phase Approximation (RPA) correction.
 - Z Expansion fit to deuterium data.
- **Scattering off correlated nucleons (2p2h)**
 - Fit to MINERvA data.
- **Resonant pion production (Non-QE, $W < 1.4$)**
 - 15% increment from re-analysis of deuterium data.
 - “Ad hoc” correction for $Q^2 < 0.7$ [GeV/c]² due to collective nuclear effects.
- **“Inelastic Scattering” (non-resonant pion production) ($1.4 < W < 2.0$)**
 - 43% reduction of the non-resonant pion production, from re-analysis of deuterium data.
- **Deep Inelastic Scattering ($W > 2.0$)**
- **Other interactions**
 - ν_e -induced and NC-induced interactions

χ^2 for Plastic Sidebands

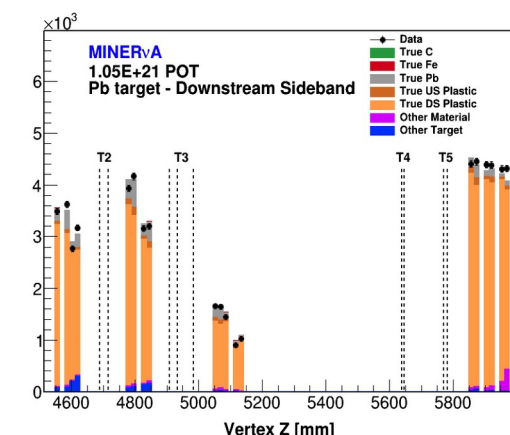
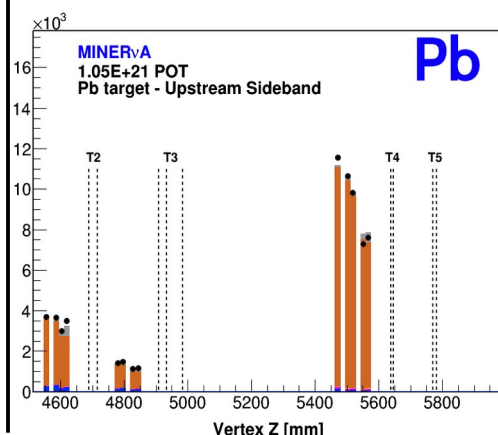
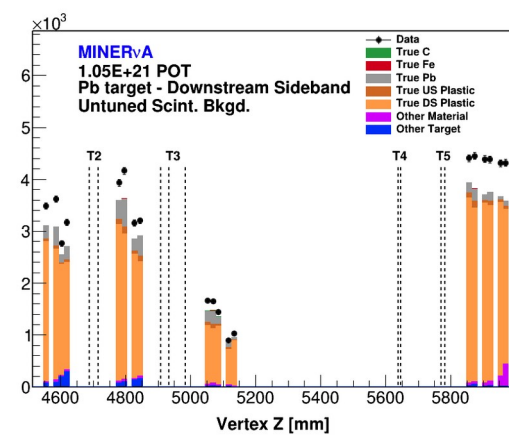
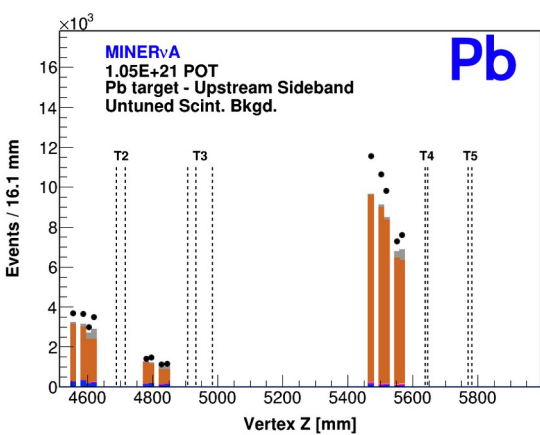
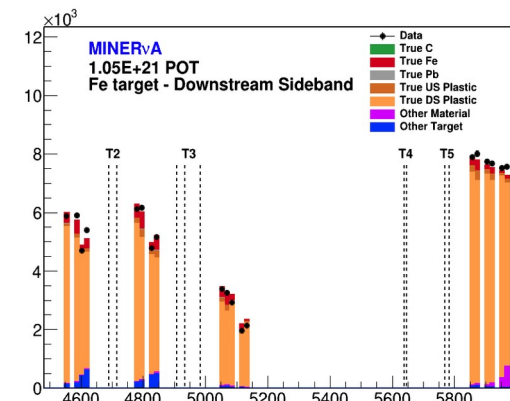
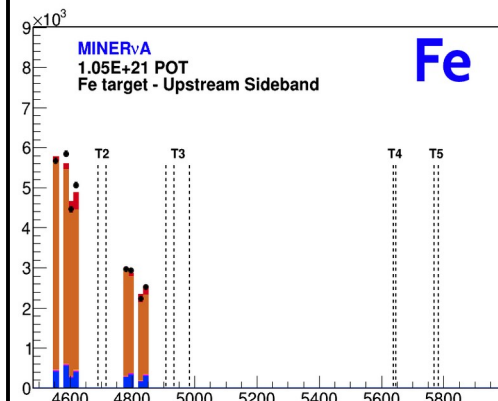
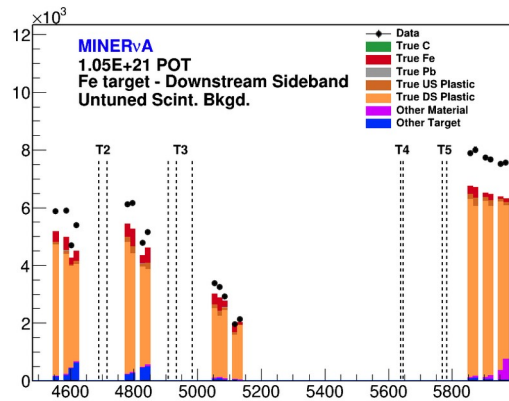
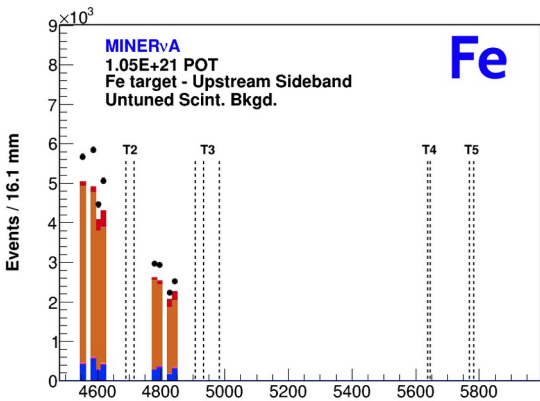
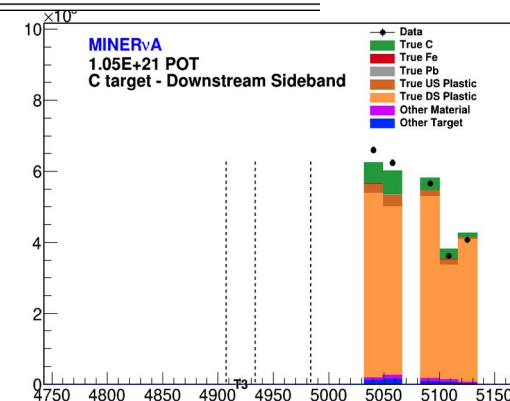
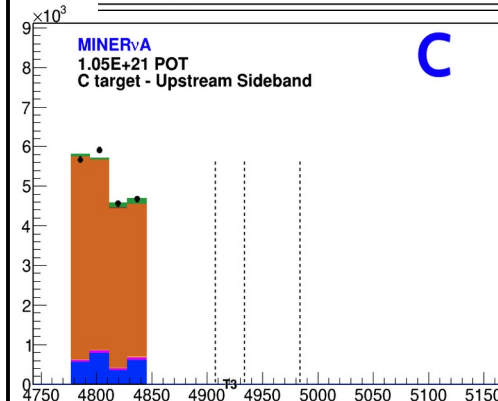
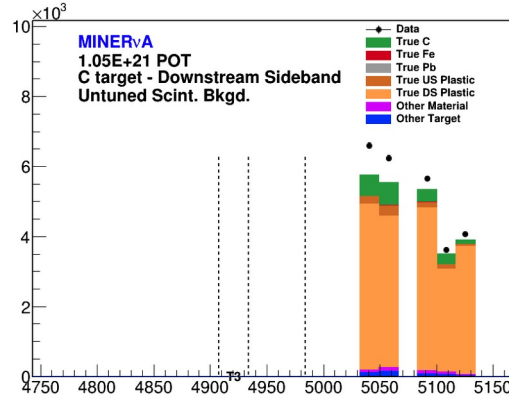
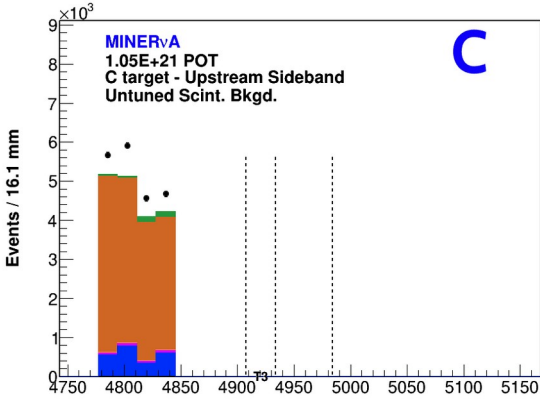
- A χ^2 hypothesis is constructed for each material (C, Fe and **Pb**) and for each plastic region: upstream (US) and downstream (DS).
- The sidebands are the plastic planes in between targets, excluding the planes immediately next to the targets, and all the planes in between targets 4 and 5.

$$\chi^2 = \sum_i \left[\frac{MC_{signal}^i + MC_{other}^i + \alpha_{us} MC_{us}^i + \alpha_{ds} MC_{ds}^i - Data^i}{\sqrt{Data^i}} \right]^2$$

- MC_{signal} = C, Fe or Pb MC contribution
- MC_{other} = Other material and other target MC contribution
- MC_{us} = Upstream plastic MC contribution
- MC_{ds} = Downstream plastic MC contribution

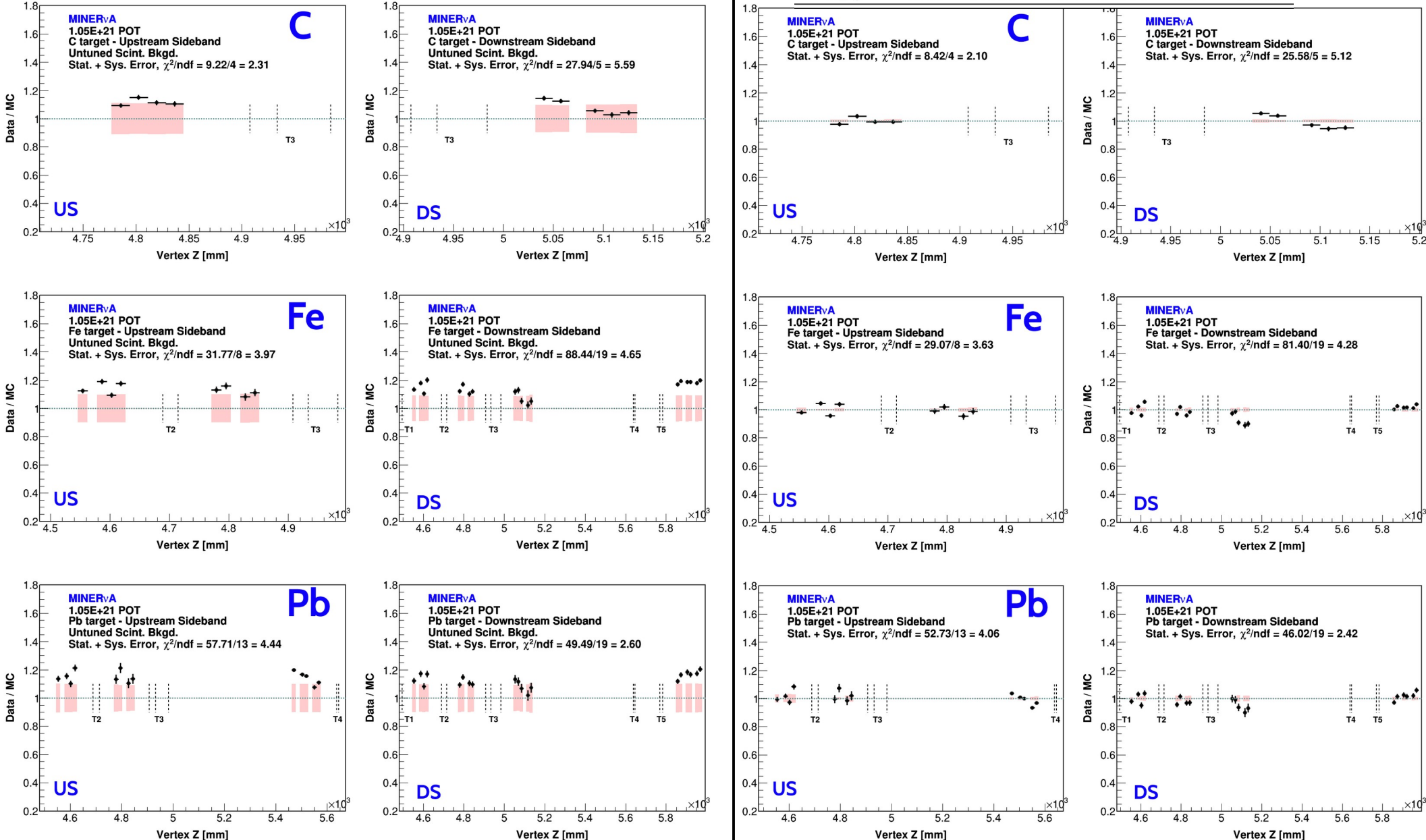
Untuned vs Tuned Sidebands

| Material | C | Fe | Pb |
|---------------|------------------|------------------|------------------|
| α_{US} | 1.15 ± 0.009 | 1.17 ± 0.004 | 1.16 ± 0.005 |
| α_{DS} | 1.11 ± 0.008 | 1.04 ± 0.005 | 1.17 ± 0.005 |

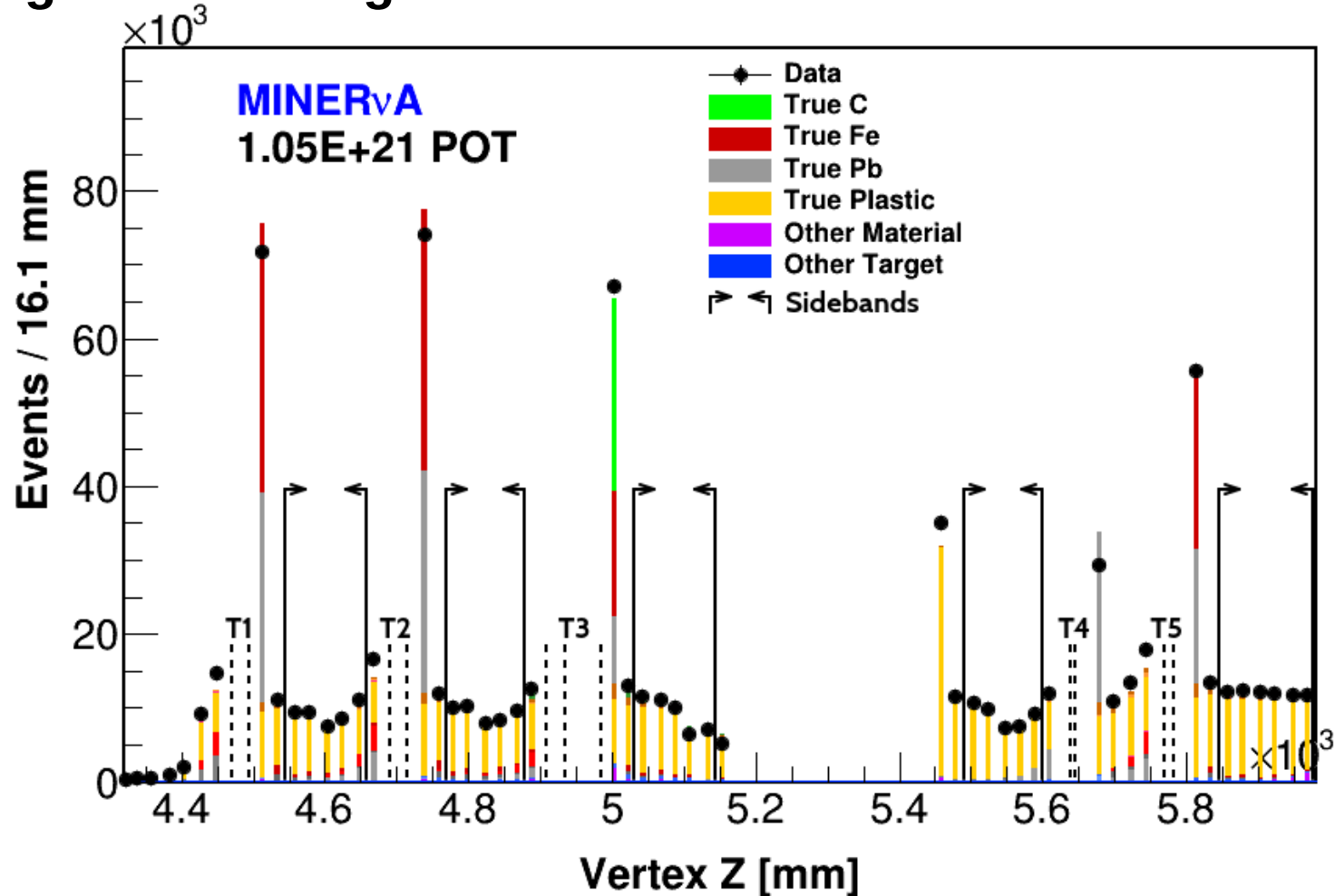


Untuned vs Tuned Sidebands

| Material | <i>C</i> | <i>Fe</i> | <i>Pb</i> |
|---------------|------------------|------------------|------------------|
| α_{US} | 1.15 ± 0.009 | 1.17 ± 0.004 | 1.16 ± 0.005 |
| α_{DS} | 1.11 ± 0.008 | 1.04 ± 0.005 | 1.17 ± 0.005 |



Background Tuning - Plastic Sidebands

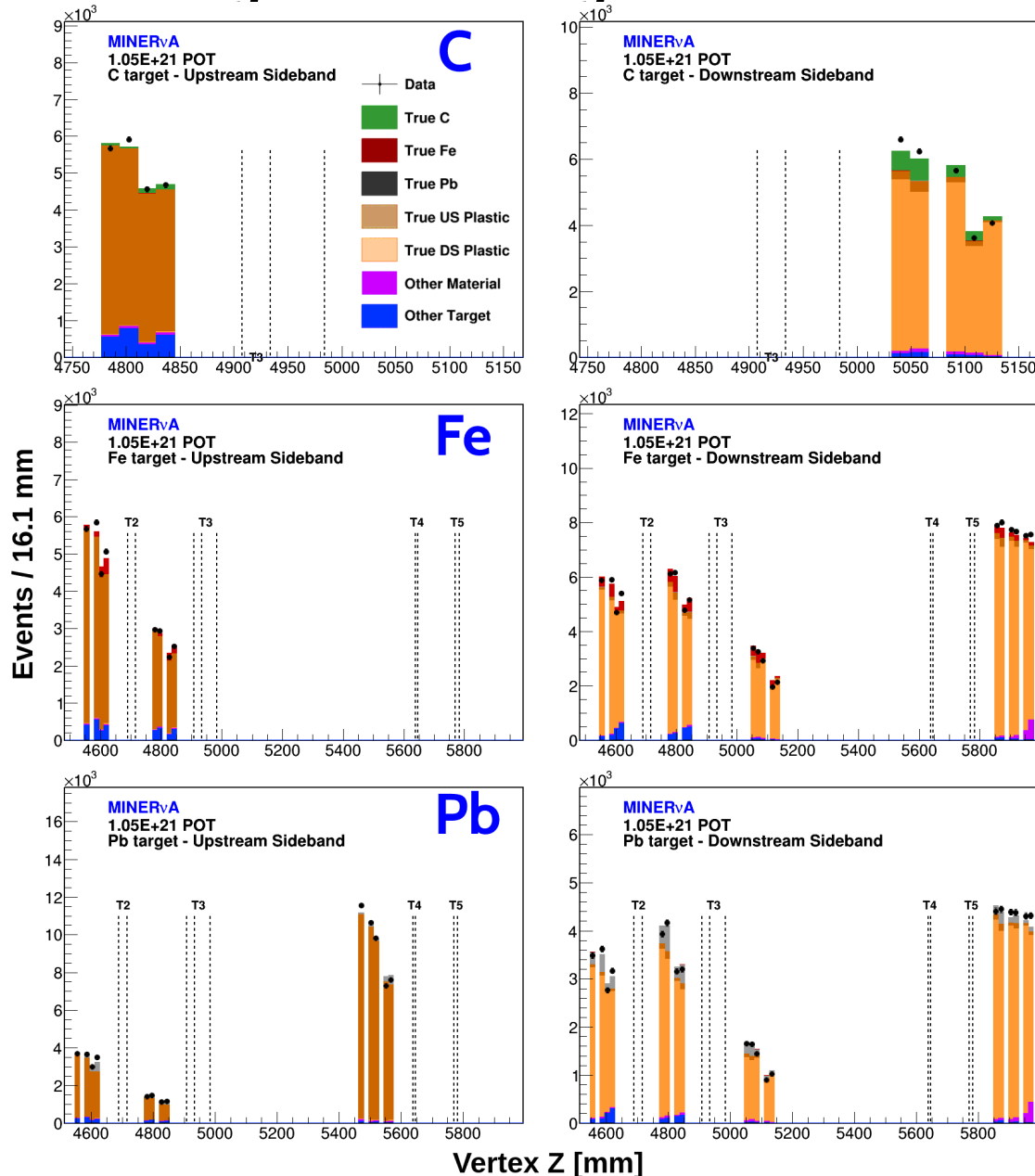


- Plastic regions between targets used as sidebands
- **Upstream** and **Downstream** plastic tuned separate
- Different sidebands for each material (C, Fe and Pb)

Scale Factors

| Material | C | Fe | Pb |
|---------------|------------------|------------------|------------------|
| α_{US} | 1.15 ± 0.009 | 1.17 ± 0.004 | 1.16 ± 0.005 |
| α_{DS} | 1.11 ± 0.008 | 1.04 ± 0.005 | 1.17 ± 0.005 |

Background Tuning - Plastic Sidebar



Plastic background
TUNED

Tuned plastic background represents:

- ~14% of the selected **C** and **Fe** samples
- ~20% of the selected **Pb** sample

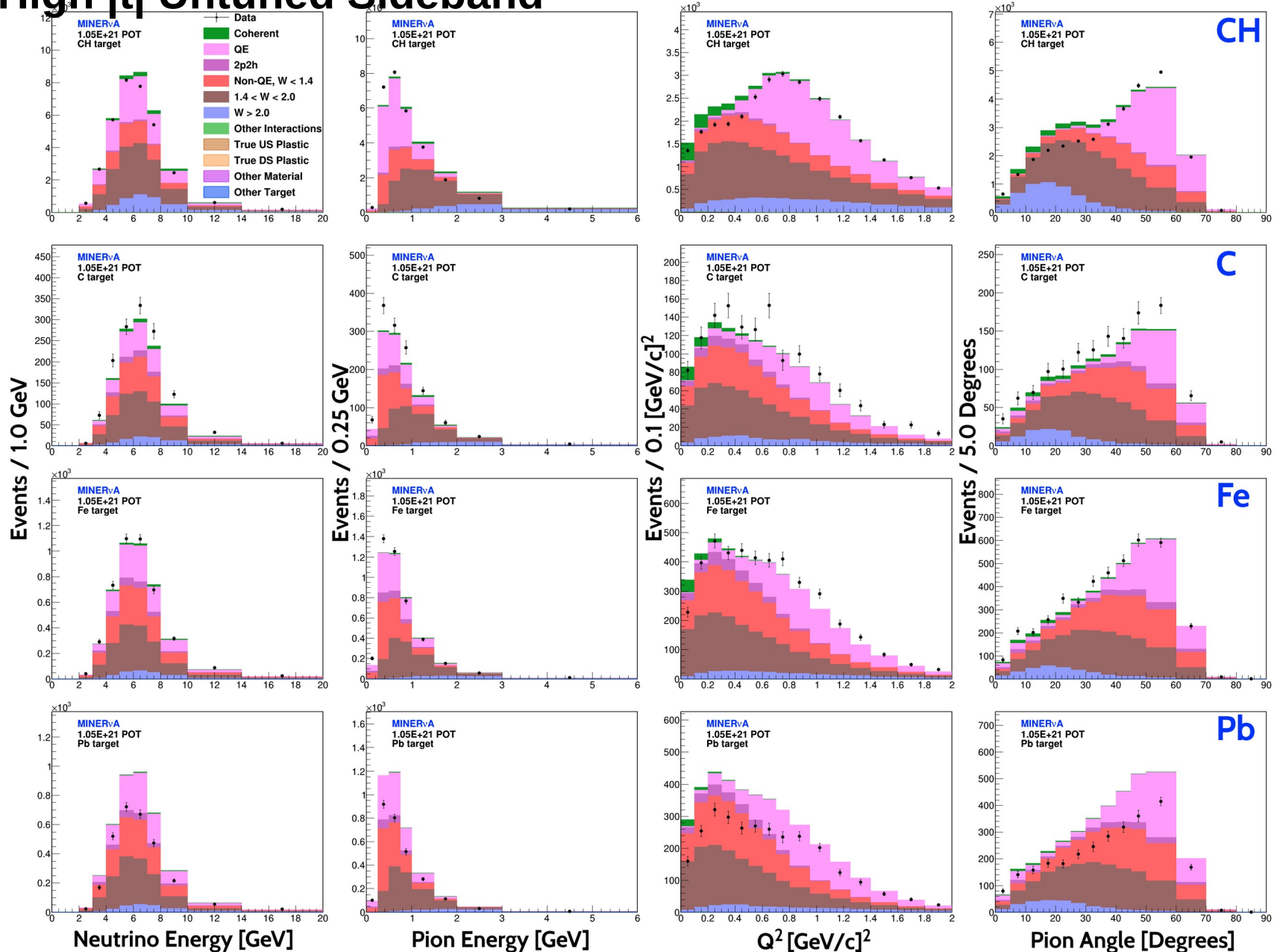
χ^2 for High $|t|$ Sideband

- The tuning is performed simultaneously in \mathbf{E}_π and \mathbf{Q}^2 variables, after the \mathbf{E}_{vtx} cut, inside the $0.2 < |t| < 0.7$ [GeV/c]² sideband.

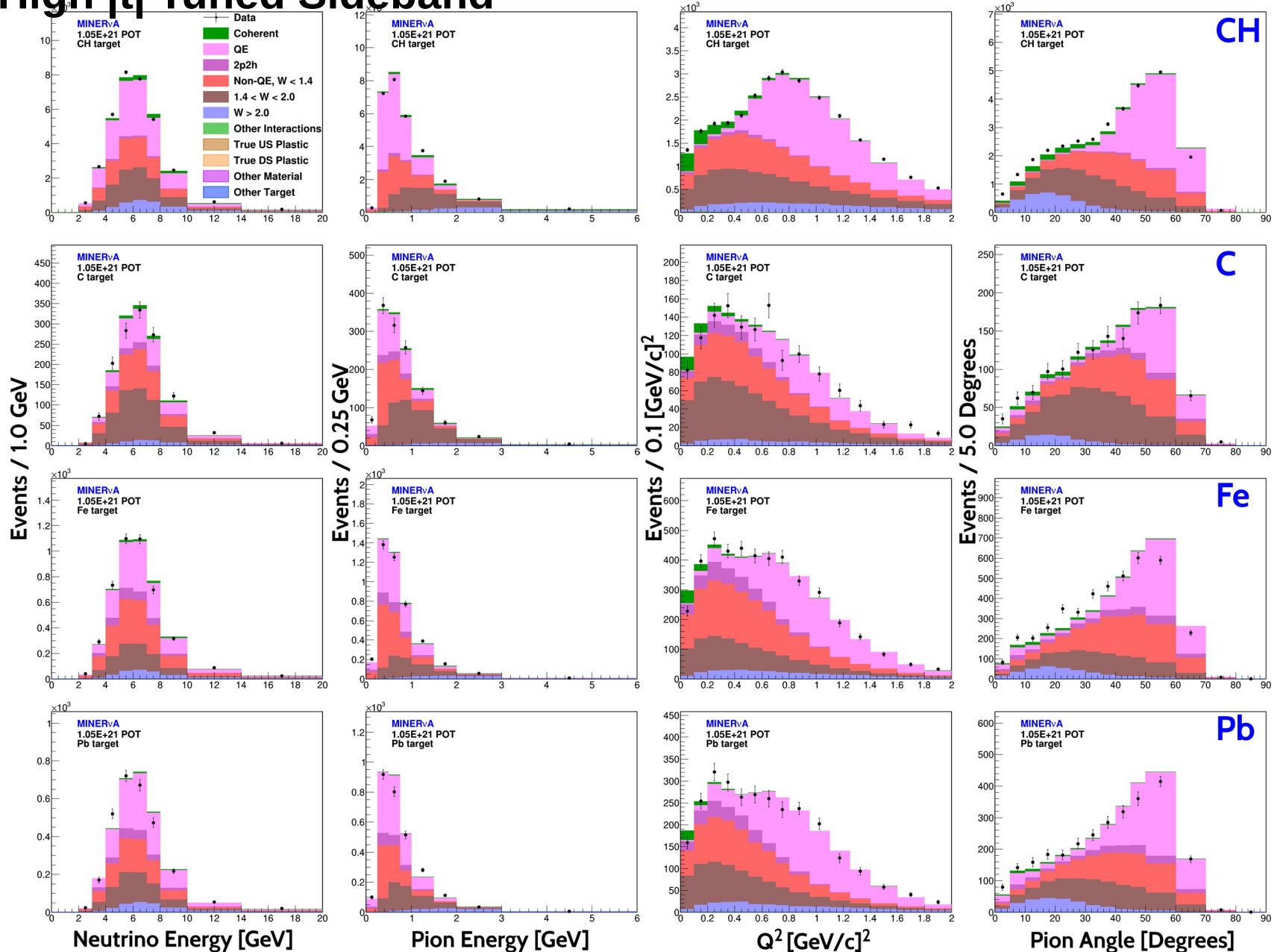
$$\chi^2 = \sum_i \sum_j \frac{\left[N_{ij}^{\text{Data}} - \sum_k \alpha_k N_{ijk}^{\text{MC}} \right]^2}{\sum_k \alpha_k N_{ijk}^{\text{MC}}}$$

- \mathbf{N}^{Data} = Number of data events in the ij bin.
- \mathbf{N}^{MC} = Number of MC events from the k background, in the ij bin.
- α_k = Scale factor for each background.

High $|t|$ Untuned Sideband



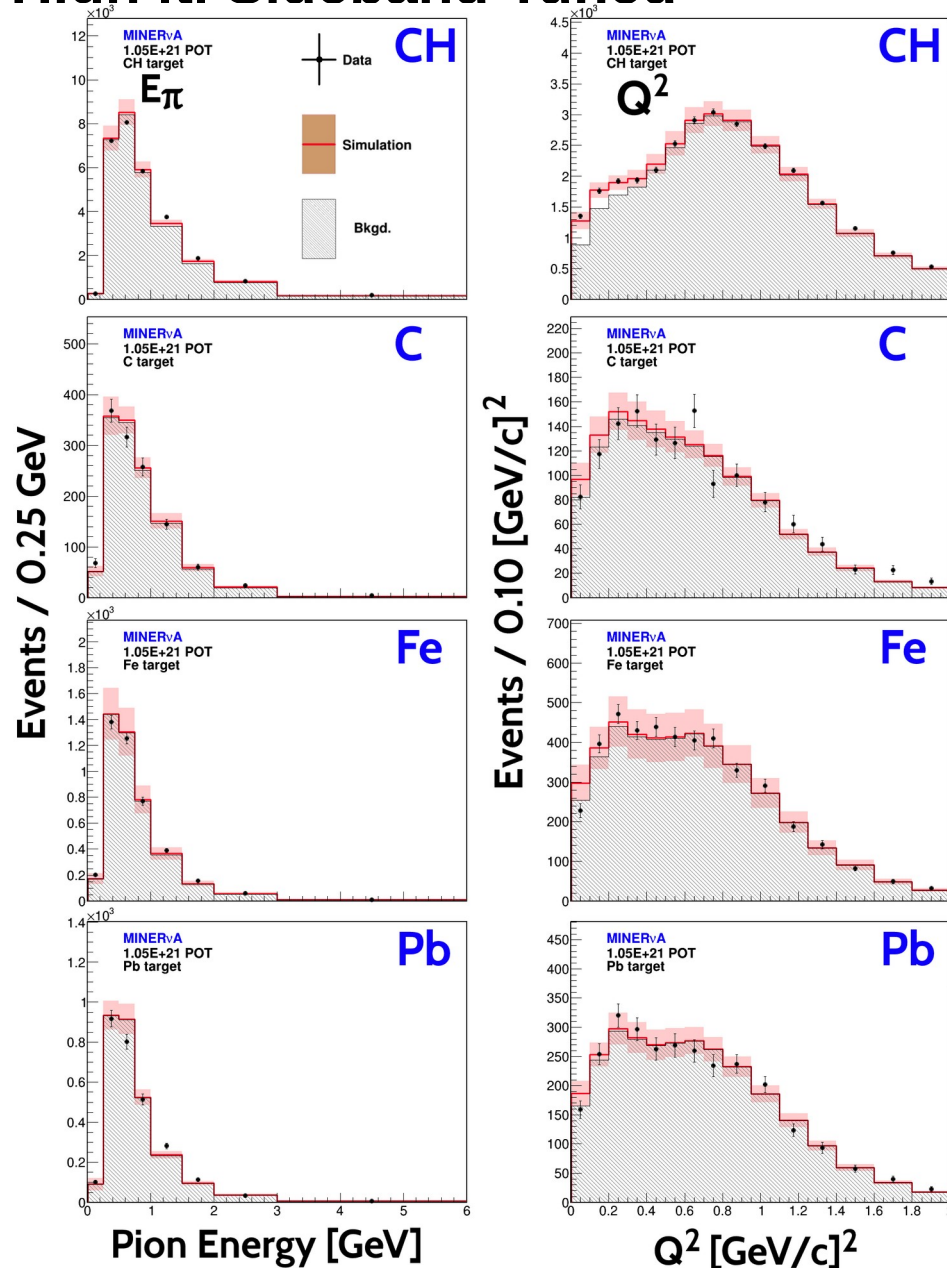
High $|t|$ Tuned Sideband



Scale Factors

| Material | CH | C | Fe | Pb |
|----------------|------------------|------------------|------------------|------------------|
| α_{QE} | 1.22 ± 0.016 | 1.22 ± 0.016 | 1.40 ± 0.067 | 1.09 ± 0.054 |
| α_{RES} | 1.29 ± 0.040 | 1.17 ± 0.046 | 1.15 ± 0.088 | 0.66 ± 0.069 |
| α_{INE} | 0.60 ± 0.016 | 1.17 ± 0.046 | 0.58 ± 0.059 | 0.50 ± 0.053 |
| α_{DIS} | 0.65 ± 0.026 | 0.65 ± 0.026 | 1.08 ± 0.137 | 0.98 ± 0.144 |

High $|t|$ Sideband Tuned

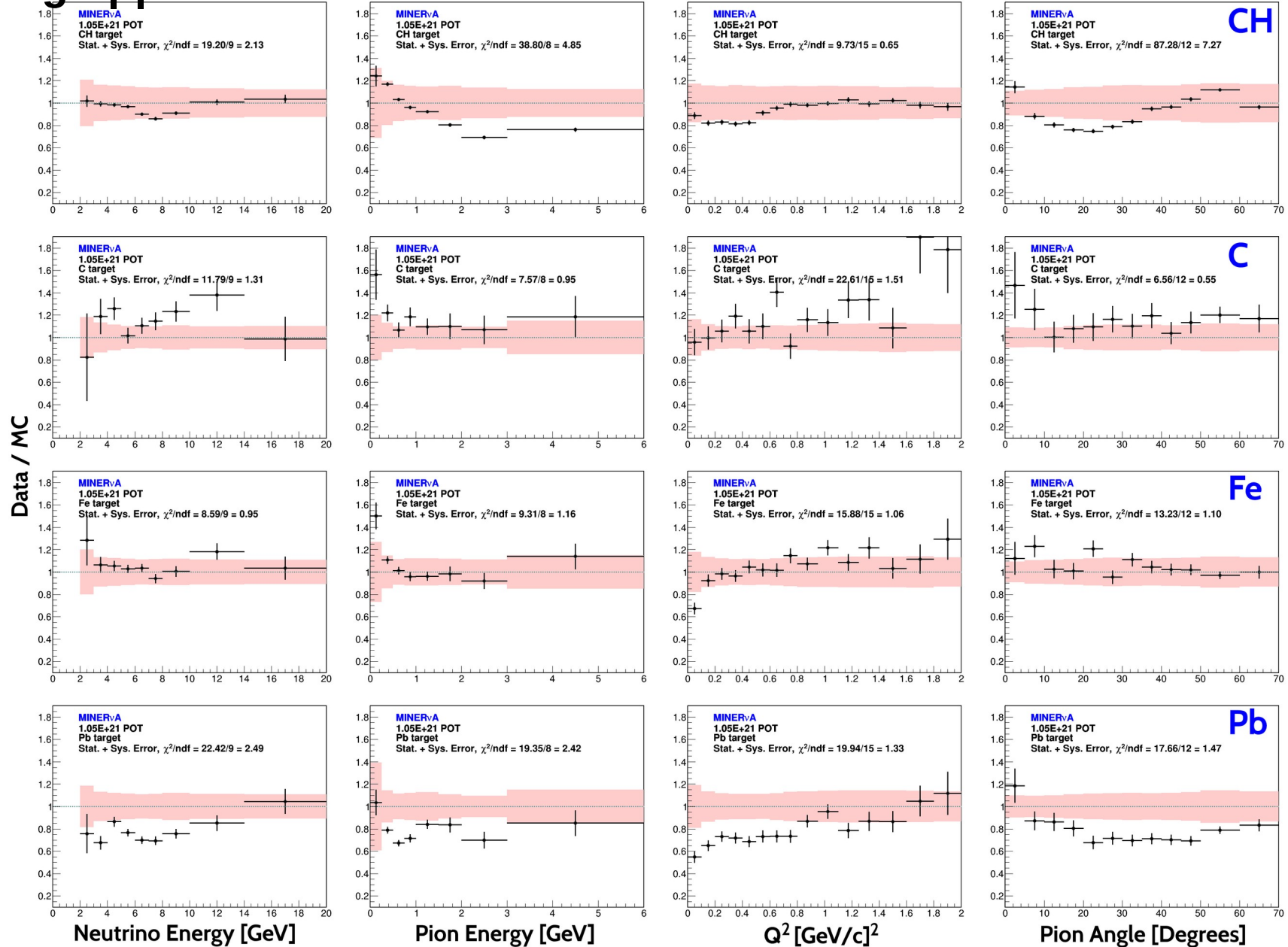


**Background
TUNED**

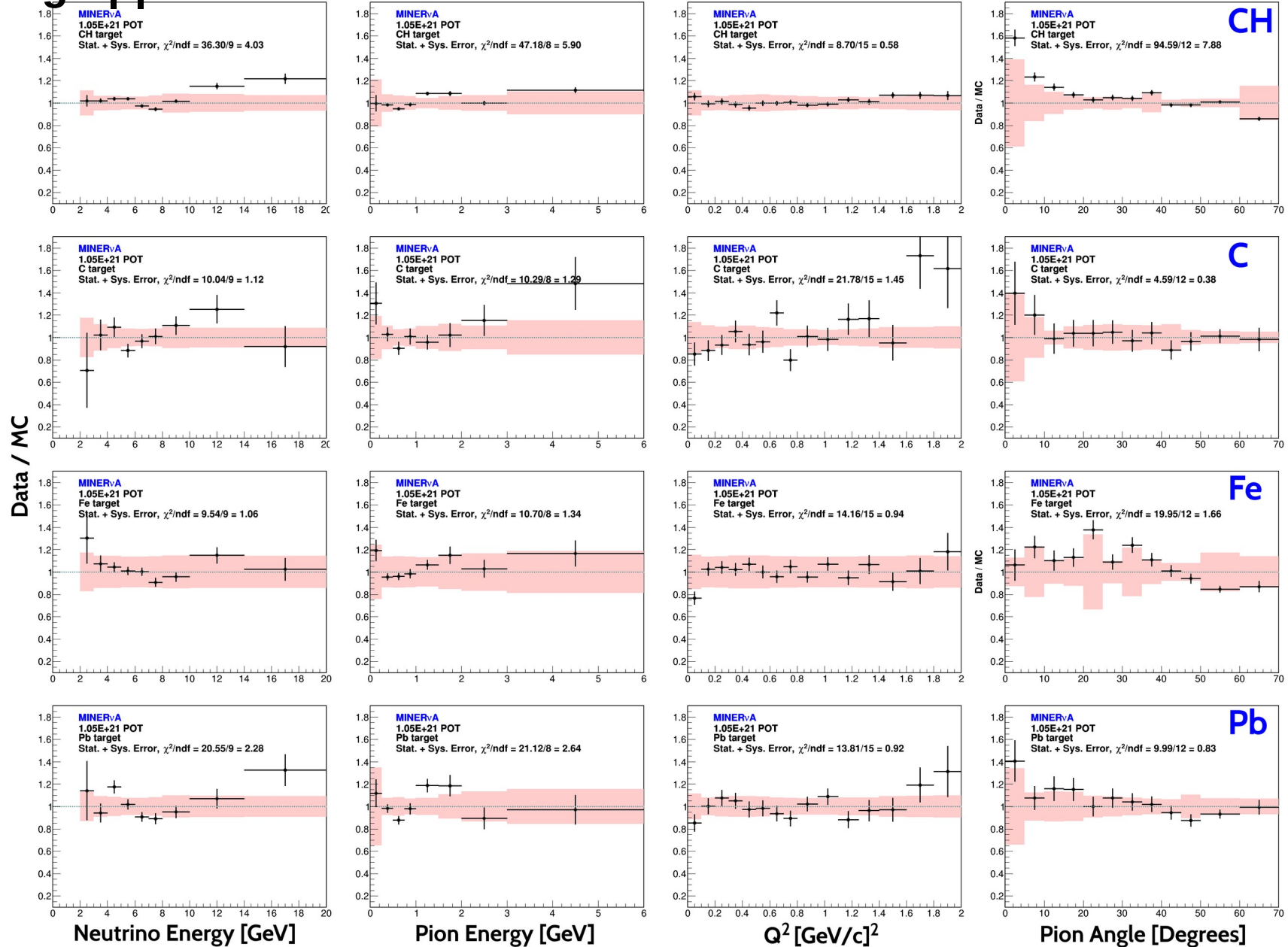
**Distributions from
high $|t|$ sidebands**

- Tuned in E_π and Q^2 simultaneously.
- Samples from $0.3 < |t| < 0.7$ [GeV/c]²

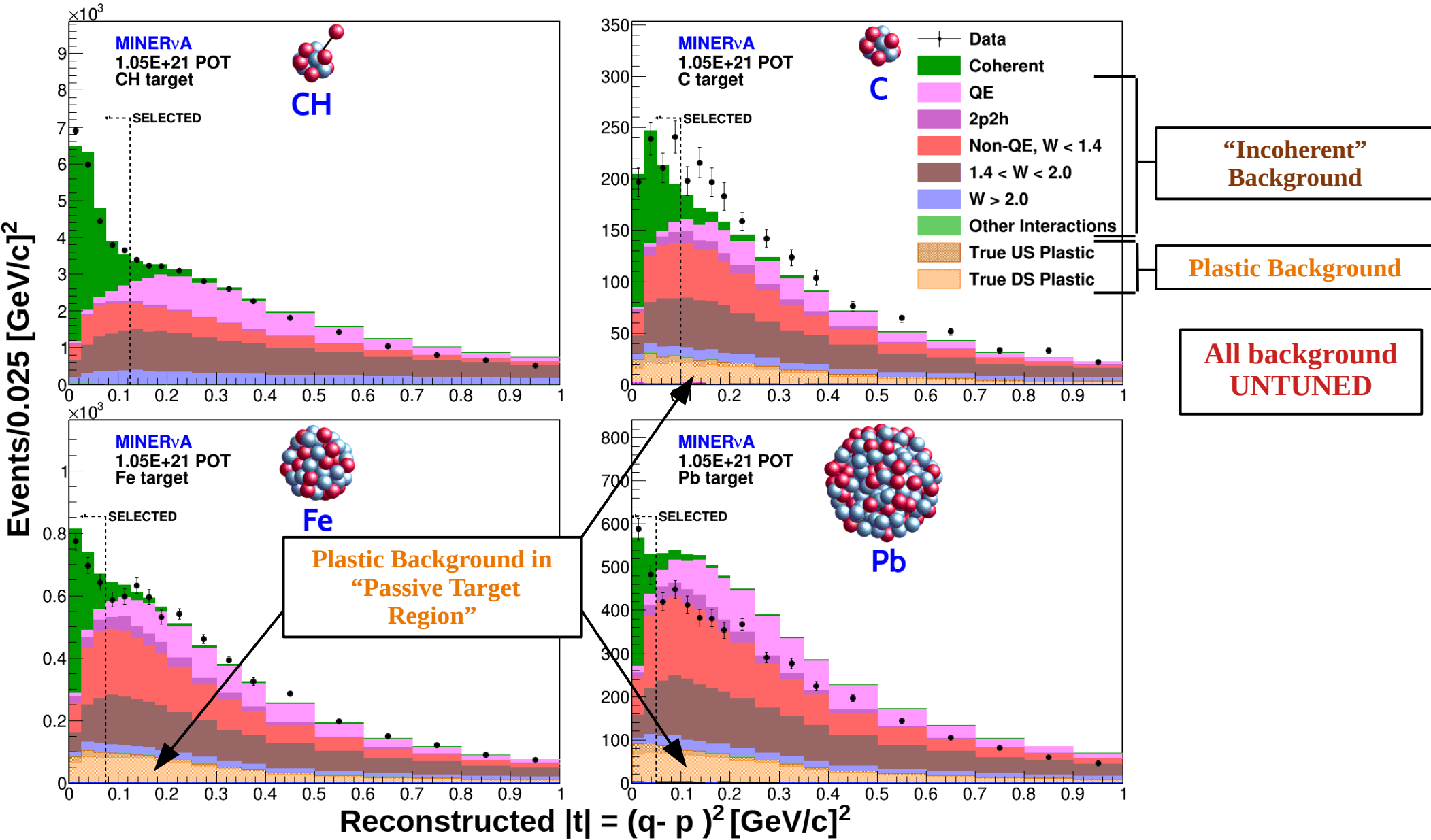
High $|t|$ Untuned Sideband – Data/MC



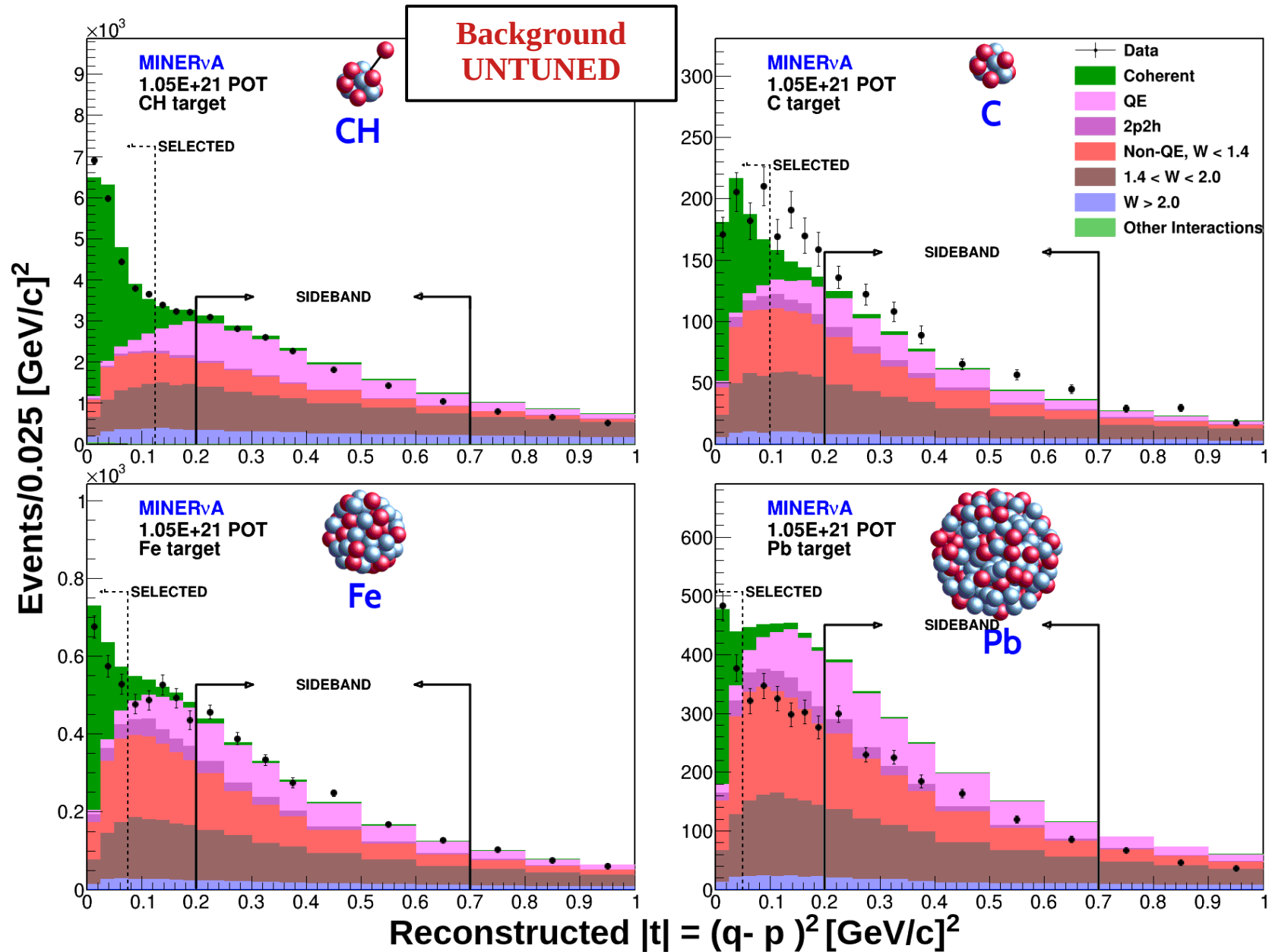
High $|t|$ Untuned Sideband - Data/MC



Event Selection – Momentum Transfer to the Nucleus $|t|$



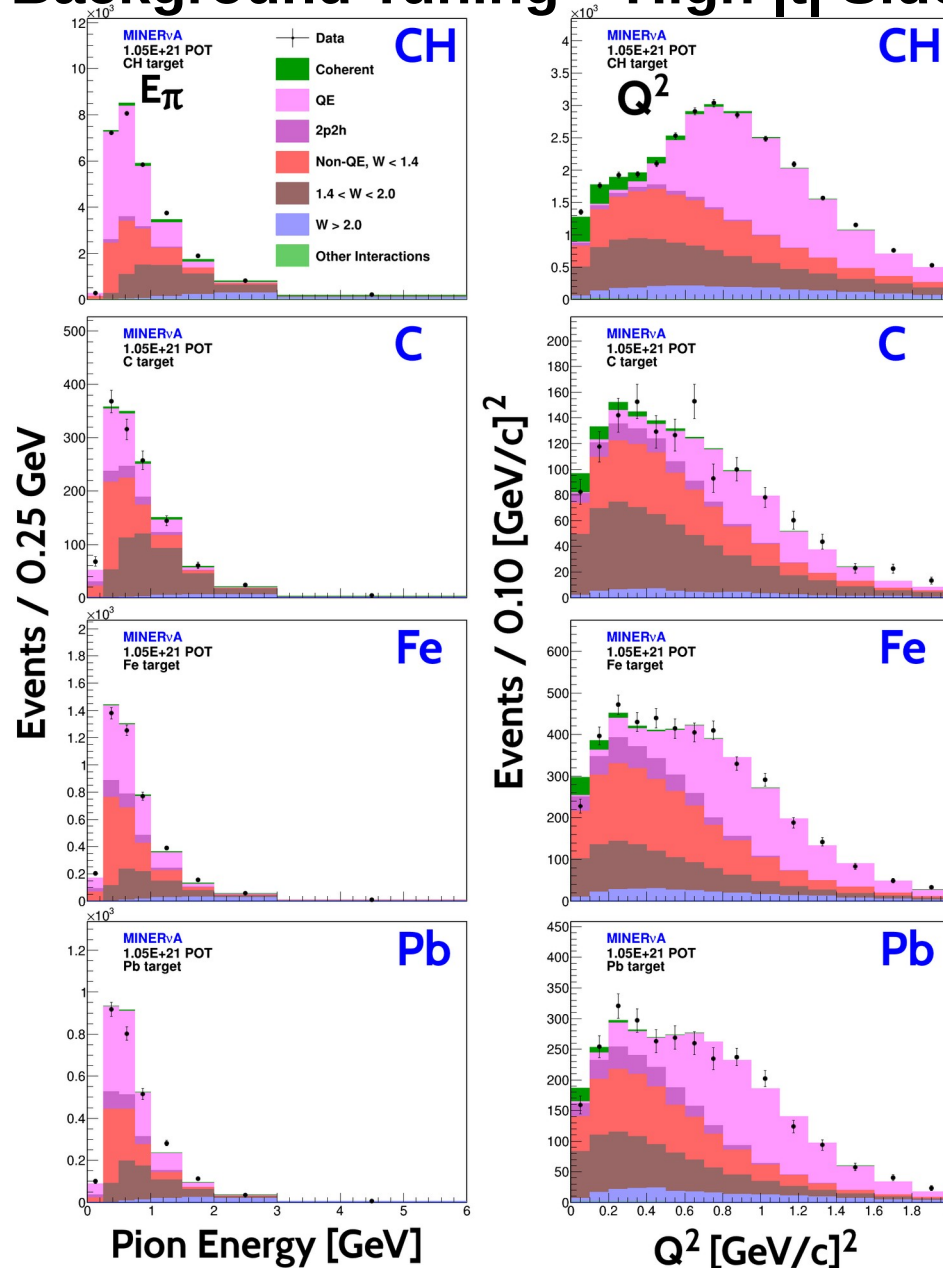
Background Tuning – High $|t|$ Sideband



Scale Factors

| Material | CH | C | Fe | Pb |
|----------------|------------------|------------------|------------------|------------------|
| α_{QE} | 1.22 ± 0.016 | 1.22 ± 0.016 | 1.40 ± 0.067 | 1.09 ± 0.054 |
| α_{RES} | 1.29 ± 0.040 | 1.17 ± 0.046 | 1.15 ± 0.088 | 0.66 ± 0.069 |
| α_{INE} | 0.60 ± 0.016 | 1.17 ± 0.046 | 0.58 ± 0.059 | 0.50 ± 0.053 |
| α_{DIS} | 0.65 ± 0.026 | 0.65 ± 0.026 | 1.08 ± 0.137 | 0.98 ± 0.144 |

Background Tuning – High $|t|$ Sideband

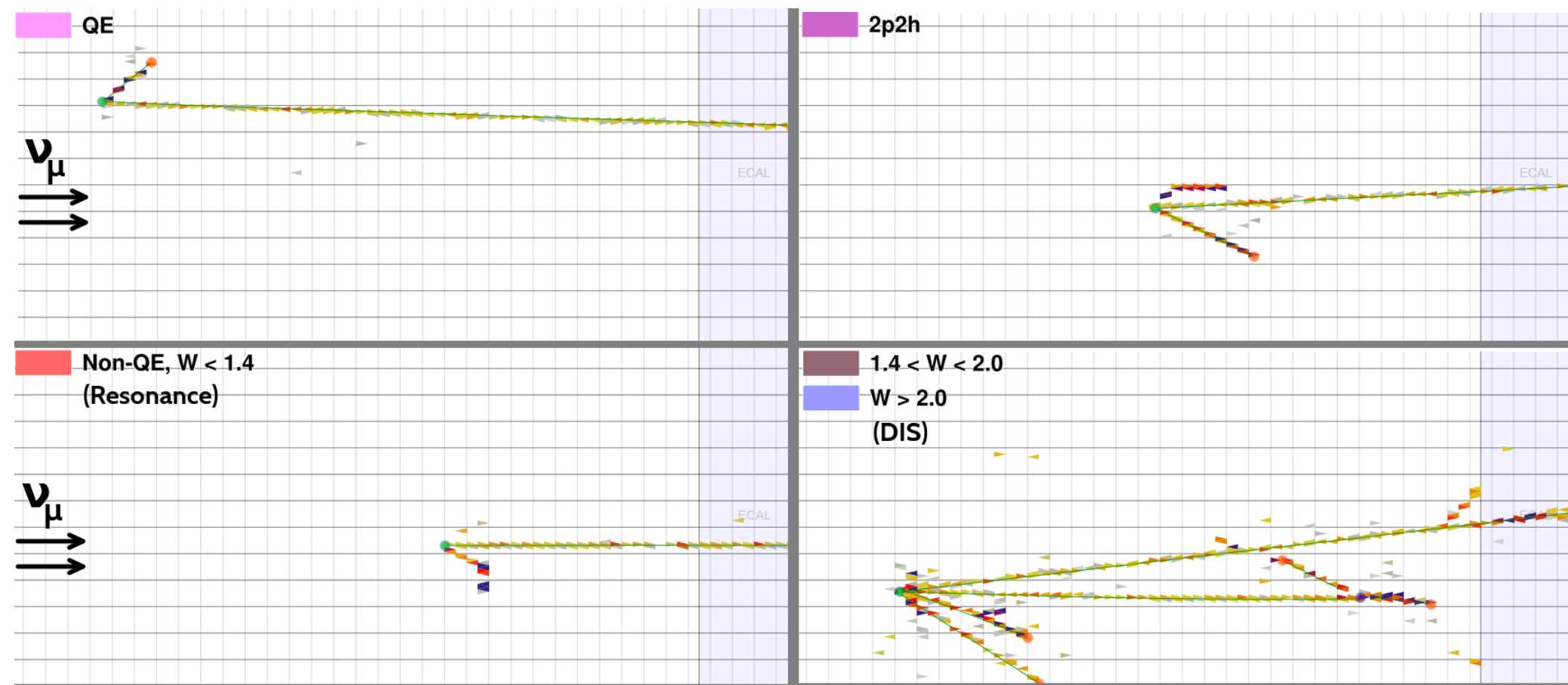


**Background
TUNED**

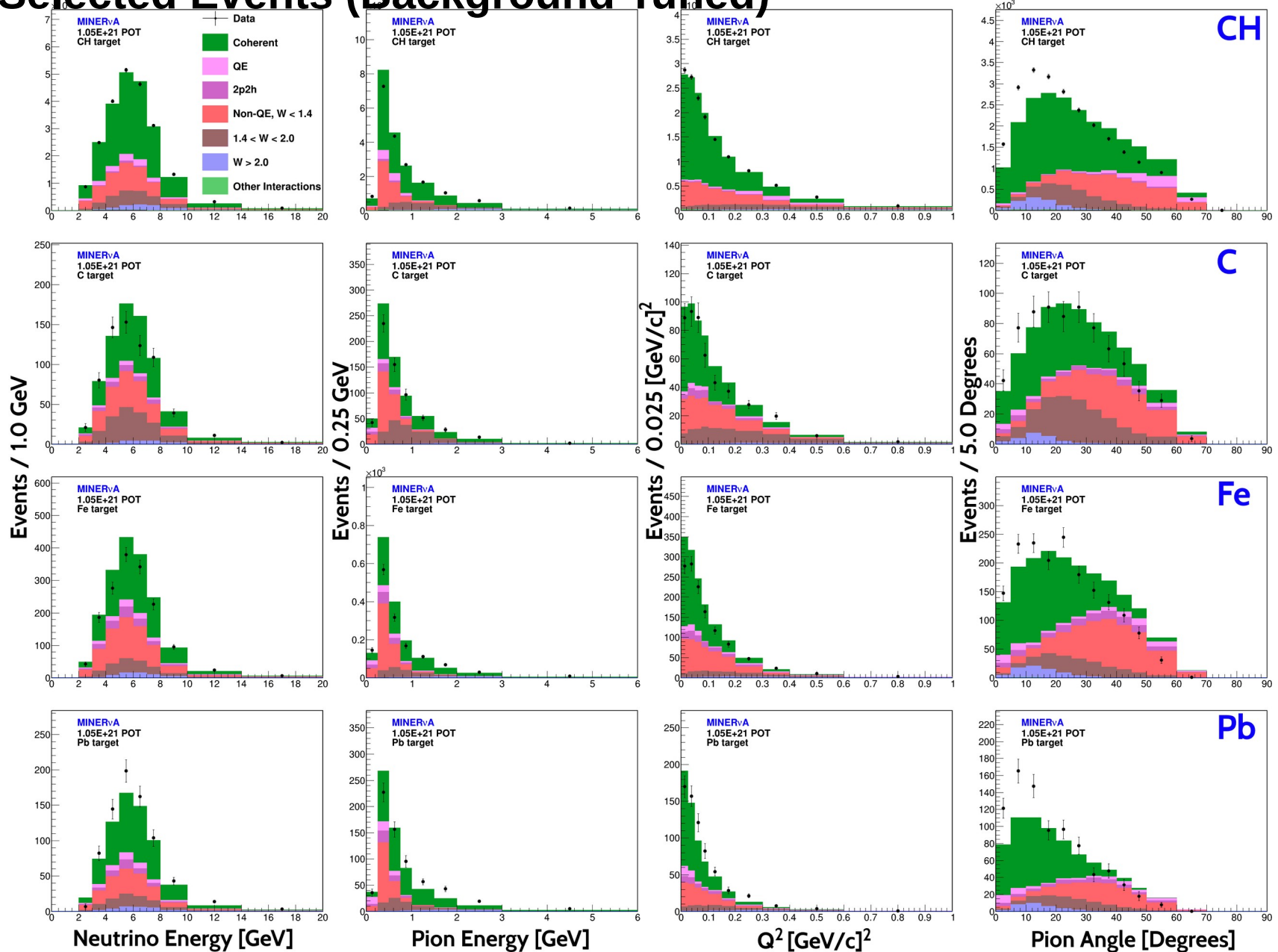
**Distributions from
high $|t|$ sidebands**

- Tuned in E_π and Q^2 simultaneously.
- Samples from $0.3 < |t| < 0.7$ [GeV/c]².
- Backgrounds in terms of W .

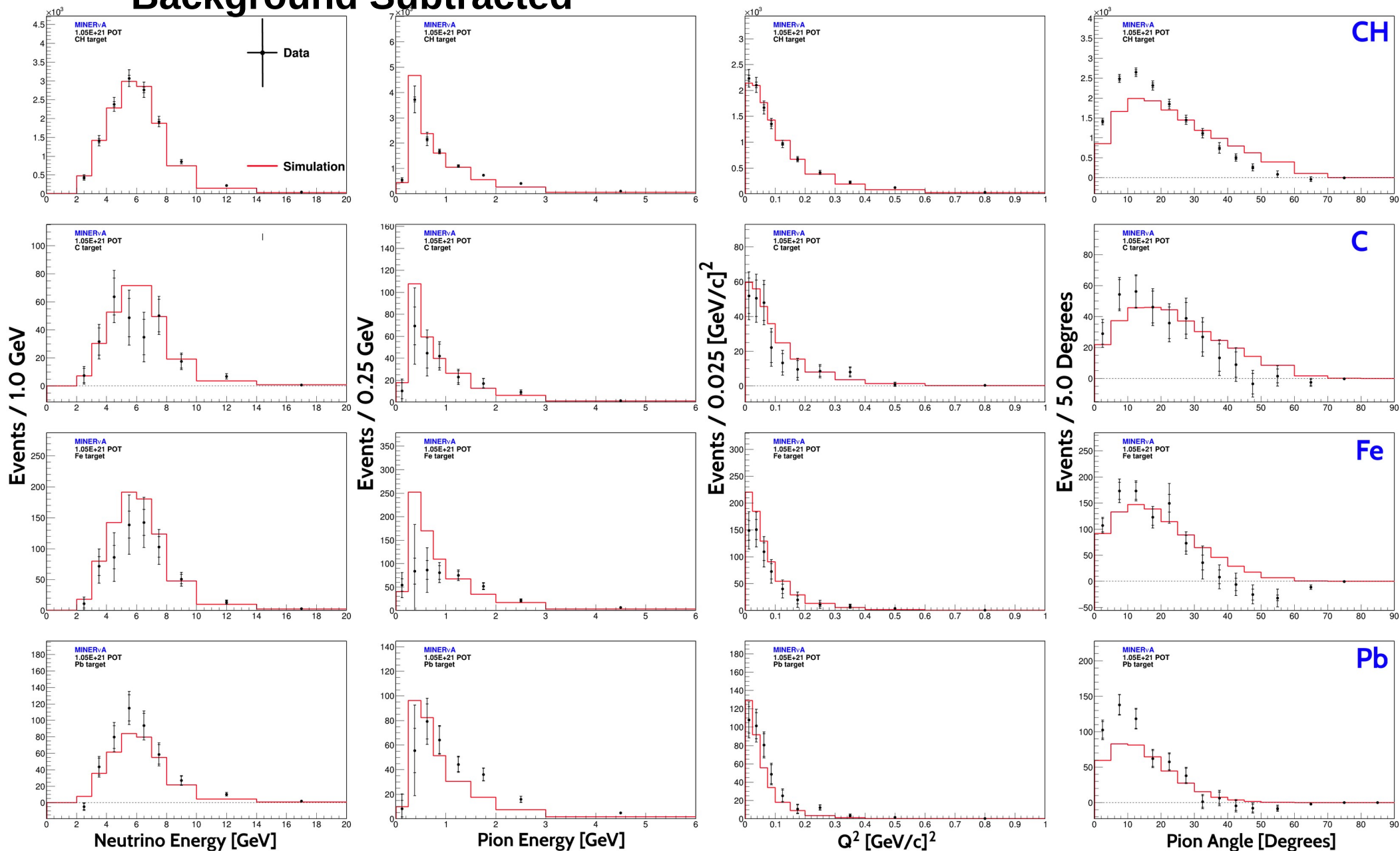
Backgrounds – In Terms of Invariant Mass (W)



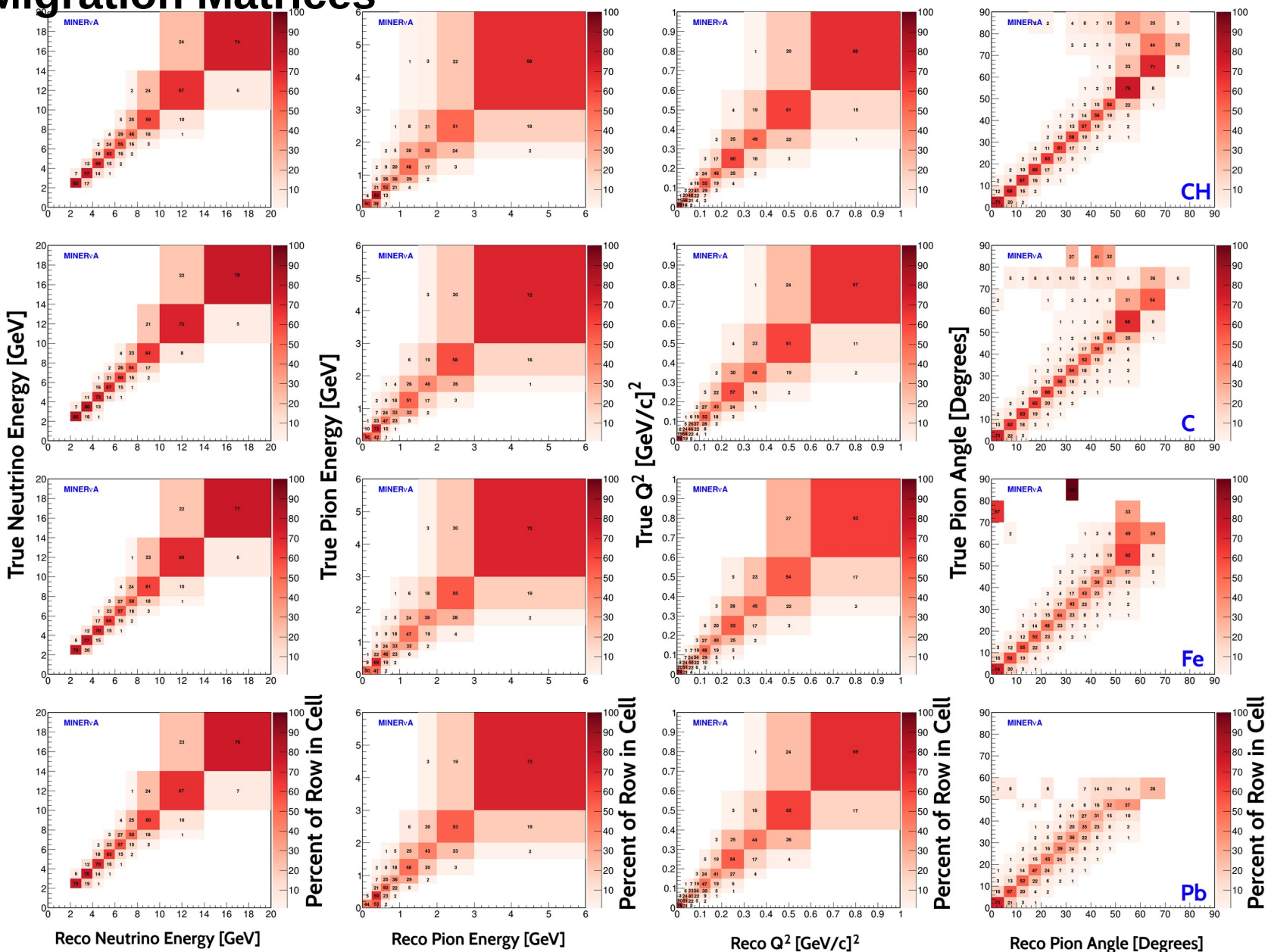
Selected Events (Background Tuned)



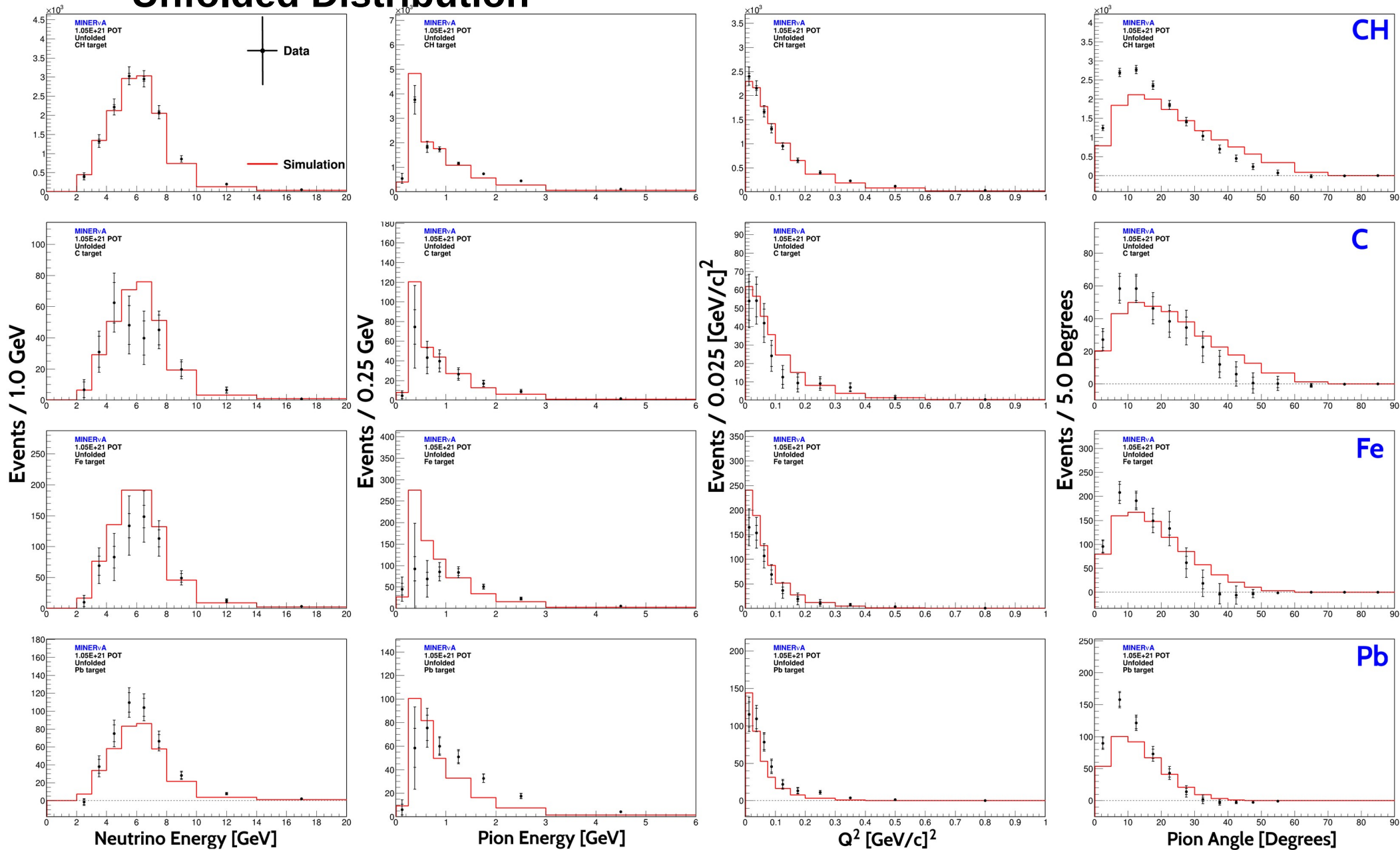
Background Subtracted



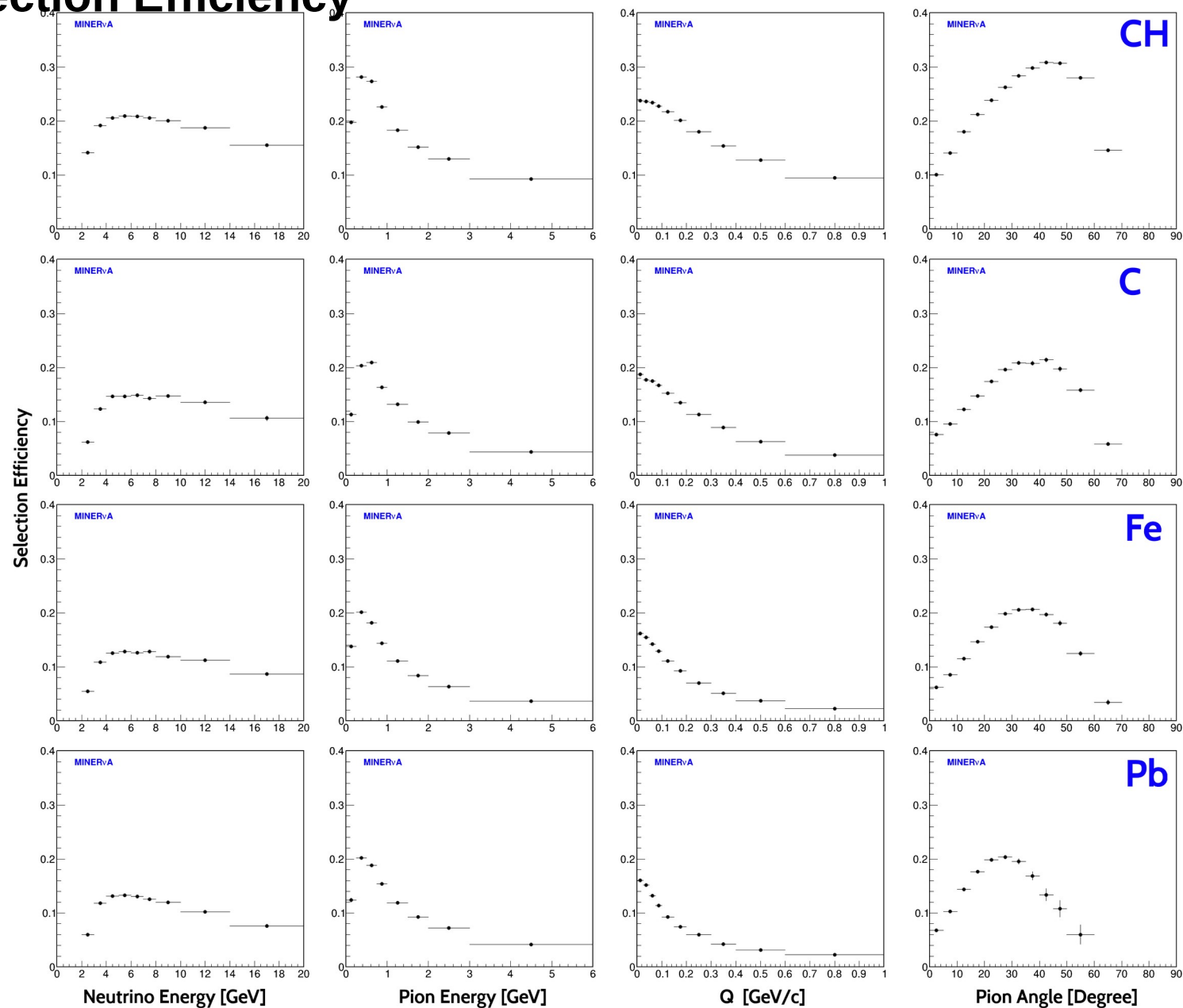
Migration Matrices



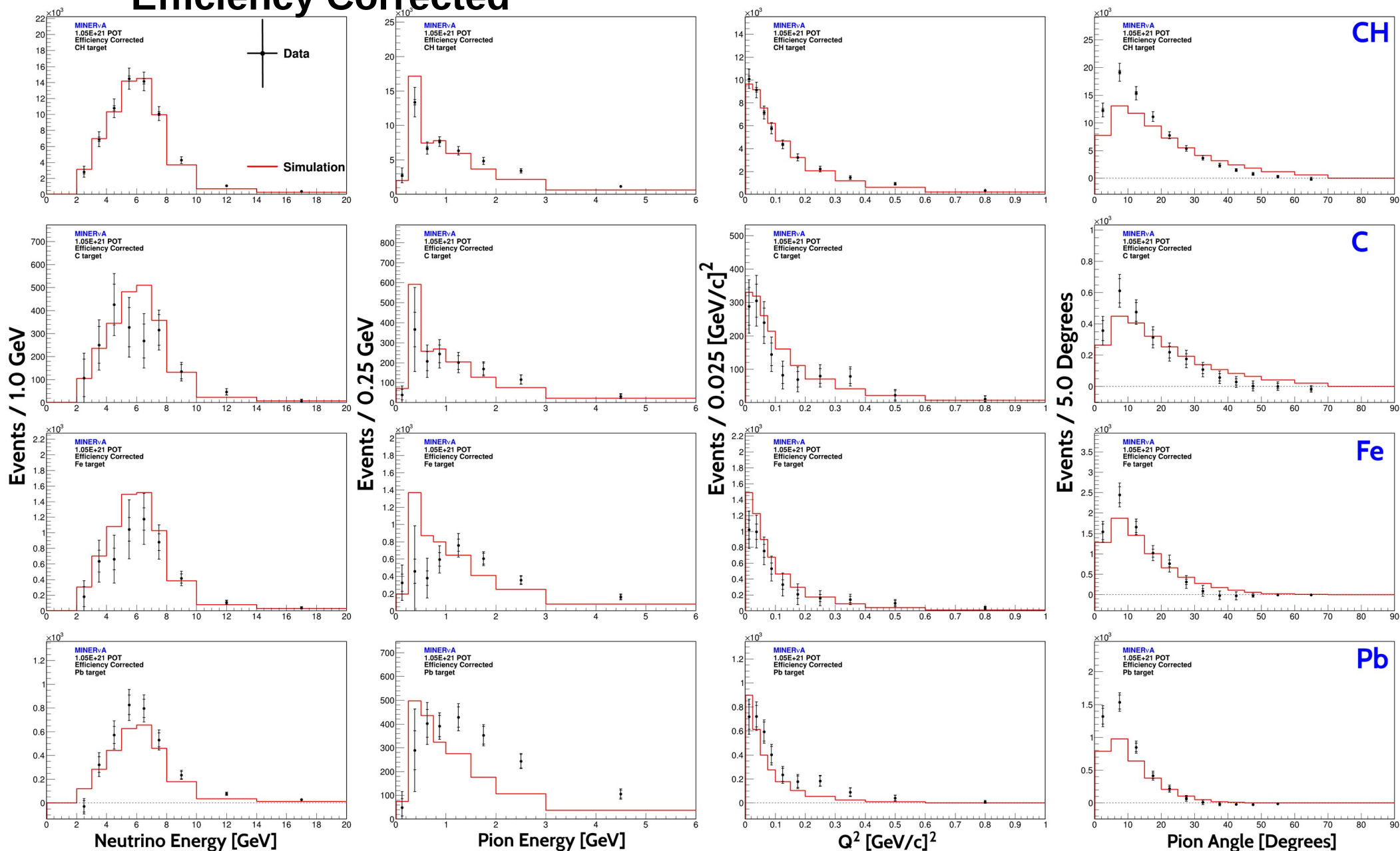
Unfolded Distribution



Selection Efficiency



Efficiency Corrected



Correction Due To Other Materials in the Fiducial Volume

The **C** and **Pb** target have less than 1% contribution from other materials. The contribution from other materials to the **CH** and **Fe** targets is specified below

| Nucleus in CH target | % of Total Mass | A | T |
|----------------------|-----------------|--------|------------------------|
| 1H | 7.4 | 1.008 | 2.425×10^{29} |
| ^{12}C | 87.6 | 12.011 | 2.404×10^{29} |
| ^{16}O | 3.2 | 15.999 | 6.548×10^{27} |
| ^{27}Al | 0.26 | 26.982 | 3.175×10^{26} |
| ^{28}Si | 0.27 | 28.085 | 3.167×10^{26} |
| ^{35}Cl | 0.55 | 35.453 | 5.511×10^{26} |
| ^{48}Ti | 0.69 | 47.867 | 4.749×10^{26} |

| Nucleus in Fe target | % of Total Mass | A | T |
|----------------------|-----------------|--------|------------------------|
| ^{12}C | 0.13 | 12.011 | 6.137×10^{25} |
| ^{26}Fe | 98.7 | 55.845 | 1.016×10^{28} |
| ^{28}Si | 0.2 | 28.085 | 4.038×10^{25} |
| ^{55}Mn | 1.0 | 54.938 | 1.032×10^{26} |

Mass fraction, mass number A, and number of nuclei from all materials present in the CH and Fe targets. Included for every material.

Correction Due To Other Materials in the Fiducial Volume

The correction β is defined as the number of coherent interactions in the material under study in the fiducial volume of a given target, over the total number of coherent interactions in the same fiducial volume

$$\beta = \left(N_M^{coh} / N^{coh} \right) = \frac{\phi \epsilon_M \sigma_M T_M}{\sum_i \phi \epsilon_i \sigma_i T_i} \approx \frac{A_M^{1/3} T_M}{\sum_i A_i^{1/3} T_i}$$

- where ϕ , ϵ_M , σ_M and T_M are the flux, efficiency, cross section and number of nuclei in each material due to **C** in the CH target, and due to **Fe** in the Fe targets
- M is either **C** or **Fe**.
- The same quantities with the i sub index, correspond to the remaining materials in the same target. The assumption of equal flux and efficiency in all materials has been made.
- The cross section has been supposed to scale as $A^{1/3}$ as in the Rein-Sehgal model. Using $A^{2/3}$ yields similar values

Correction Due To Other Materials in the Fiducial Volume

$$\sigma_i = \underbrace{\beta}_{\text{Material Correction Factor}} \frac{\sum_j U_{ij} (N_j^{DATA} - N_j^{BKGD})}{\epsilon_i \phi_i T}$$

Total Cross Section (points to σ_i)
 Unfolding Matrix (points to U_{ij})
 Number of Data Events (points to N_j^{DATA})
 Number of Background Predicted Events (points to N_j^{BKGD})
 Efficiency (points to ϵ_i)
 Flux Per Bin (points to ϕ_i)
 Number of Nuclei (points to T)

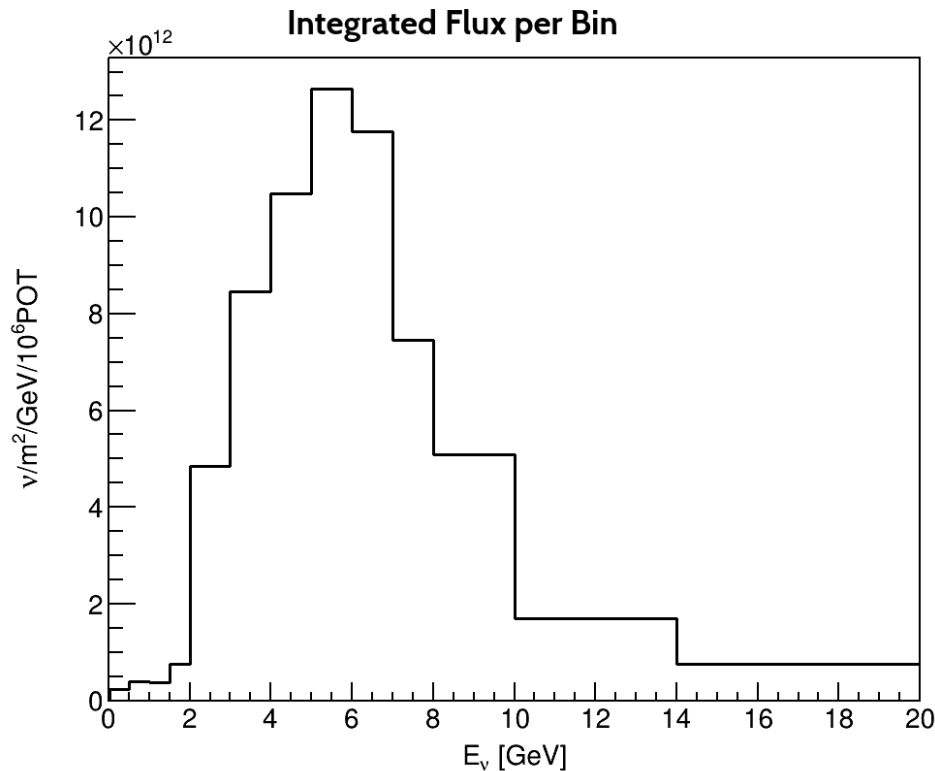
| Material | β |
|-----------|---------|
| <i>CH</i> | 0.96 |
| <i>C</i> | 1.0 |
| <i>Fe</i> | 0.98 |
| <i>Pb</i> | 1.0 |

Cross Section Extraction

Flux and Number of Targets

$$\sigma_i = \frac{\sum_j U_{ij} (N_j^{DATA} - N_j^{BKGD})}{\epsilon_i \phi_i T}$$

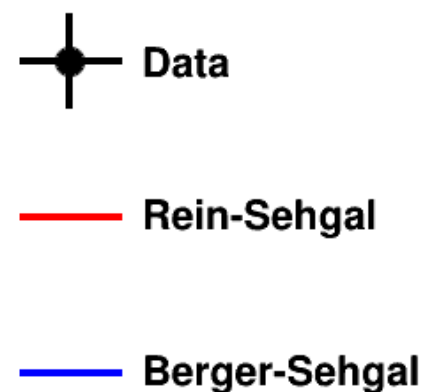
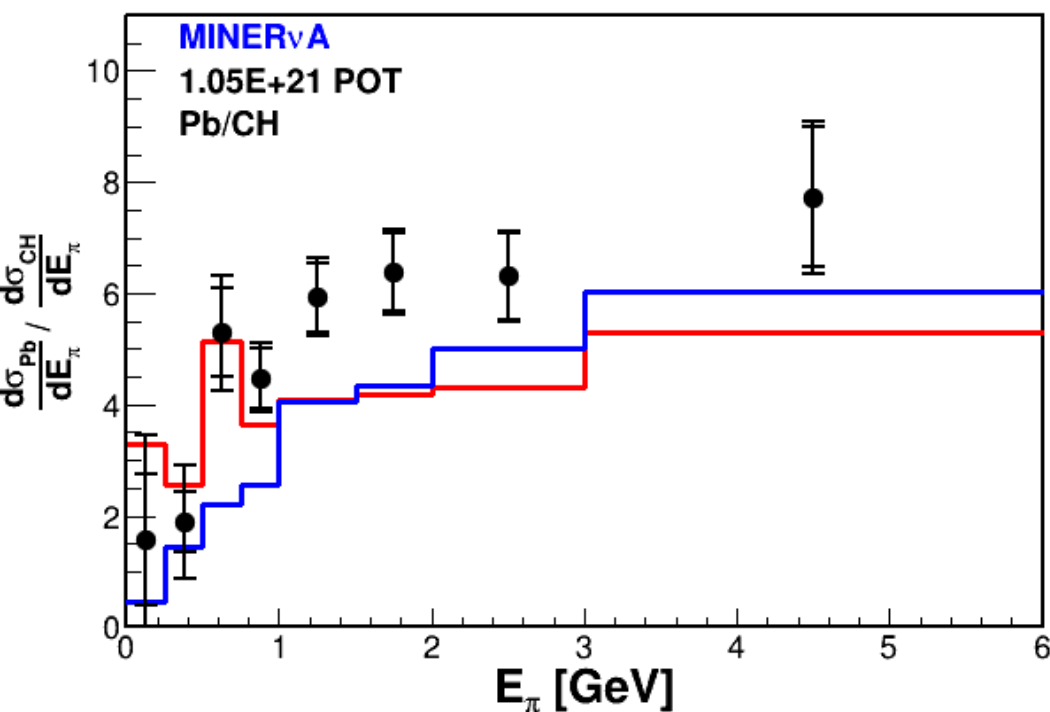
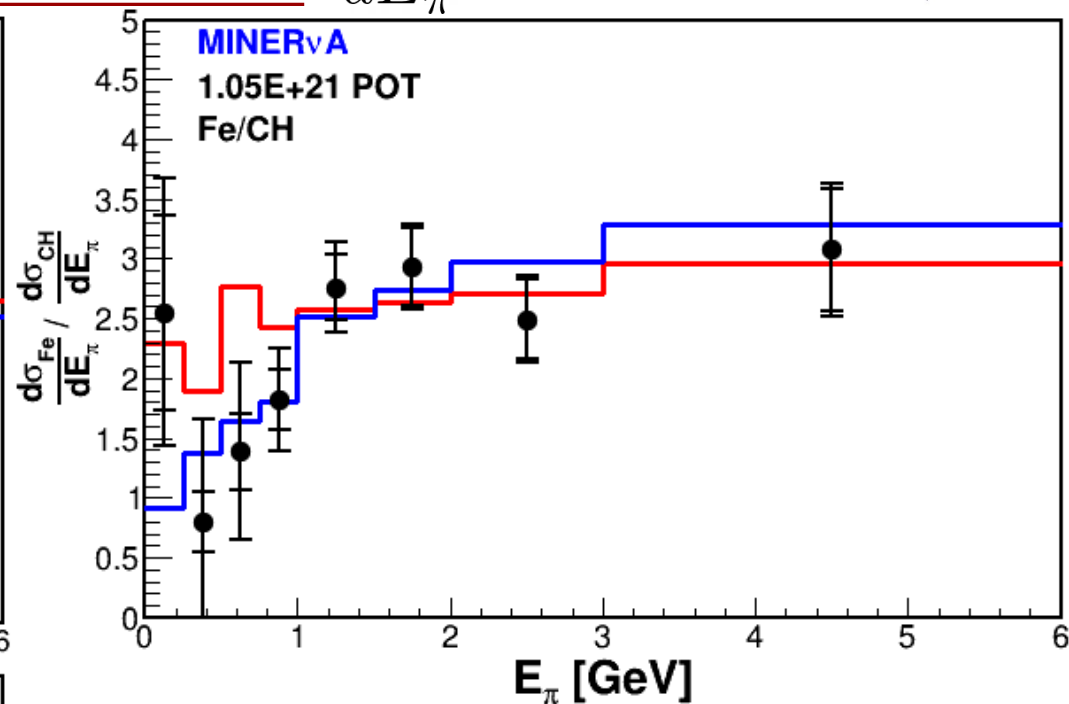
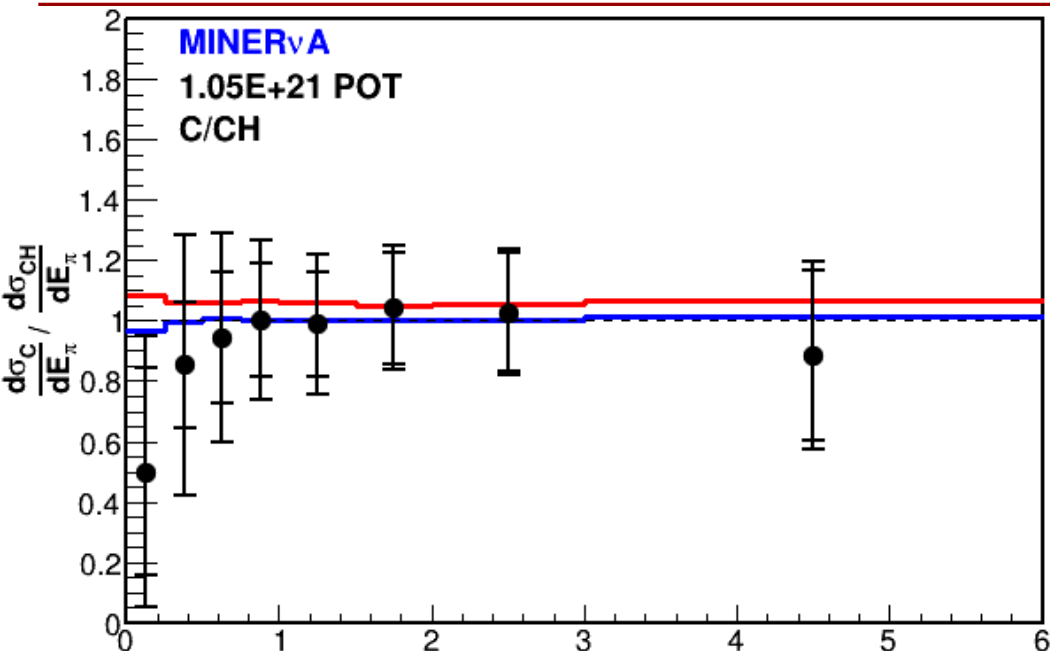
Total Cross Section (points to σ_i)
 Unfolding Matrix (points to U_{ij})
 Number of Selected Data Events (points to N_j^{DATA})
 Number of Predicted Background Events (points to N_j^{BKGD})
 Reco Bin (points to j)
 True Bin (points to i)
 Efficiency (points to ϵ_i)
 Flux Per Bin (points to ϕ_i)
 Number of Nuclei (points to T)



| Material | No. of Nuclei |
|-----------|---------------|
| <i>CH</i> | 23.6E+28 |
| <i>C</i> | 0.79E+28 |
| <i>Fe</i> | 1.02E+28 |
| <i>Pb</i> | 0.28E+28 |

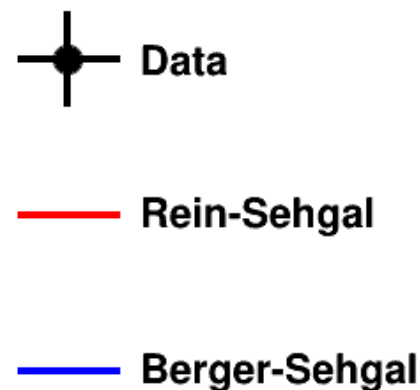
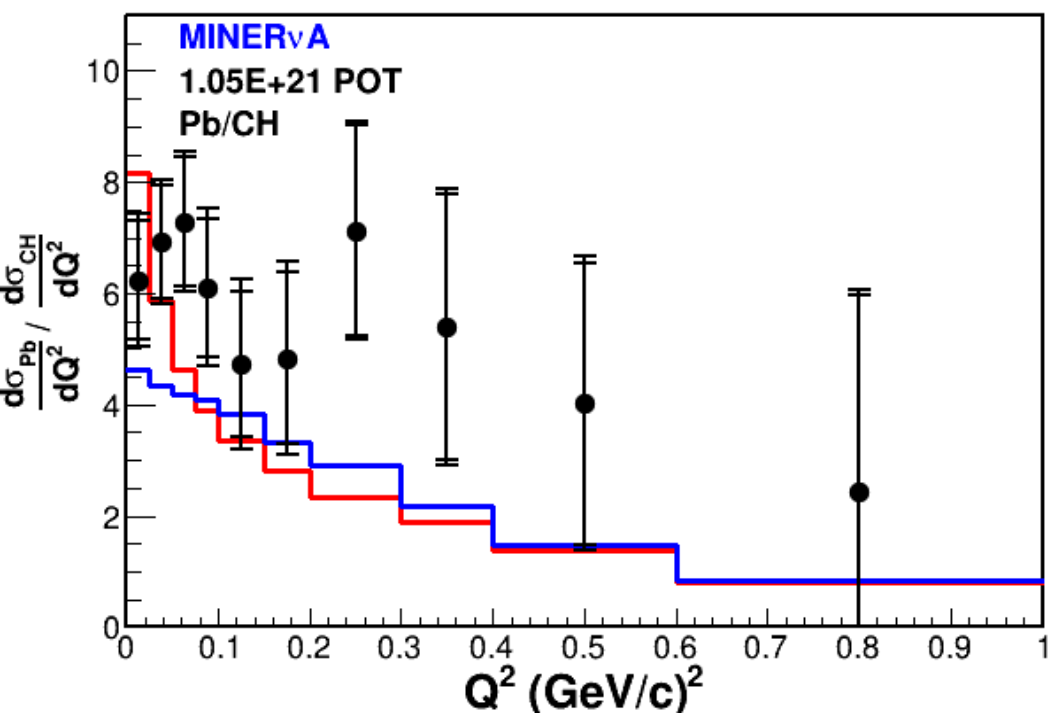
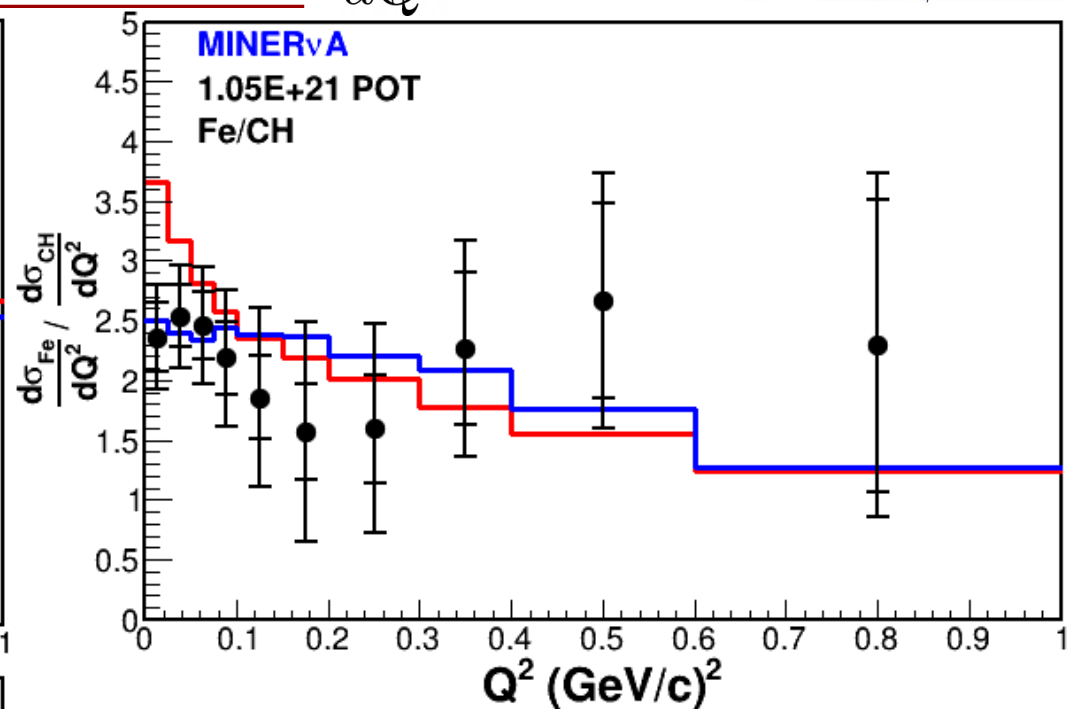
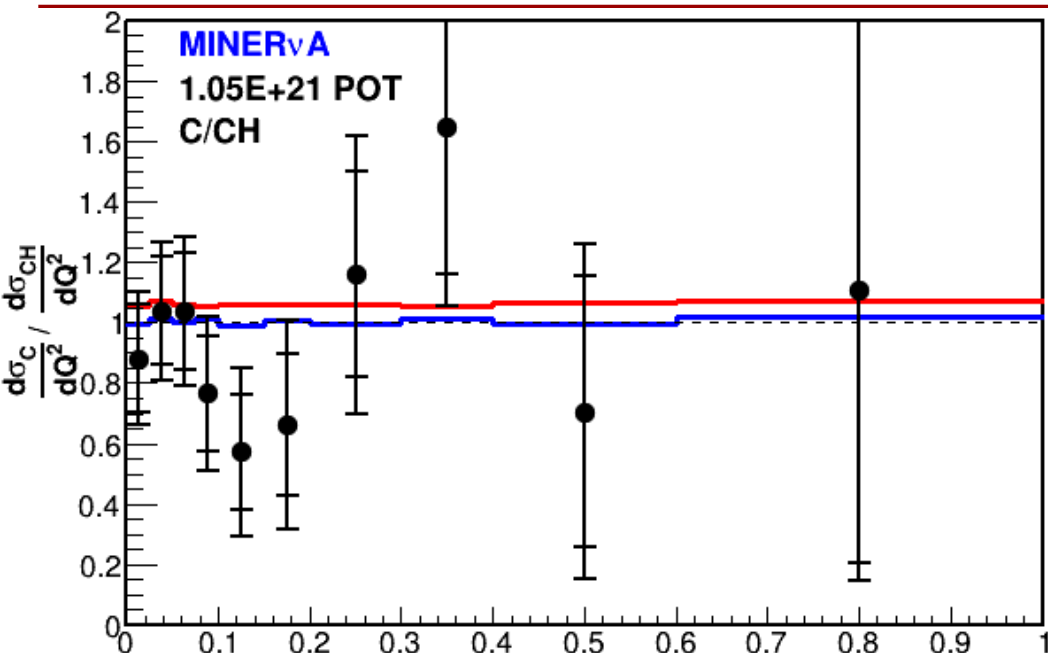
Backup – Results – Cross Section Ratios

$$\frac{d\sigma}{dE_\pi}$$



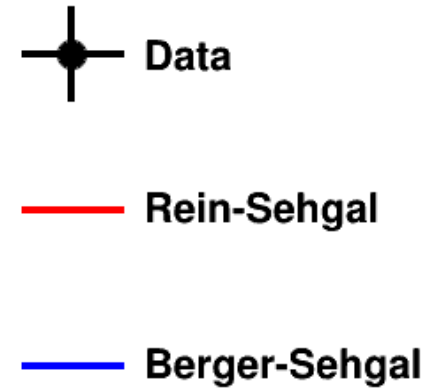
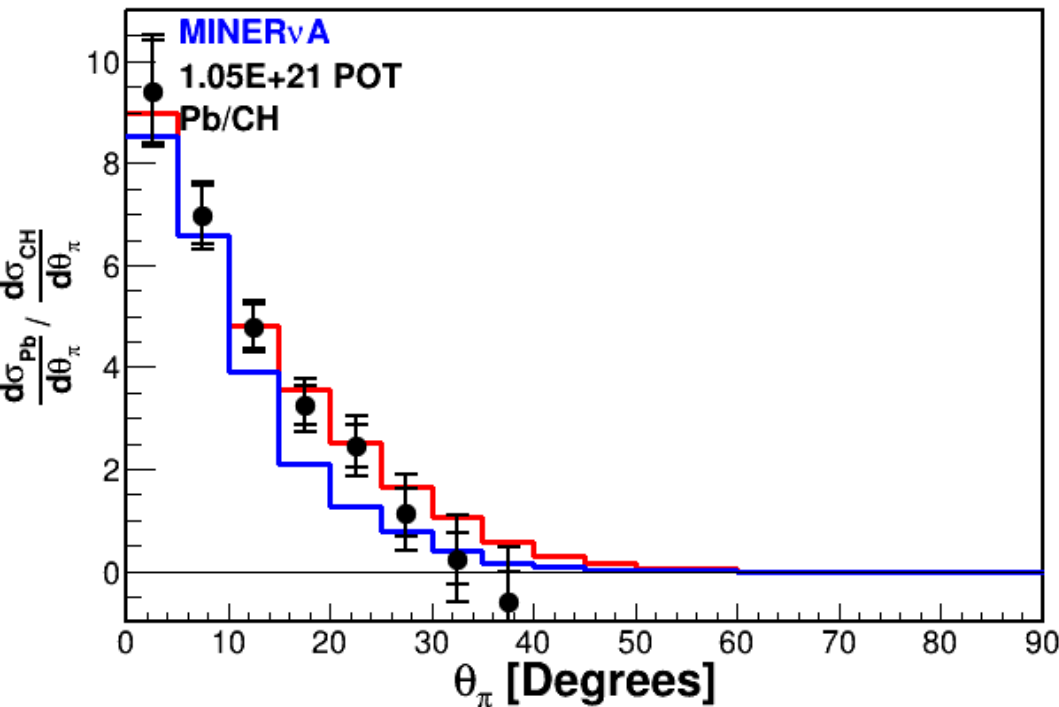
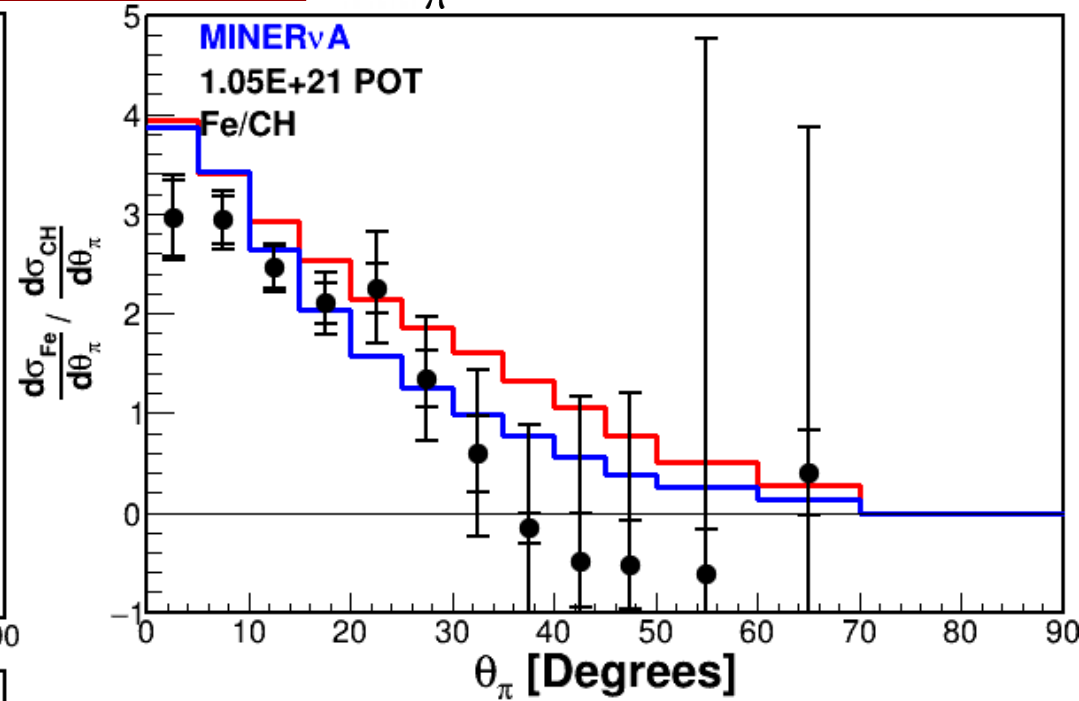
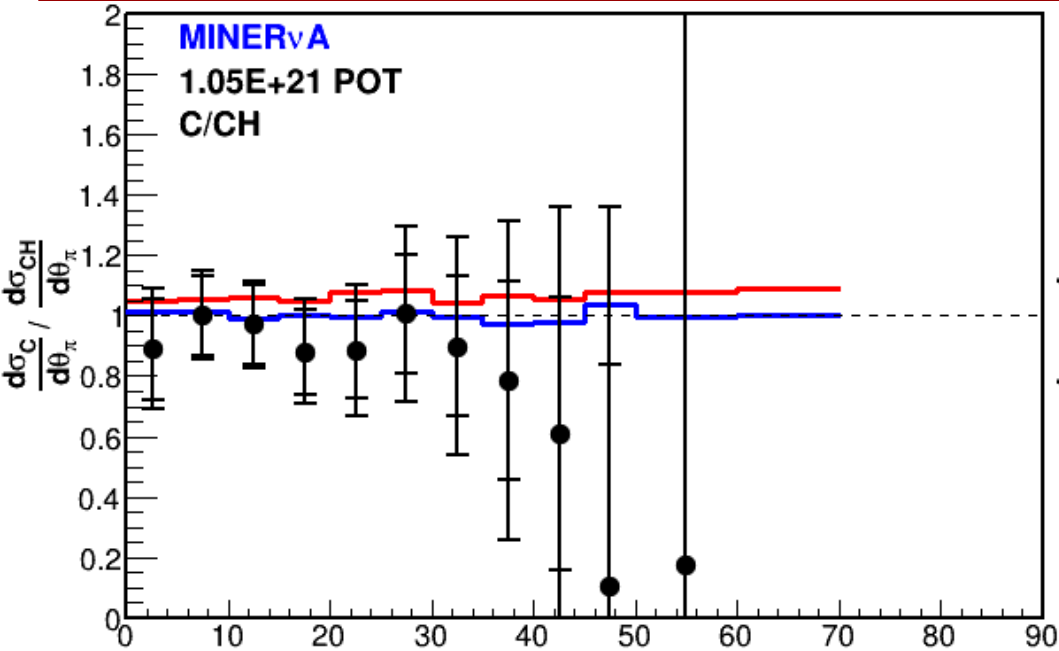
Backup – Results – Cross Section Ratios

$$\frac{d\sigma}{dQ^2}$$



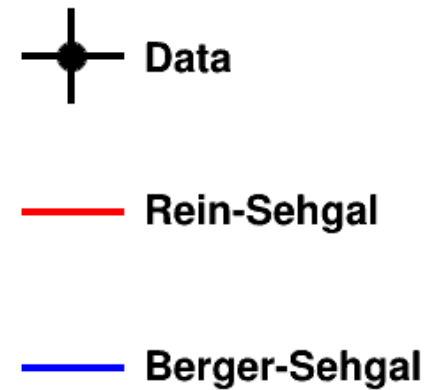
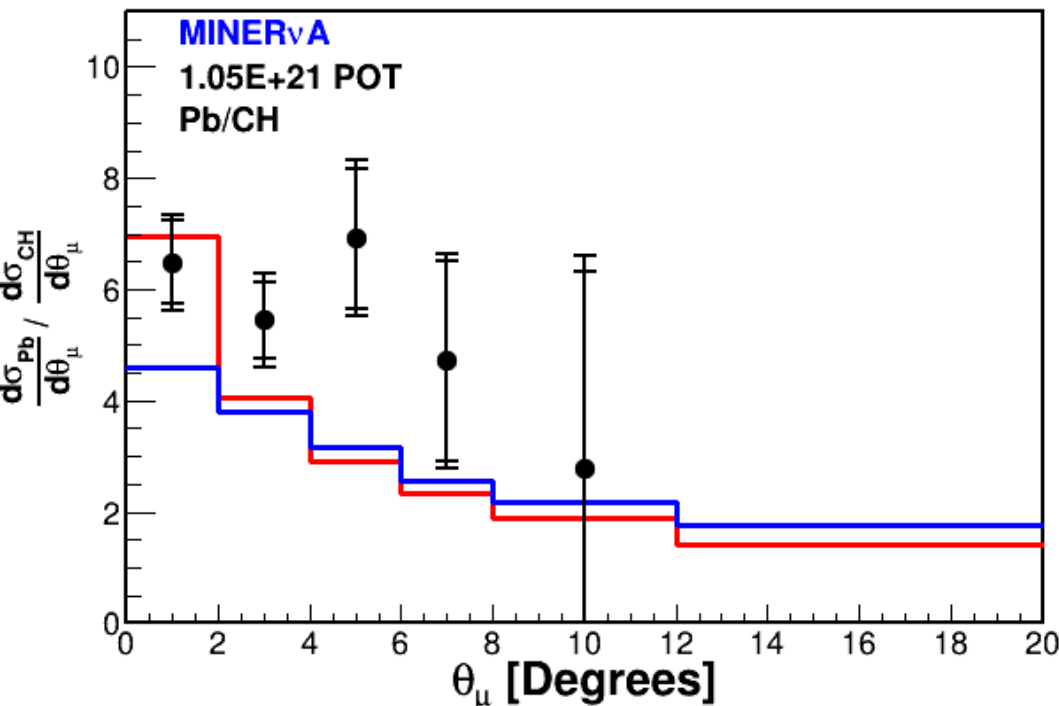
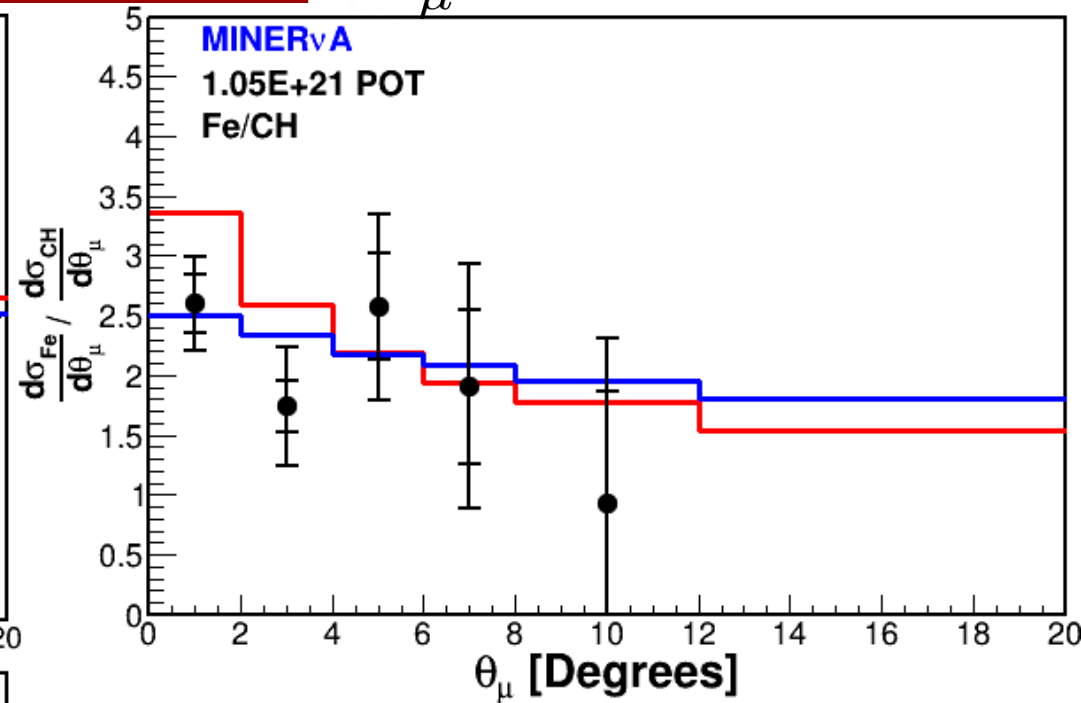
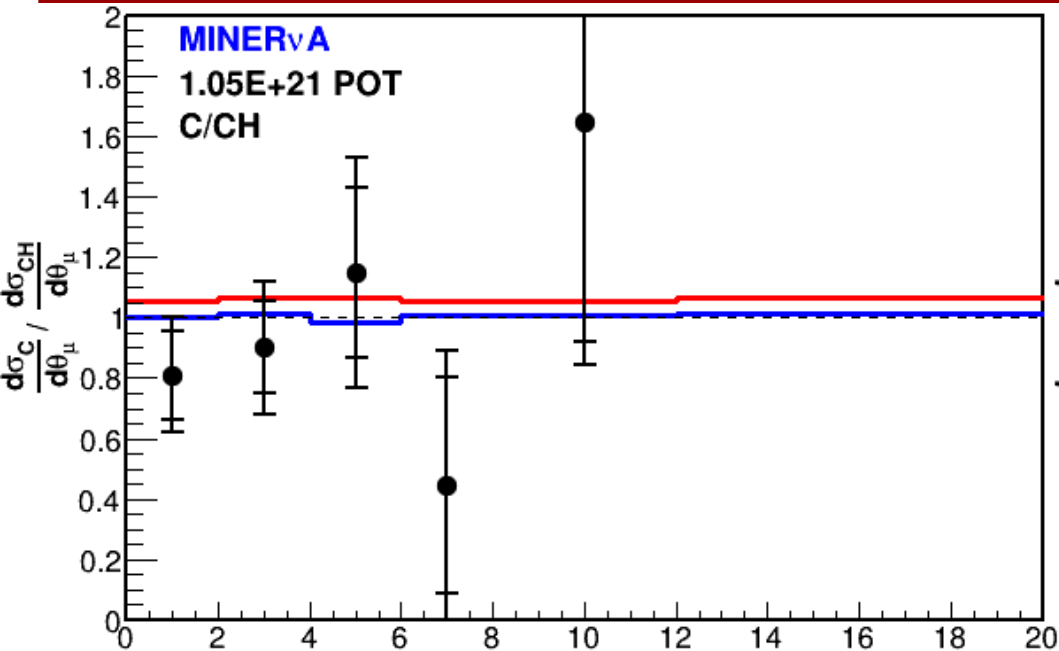
Backup – Results – Cross Section Ratios

$$\frac{d\sigma}{d\theta_\pi}$$



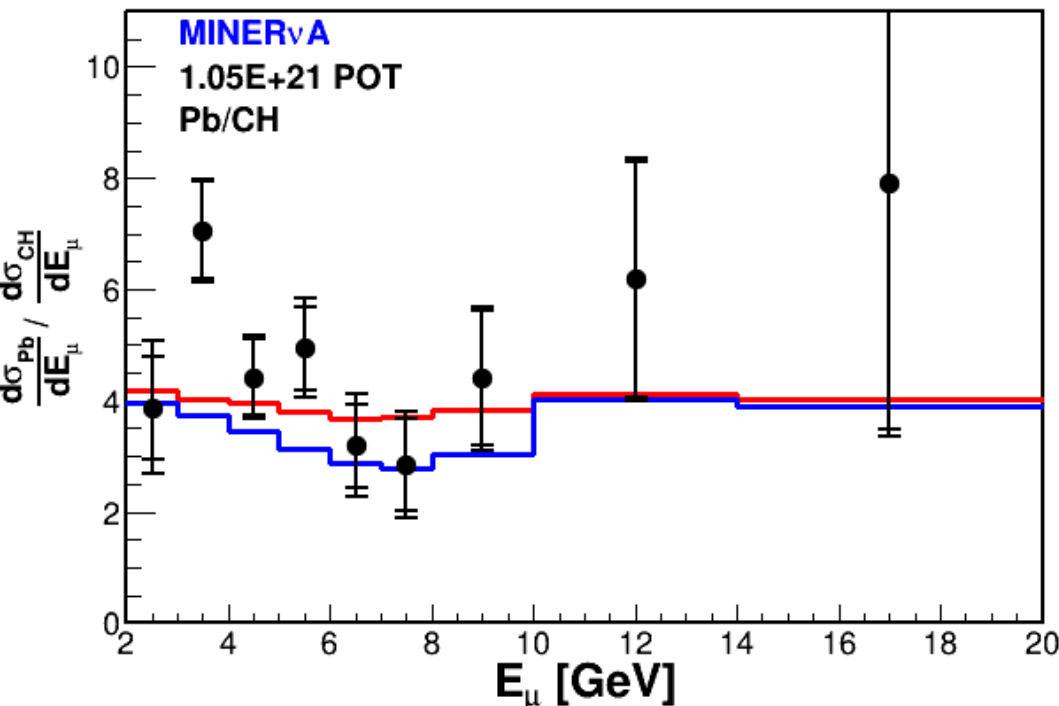
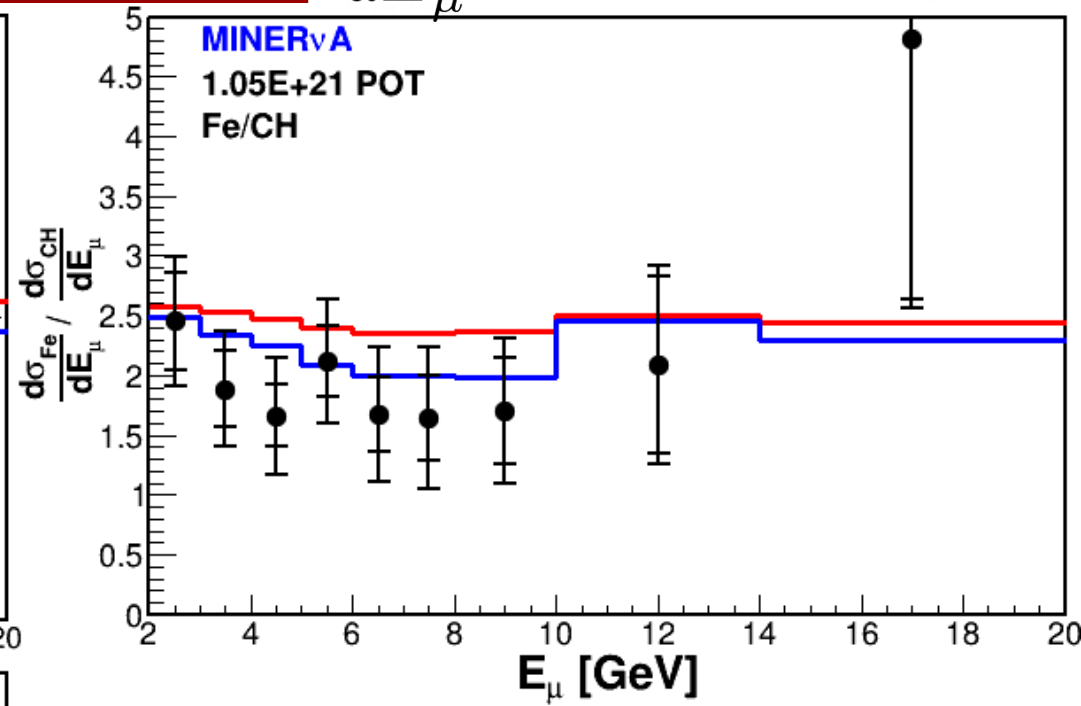
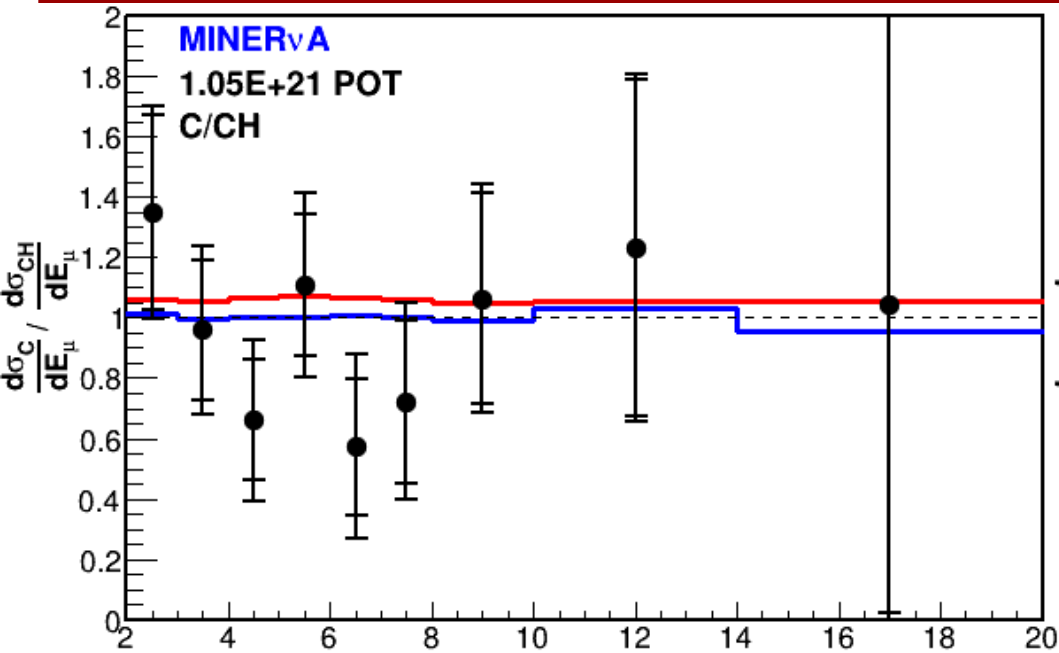
Backup – Results – Cross Section Ratios

$$\frac{d\sigma}{d\theta_\mu}$$



Backup – Results – Cross Section Ratios

$$\frac{d\sigma}{dE_\mu}$$



● Data

— Rein-Sehgal

— Berger-Sehgal

The Rein-Sehgal Model

- It extrapolates the CC cross section

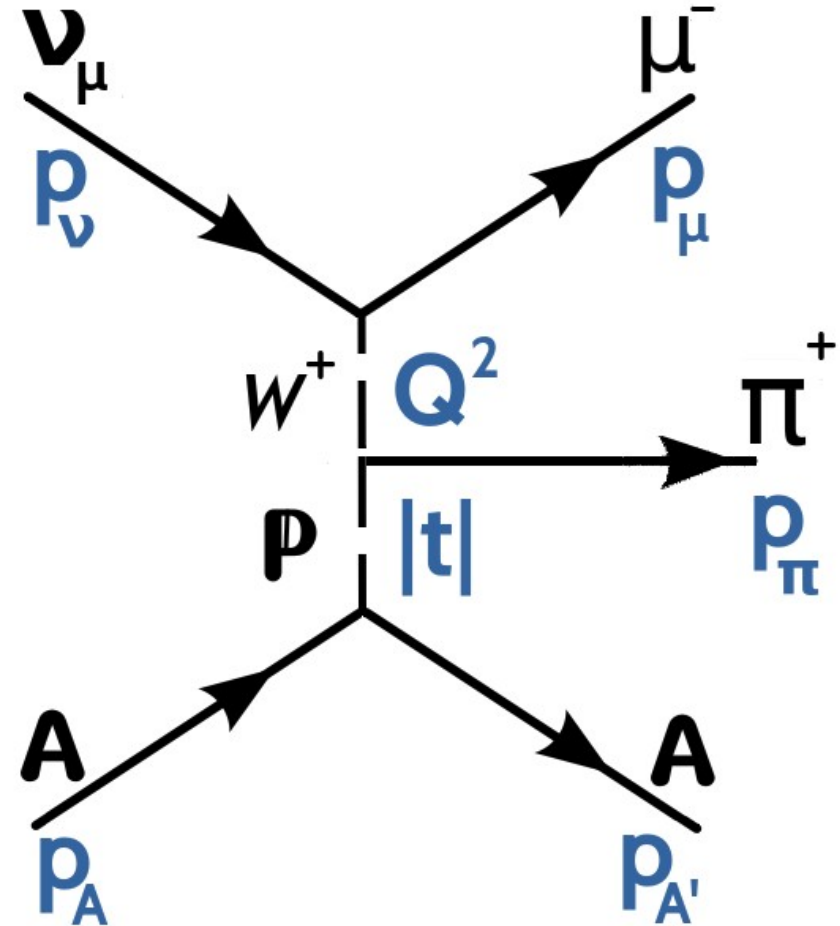
$$\left. \frac{d^3 \sigma_{coh}^{CC}}{dQ^2 dy d|t|} \right|_{Q^2=0} = \frac{G_F^2 f_\pi^2}{2\pi^2} \frac{1-y}{y} \frac{d\sigma^{\pi^\pm A}}{d|t|}$$

to $Q^2 > 0$

- Using a form factor

$$\left[m_A^2 / (m_A^2 + Q^2) \right]^2$$

- Pion-nucleus scattering is modeled using pion-nucleon data.



Other Models

Berger-Sehgal (B-S) [Phys.Rev. D79, 053003 (2009)]

- It uses π -carbon data for the $\pi+A \rightarrow \pi+A$ scattering.
- It predicts lower cross section at low P_π (see figure).
- Includes lepton mass

Belkov-Kopeliovich (B-K) [Sov.J.Nucl.Phys. 46 (1987) 499]

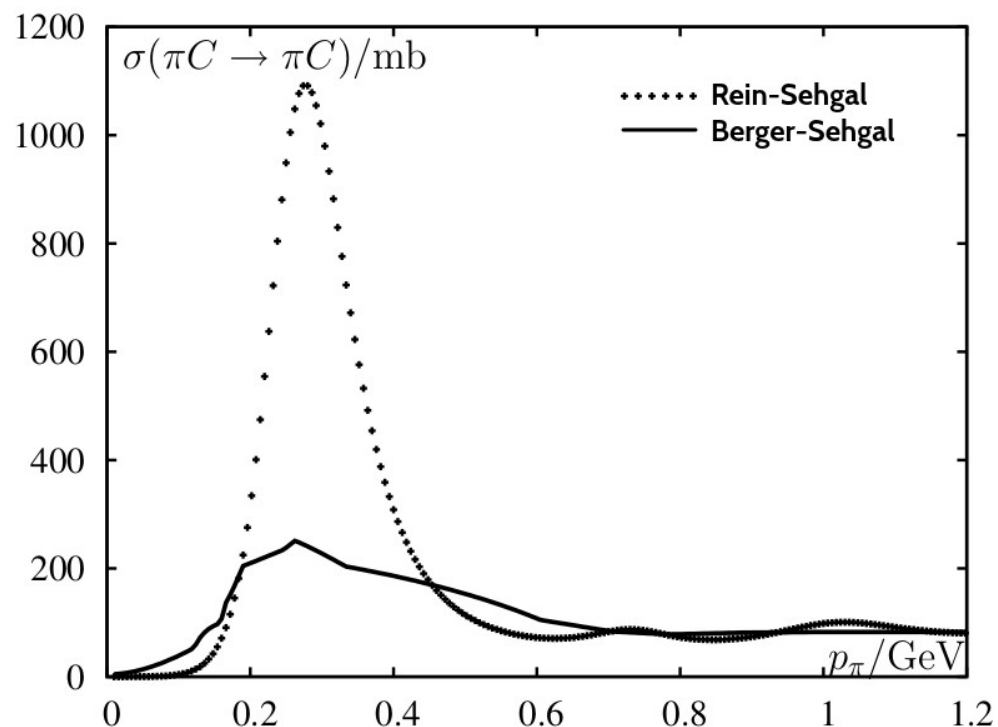
- Axial current dominated by heavy meson fluctuations, \mathbf{a}_1 or $\rho\pi$ system.
- Predicts energy-dependent A-scaling of the cross section.

Paschos-Schalla (P-S) [Phys.Rev. D80, 033005 (2009)]

- Similar to B-S. It also uses π -carbon data for the $\pi+A$ elastic scattering.
- Focuses on $Q^2 < 0.1 \text{ GeV}^2$ region, also including the lepton mass.

Microscopic Models (M-M) [Phys.Rev. C75, 055501 (2007)]

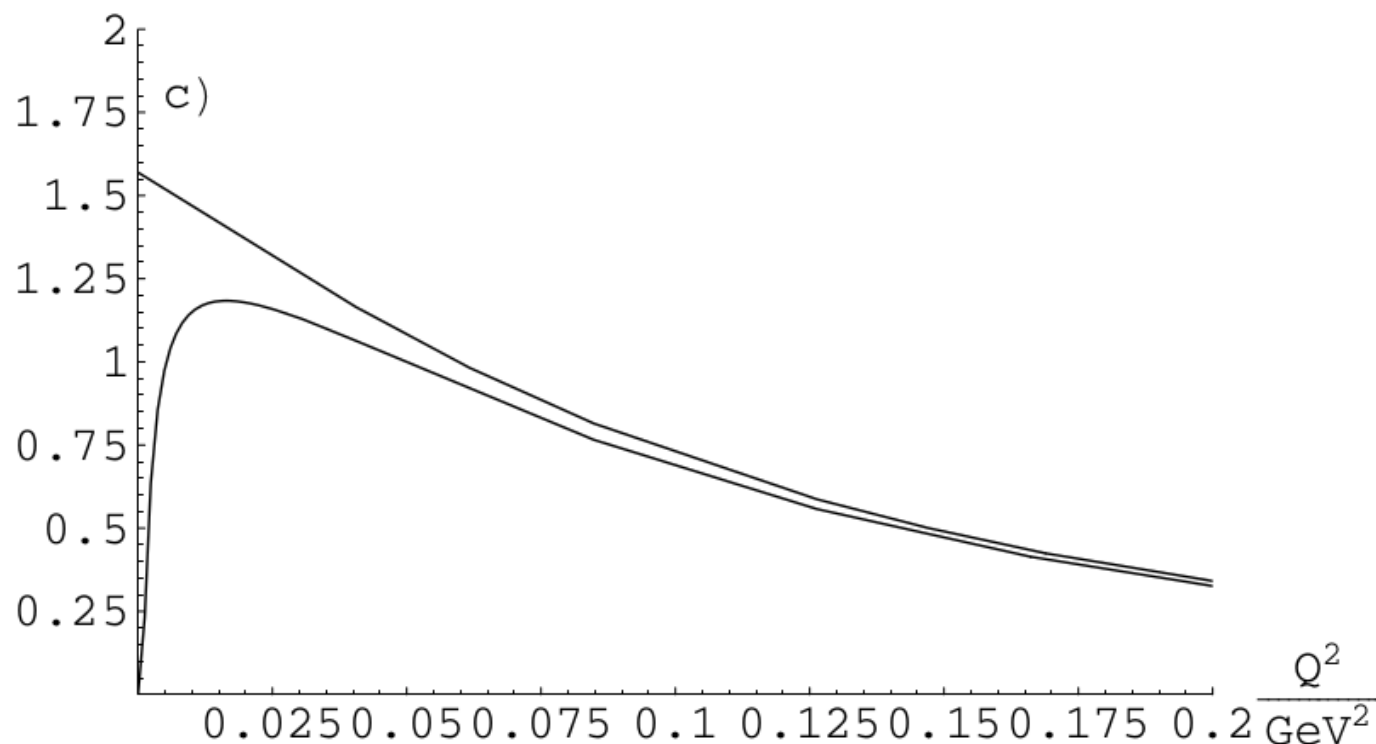
- Consider the individual contribution of nucleons to the cross section. π production obtained through baryon Δ resonances.
- Valid for $E_\nu < 2 \text{ GeV}$.



Elastic pion-Carbon cross section.
Berger-Sehgal vs Rein-Sehgal predictions

Lepton Mass in the R-S Model

Suppression of the CC cross section on carbon for $Q^2 < 0.1$ [GeV/c]² and $E_\nu = 2.0$ GeV. The upper (lower) distribution corresponds to the cross section without (with) the lepton mass correction.



MINERvA will also be adding **Fe** and **Pb** to the literature!

| EXPERIMENT | YEAR | BEAM | $\langle E_{\nu(\bar{\nu})} \rangle$, range [GeV] | MATERIAL | $\langle A \rangle$ |
|---------------|------|-----------------|--|----------------------------------|---------------------|
| NC | | | | | |
| Aachen-Padova | 1983 | $\nu/\bar{\nu}$ | 2 | <i>Al</i> | 27 |
| Garmamelle | 1984 | $\nu/\bar{\nu}$ | 2 | <i>CF₃Br</i> (Freon) | 36 |
| SKAT | 1985 | $\nu/\bar{\nu}$ | 7 | <i>CF₃Br</i> (Freon) | 36 |
| CHARM | 1985 | $\nu/\bar{\nu}$ | 31 (24) | <i>CaCO₃</i> (Marble) | 20 |
| 15' BC | 1986 | ν | 20 | <i>NeH₂</i> | 20 |
| MiniBooNE | 2008 | ν | 0.7 | <i>CH₂</i> | 12 |
| NOMAD | 2009 | ν | 24, 2.5-300 | <i>C</i> | 12.8 |
| SciBooNE | 2010 | ν | 0.8 | <i>C</i> | 12 |

| EXPERIMENT | YEAR | BEAM | $\langle E_{\nu(\bar{\nu})} \rangle$, range [GeV] | MATERIAL | $\langle A \rangle$ |
|---------------------|------|-----------------|--|---------------------------------|---------------------|
| CC | | | | | |
| WA59 | 1984 | $\bar{\nu}$ | 40 | <i>NeH₂</i> | 20 |
| SKAT | 1986 | $\nu/\bar{\nu}$ | 7 | <i>CF₃Br</i> (Freon) | 36 |
| BEBC WA59 | 1986 | $\bar{\nu}$ | 5-150 | <i>Ne</i> | 20 |
| E632 | 1989 | $\nu/\bar{\nu}$ | 150 (110) | <i>Ne</i> | 20 |
| BEBC WA59 | 1989 | ν | 5-150 | <i>Ne</i> | 20 |
| CHARM II | 1993 | $\nu/\bar{\nu}$ | 20 | Glass | 20.7 |
| E632 | 1993 | $\nu/\bar{\nu}$ | 80 (70) | <i>Ne</i> | 20 |
| K2K | 2005 | ν | 1.3 | <i>C</i> | 12 |
| SciBooNE | 2009 | ν | 1.1 | <i>C</i> | 12 |
| MINERvA (LE) | 2014 | $\nu/\bar{\nu}$ | 3.6 | <i>C</i> | 12 |
| ArgoNeuT | 2015 | $\nu/\bar{\nu}$ | 9.6 (3.6) | <i>Ar</i> | 40 |
| T2K | 2016 | ν | < 1.5 | <i>C</i> | 12 |
| MINERvA (ME) | 2022 | ν | 6 | <i>C, Fe, Pb</i> | 12, 56, 207 |